ACTA ODONTOLOGICA LATINOAMERICANA

aol

ACTA ODONTOLÓGICA LATINOAMERICANA
An International Journal of Applied and Basic Dental Research

EDITORIAL POLICY

Although AOL will accept original papers from around the world, the principal aim of this journal is to be an instrument of communication for and among Latin American investigators in the field of dental research and closely related areas.

Particular interest will be devoted to original articles dealing with basic, clinic and epidemiological research in biological areas or those connected with dental materials and/or special techniques.

Clinical papers will be published as long as their content is original and not restricted to the presentation of single cases or series.

Bibliographic reviews on subjects of special interest will only be published by special request of the journal.

Short communications which fall within the scope of the journal may also be submitted.

Submission of a paper to the journal will be taken to imply that it presents original unpublished work, not under consideration for publication elsewhere. To this end, the authors will state their agreement with the editorial policy. The papers cannot later be published elsewhere without the express consent of the editors.

To favour international diffusion of the journal, articles will be published in English with an abstract in Spanish or Portuguese.

Acta Odontológica Latinoamericana may use Internet programs and tools to detect plagiarism, self-plagiarism, duplication and fragmentation.

Regarding the ethics of the publication process, Acta Odontológica Latinoamericana complies with the Recommendations for the Conduct, Reporting, Editing and Publication of Scholarly Work in Medical Journals, International Committee of Medical Journal Editors. (https://www.icmje.org/icmje-recommendations.pdf)

The editors of Acta Odontologica Latinoamericana have no commercial interest, nor do they endorse or vouch for commercial products or diagnostic and therapeutic procedures mentioned in the publications.

Articles accepted for publication will be the property of Acta Odontológica Latinoamericana and express the opinion of the authors.

Acta Odontológica Latinoamericana is an open access publication. The content of the publication is licensed under a Creative Commons Attribution-Noncommercial 4.0 International License (CC BY-NC 4.0)

Peer review process
Acta Odontologica Latinoamericana uses double-blind review, which means that both the reviewer and author identities are concealed from the reviewers, and vice versa, throughout the review process.

The review process will be carried out by two reviewers selected by the editorial board, from specialists in each field. The reviewers will undertake the review process in order to achieve the highest possible standard of scientific content. Confidentiality, impartiality and objectivity will be maintained during the entire peer review process. If discrepancies arise, a third reviewer will be invited to participate. The reviewers will have a period of 4 weeks to review the manuscript and based on their report, the Editorial Committee may request modifications and decide on acceptance or rejection of the manuscript. The revised version of manuscripts with a recommendation of major modifications, will be sent back to the reviewers for final evaluation.

The manuscripts accepted for publication will be submitted to idiomatic evaluation and revision, edition and layout. The authors will proofread their manuscript and must approve the final version prior to publication.

Policies on Conflict of Interest
All authors must state any financial or other conflict of interest that could be interpreted as a bias in the results or interpretation of the results reported in their manuscript.

Human and Animal Rights, and Informed Consent
All investigators should ensure that the planning, conduct, and reporting of human research are in accordance with the Helsinki Declaration as revised in 2013. The authors must state in their manuscript that they have obtained informed consent of the people involved and that the project has been approved by an institutional ethics committee
Studies involving laboratory animals must comply with the "Guide for the Care and Use of Laboratory Animals", National Academy of Sciences. Washington DC and have the approval of an institutional committee

CONTENTS

Precision of polyether ether ketone (PEEK) or cobalt-chrome implant bar fit to implants after mechanical cycling

Eduardo V Silva Júnior ⓘ, Roberta T Basting ⓘ, Cecilia P Turssi ⓘ, Fabiana MG França ⓘ

Faculdade São Leopoldo Mandic, Programa de Pós-Graduação, Campinas, Brasil.

ABSTRACT

*Based on its mechanical properties, PEEK (polyether-ether-ketone) might be useful in restorative procedures. In oral rehabilitation, its viability has been studied mainly for prostheses and dental implants. **Aim:** The aim of this study was to evaluate the fit accuracy of dental implant bars made of either PEEK or cobalt-chrome submitted to cycling mechanics. **Materials and Method:** This was an experimental in vitro study, where units were treated with two implants and mini-abutments, joined by cobalt-chrome or polyether-ether-ketone PEEK bars. A total 20 bars were prepared (n=10 per group) and subjected to mechanical cycling tests (1 million cycles on the distal cantilever of the bar in the vertical direction, 120N and sinusoidal loading, at a frequency of 2Hz). The fit at the abutment/implant interface was measured before and after cycling, and the counter-torque of the vertical screw of the mini abutments was measured after cycling, using a digital torquemeter. Data were analyzed by three-way ANOVA and Tukey's test at 5% significance level. **Results:** No statistically significant interaction was found among the three factors considered (bar material, implant positioning and mechanical cycling) (p = 0.592). No significant difference was identified in the interaction between bar material and implant positioning (p = 0.321), or between implant positioning and mechanical cycling (p = 0.503). The association between bar material and mechanical cycling was statistically significant (p = 0.007), with the cobalt-chrome bar resulting in greater misfit with mechanical cycling. There was no difference in counter-torque values between groups. **Conclusions:** The PEEK bar provided better fit of the mini abutments to the implants, even after mechanical cycling. The counter-torque of the screws was similar in all scenarios considered.*

Keywords: PEEK - Dental prosthesis - Mouth rehabilitation.

Precisão da adaptação de barras tipo protocolo confeccionados em polyetheretherketone (PEEK) ou cobalto cromo sobre implante após ciclagem mecânica

RESUMO

*O PEEK (Poli-éter-éter-cetona) é um material considerado para uso em procedimentos restauradores devido às suas propriedades mecânicas. Na reabilitação oral, sua viabilidade tem sido estudada principalmente para uso em próteses e implantes dentários. **Objetivos:** O objetivo deste estudo foi avaliar a precisão da adaptação de duas barras diferentes do tipo protocolo confeccionadas em PEEK ou Cobalto-Cromo, após serem submetidas à mecânica ciclística. **Materiais e Método:** As unidades experimentais foram constituídas por barras confeccionadas em Poli-ether-ether-Ketone (PEEK) e em Cobalto-Cromo (Co-Cr). Trata-se de um estudo experimental, in vitro, onde verificou-se unidades constituídas por dois implantes e mini pilares unidos com barras de Cobalto-Cromo ou PEEK. Foram confeccionados um total de 20 barras (n=10 em cada grupo) e as barras foram submetidas a ensaios de ciclagem mecânica (1 milhão de ciclos no cantilever distal da barra no sentido vertical, 120N e carregamento senoidal, a uma frequência de 2Hz). Antes e após a ciclagem realizou-se a mensuração da desadaptação na interface pilar/implante e após a ciclagem foi medido o contra-torque do parafuso vertical dos mini-pilares através de torquímetro digital TQ 8800 (LT Lutron, Taiwan). Os dados foram submetidos a ANOVA a três critérios e teste de Tukey ao nível de significância a 5%. **Resultados:** Constatou-se que não houve interação estatisticamente significativa entre os três fatores estudados, ou seja, entre o material da barra, o posicionamento do implante e a ciclagem mecânica (p = 0,592). Também não se identificou diferença estatística significativa da interação entre o material da barra e o posicionamento do implante (p = 0,321), nem entre o posicionamento do implante e a ciclagem mecânica (p = 0,503). Já a associação entre o material da barra e a ciclagem mecânica foi estatisticamente significativa (p = 0,007), onde a barra de Cobalto-Cromo resultou em maior desadaptação com a ciclagem mecânica. Não houve diferença nos valores dos contra-torques entre os grupos. **Conclusões:** Conclui-se que a barra de protocolo fabricada em PEEK proporcionou melhor adaptação dos mini pilares aos implantes mesmo após a ciclagem mecânica. Por fim, o contra-torque dos parafusos foi semelhante em todos os cenários avaliados.*

Palavras-chave: PEEK - Prótese dentária - Reabilitação bucal.

INTRODUCTION

Science and technology are increasingly investing in implant dentistry, which is one of the main specialties requiring innovative materials[1]. One of these materials is PEEK (polyether-ether-ketone), an aromatic semicrystalline polymer developed in England in the late 1970s. PEEK is a high-performance thermoplastic material being researched in dentistry[2-5].

PEEK has been considered for use in restorative procedures due to its mechanical properties[6]. In oral rehabilitation, its viability has been studied mainly for prostheses and dental implants. In Implantology specifically, it is studied as a potential alternative to titanium and zirconia, considering its biocompatibility and physical properties such as elasticity, resistance and radiolucency[7-9].

PEEK has high resilience, resistance to fracture and corrosion and shock absorption, and low transmission of forces to the adjacent bone[10], which can prevent abutment screw fractures, transmission of occlusal overloads to the marginal bone around dental implants, and bone loss[10].

PEEK has an elastic modulus similar to that of bone, so it can absorb mechanical shocks. Prosthetic abutments and dental implants made from PEEK can therefore absorb and foster dissipation of masticatory loads to the peri-implant bone, thereby preventing implant failures[10]. Its main disadvantages are that it is bioinert, which may be a problem for osseointegration, and susceptible to stress deformation[9-10]. In thermal cycling with artificial saliva, PEEK has low retention in prostheses, especially at very acidic or very alkaline pH values[11-12]. There are few randomized controlled clinical studies to ensure effectiveness in its clinical use[9-10].

Passive fit is one of the most important prerequisites for maintaining the implant-bone interface. To achieve a passive fit or stress-free framework, the framework should theoretically not induce stress on the implant components or surrounding bone in absence of external load application[13]. However, according to the available literature, it is practically impossible to achieve completely passive fit[13]. Prosthetic complications such as loosening or fracture of the prosthetic abutment screw, infrastructure and ceramic covering have been documented and may be related to poor fit of the framework[13]. In bone tissue, complications such as infections, oronasal communication or peri-implantitis are quite rare[14].

In implant-supported bars, there is a direct relationship between the amount of deformation and the force of occlusion, while there is an inverse relationship with the modulus of elasticity of the framework material of the implant-supported bar[15]. The most usual techniques for making bars for protocol-type prostheses ultimately produce heavy structures and use laboratory procedures requiring extensive execution time, fostering failures in their manufacture. In this regard, PEEK could be an alternative material. However, due to the scarce evidence and protocol-type prostheses, further studies are required. Considering as a null hypothesis that PEEK promotes fit similar to that of cobalt-chrome, which is the material traditionally used, the aim of this study was to evaluate the fit accuracy of PEEK and cobalt-chrome implant bars, after being submitted to cycling mechanics.

MATERIALS AND METHOD
Experimental design

This was an experimental in vitro study. Experimental units consisted of two implants and mini abutments seated on them, numbered as mini abutment I and mini abutment II, the latter being closest to the cantilever. The mini abutments were connected with bars that had two levels, one made of cobalt-chrome and other made of PEEK. The positioning of the implant/mini prosthetic abutment and bars was measured before and after dry mechanical cycling. As a dependent variable, there was an assessment of the mismatch between mini abutments I and II to cylinders made of Co-Cr alloy and PEEK and the counter-torque of the screws of the mini abutments after the dry mechanical cycling test.

Sample and master model preparation

Twenty solid rectangular bars were prepared, half of them (n=10) made of polyether-ether-ketone (PEEK), and the other half (n=10) of cobalt-chrome, to be used as a control group.

Aluminum molds 30 mm long x 6.97 mm wide x 12.60 mm tall were made for fixing the implants. To guide the positioning of the two external hexagon implants (3.75 x 11mm) and 4.1mm platform (Neodent), a lathe was used to make perforations 3.5 mm in diameter in the aluminum mold.

The perforations were equidistant and parallel, with precision of one micrometer (1 μm), and numbered I and II. The implants were subsequently placed using

a ratchet, and standardized with torque of 60 N.cm (Fig. 1).

HE 4.1 mini conical abutments (Neodent, Curitiba, Brazil) were installed on the implants with a regular transmucosal height of 1 mm and torque 32N.cm, as recommended by the manufacturer. Then, proto-col-type bars were made, a PEEK-type polymeric disc (Juvora Dental Discs, Cleveleys, UK) and a wax disc (Vitazanfabrik, Bad Säckingen, Germany) were positioned on a five-axis milling machine for machining the bars (Juvora Dental Discs, Cleveleys, UK).

After installing all the implants in the master molds with their respective mini abutments, they were scanned with a 3shape scanner, and an adapted solid body protocol-type bar project[16] was executed in the Dental System 3Shape program (Fig. 2). Ten PEEK polymer bars and ten wax bars were made in the same design, as a quadrilateral figure with dimensions 30 mm long x 6.97 mm wide x 12.60 mm tall. The wax bars were subjected to the induction casting process. The passivity of all bars was tested by visual verification in their respective metallic molds. The metal bars and polymer (PEEK) bars were screwed into the mini abutments on the implants with torque of 10N.cm, as recommended by the manufacturer, and then submitted to the dry mechanical cycling test.

Mechanical cycling

The cyclic load tests were performed in a device for mechanical cycling (MSFM, Elquip, São Carlos, SP, Brazil), dry and at room temperature, applying

Fig. 2: Digital design of the bars to be milled. Dimensions: 6.07 mm high x 33.3 mm long X 4.03 mm thick.

1 million cycles on the distal cantilever of the bar in the axial direction, which simulates 50 years[17]. The cylinder drive speed and frequency were controlled by the control box that moved the pistons located inside these cylinders, compressing the specimens with a controlled force of 120N and sinusoidal loading, at a frequency of 2Hz[18] (Fig. 3).

Mini abutment/implant interface fit assessment

Before and after the mechanical cycles, the samples of the implant - mini abutment/bar set were positioned in a microhardness tester to measure the mismatch of the implant/prosthetic abutment interface and respective bars, with an increase of 100 times (Pantec, Campinas, SP – Brazil). Eight readings were performed, two on the anterior face and two on the posterior face of each implant/mini-abutment and bar set, totaling 80 measurements for each group of 10 sets. Two measurements were taken on each mini-plier, I and II, at the point where the bar was adapted to the mini-abutment. The other measurements were taken in exactly the same locations on the opposite side. Thus, four measurements were
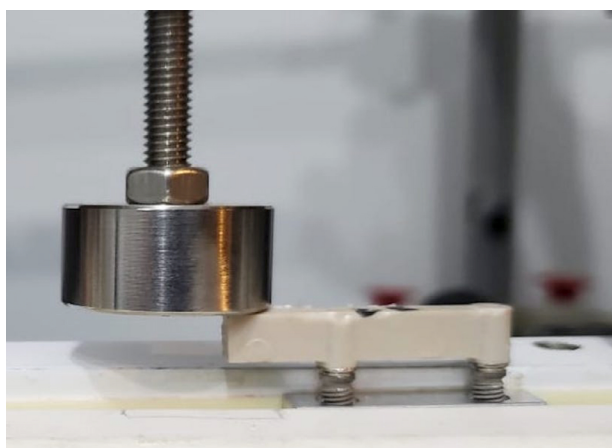

Fig. 1: Master die. Dimensions: 12.60 mm high x 30 mm long x 6.97 mm thick. The distance between implants I and II was 15.24 mm.

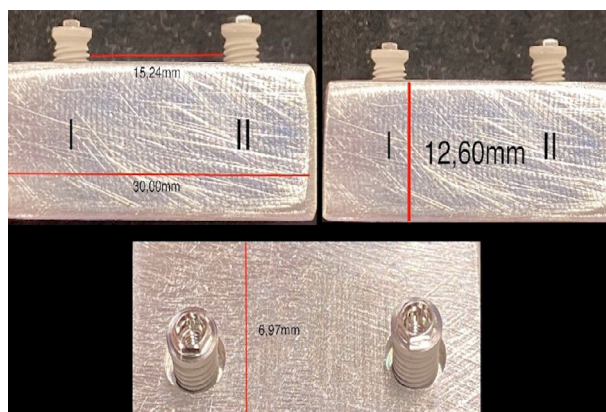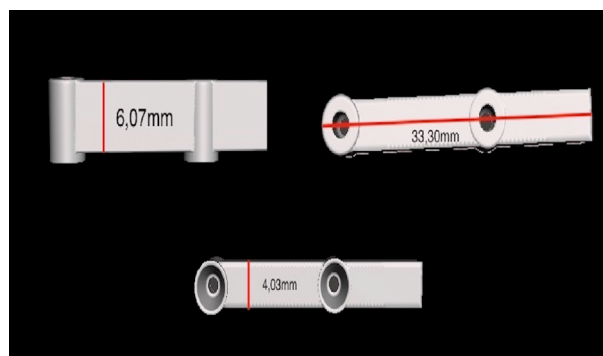Fig. 3: Loading positioning during mechanical cycling.

taken on the anterior side and four on the posterior side, totaling eight measurements. An arithmetic mean of the measurements of each implant was used for analysis.

Counter-torque

Before and after the mechanical cycles, the samples of the implant - mini abutment/bar set were placed in a microhardness tester (Pantec, Campinas, SP, Brazil) to measure the mismatch of the implant/prosthetic abutment interface and respective bars, with an increase of 100 times. A TQ 8800 digital torquemeter (LT Lutron, Taiwan) was used to measure the counter-torque of the mini abutment screws after cycling and check the abutment/implant interface mismatch. All the analyses were performed by the same operator.

Statistical analysis

Fit data were checked for adherence to normal distribution. In order to investigate the effects of bar material, implant positioning and mechanical cycling, as well as the triple and dual interactions among these three factors, the three-way analysis of variance for repeated measures was used. For multiple comparisons, Tukey's test was used. For counter-torque values, the effects of bar material and implant positioning, non-parametric Mann-Whitney tests were used. Statistical calculations were performed using SPSS 23 software (SPSS Inc., Chicago, IL, USA), setting the significance level at 5%.

RESULTS

Table 1 summarizes the mean values and standard deviations of the fit between the mini abutments and the protocol-type cylinder made of PEEK or cobalt-chrome, before and after mechanical cycling. Three-way analysis of variance for repeated measurements showed that there was no statistically significant interaction among the three study factors (bar material, implant positioning and mechanical cycling) (p = 0.592). No statistically significant effect was identified between the bar material and implant positioning (p = 0.321), or between implant positioning and mechanical cycling (p = 0.503). The association between bar material and mechanical cycling was statistically significant (p = 0.007). Table 2 shows the results of the statistically significant interaction. Both before and after mechanical

Table 1. Means and standard deviations of the fit (µm) between the mini abutments and the cylinder of protocol-type bars made of PEEK or cobalt-chrome, before and after mechanical cycling.

Bar material	Before cycling		After cycling	
	Mini abutments I	Mini abutments II	Mini abutments I	Mini abutments II
PEEK	6.02 (0.93)	6.32 (1.24)	5.81 (1.48)	5.97 (1.10)
Cobalt-Chrome	7.35 (1.04)	7.17 (0.82)	10.62 (5.88)	9.17 (1.21)

Table 2. Means and standard deviations of misfit (µm) between the cylinder of protocol-type bars made of PEEK or cobalt-chrome and the mini abutments, without considering their positioning, before and after mechanical cycling.

Bar material	Before cycling*	After cycling*
PEEK	6.17 Aa (1.08)	5.89 Aa (1.27)
Cobalt-Chrome	7.26 Ba (0.92)	9.89 Bb (4.20)

* Not considering whether they were mini-abutments I or II. Means followed by different capital letters indicate significant difference between materials (comparisons within each column). Means followed by different lowercase letters indicate a significant difference before and after cycling (comparisons within each row).

cycling, the misfit was significantly greater with the cobalt-chrome bar than with the PEEK bar. Only cobalt-chrome resulted in greater misfit with mechanical cycling. For the PEEK bar, the misfit between the mini abutments and their cylinder was not significantly affected by mechanical cycling.

The Mann-Whitney tests showed no significant difference (Table 3) in the values of counter-torque in

Table 3. Medians, means and standard deviations of the counter-torque (N.cm) of mini abutment screws, according to their positioning and the material used in making the protocol-type bar.

Bar material	Mini abutment I	Mini abutment II
PEEK	3 Aa 2.50 (1.4)	2 Aa 1.90 (1.4)
Cobalt-Chrome	4 Aa 2.3 (5.36)	1 Aa 0.40 (3.9)

Medians in the first line of each group. Means and standard deviation in the second line of each group. Medians followed by the same capital letters indicate no significant difference between materials (comparisons within each column). Medians followed by different lowercase letters indicate a significant difference between mesial and distal miniscrews (comparisons within each row).

the screws of the mini-abutments I and II with either cobalt-chrome (p = 0.257) or PEEK (p = 0.473) bars.

DISCUSSION

The search for alternative materials for implant-supported bars is justified by the concern about a possible release of metals from cobalt-chrome alloys into the bloodstream[3]. The present study sought to evaluate the properties of PEEK by comparing fit accuracy between PEEK and conventional Co-Cr bars. The findings refuted the null hypothesis because the experimental bar had lower misfit values.

The results demonstrated that the interaction between the bar's composition material and the performance of mechanical cycling affected the marginal fit of the mini abutment. In this context, PEEK bars achieved better marginal fit before and even after mechanical cycling. This might be explained by the fact that PEEK has a lower modulus of elasticity and absorbs more tension, distributing the load on the bar more evenly[18-20].

These findings complement existing evidence for use in dentistry, which point to aesthetic feasibility[21], biocompatibility and elasticity[10], with several studies suggesting optimistic results regarding physical, chemical and mechanical properties[19-21]. In the present study, the cantilever region was chosen because it is the most affected by masticatory forces, as noted in other studies[16,23]. Room temperature was used without impact on the results since the critical temperature to modify the properties of PEEK is above 75 °C[24].

PEEK is limited to use in healing abutments or prosthetic dental devices. Further, more complex investigations are needed, including histopathological studies investigating how to improve osseointegration, since PEEK is bioinert[9,10-25]. However, it has been proven that osseointegration occurs in implants with PEEK[26], and surface modification with laser, bioactive materials or chemical treatments has been proposed [27].

The need for further research on protocol bars is confirmed by the fact that the literature is mainly related to overdentures. Corroborating the results of the present research, other studies have reported that structures made of PEEK provide better retention, and lower stress concentration or misfit than those made of Co-Cr alloy[20,28,29]. Clinical and longer-term studies have shown good outcomes and patient satisfaction with PEEK[30]. Despite the lack of studies with protocol bars, the findings mentioned above suggest that PEEK is a promising material for implant dentistry.

In other situations, for example, when the All-on-Four® technique was used, the stress peak was higher for PEEK bars than conventional bars[31]. For zygomatic implants, there was no difference in tension between PEEK and the cobalt-chrome alloy[32]. Compressive strength was lower in PEEK bars than in nickel-chrome bars[16].

The results of this study support the use of PEEK as an alternative for protocol bars, since it promoted a smaller misfit, being a functionally viable option, in addition to being a good aesthetic option, according to other studies[31,33]. The differences between PEEK and cobalt-chrome bars can be explained by their surface features, regarding which the influence of particle size and uniformity, as well as the mechanical properties, have been reported[3]. Moreover, evidence is emerging that PEEK bars improve mastication performance, bite force capacity and occlusal pattern, in addition to providing greater patient satisfaction[34].

The "counter-torque" response variable did not indicate any difference between materials. It is speculated that PEEK promoted the same passivity as the cobalt-chrome alloy, protecting the screw similarly. Like the current study, most studies on PEEK in oral rehabilitation are still experimental. Despite the need for larger long-term clinical studies, it is important to reinforce the evidence of experimental studies that support and increase the safety of using the material in clinical practice, which reinforces the relevance of the present study.

It is concluded that the PEEK protocol bar provided better fit of the mini abutments to the implants, even after mechanical cycling. The counter-torque of the screws was similar in all evaluated scenarios.

DECLARATION OF CONFLICTING INTERESTS
The authors declare no potential conflicts of interest regarding the research, authorship, and/or publication of this article.

REFERENCES

1. Valadas LAR, Oliveira Filho RD, Francischone CE, Lotif MAL, Bandeira MAM, Fonteles MMF, Simões TC, Girão Júnior ACM, Martiniano CRQ. Prospective study of dental implantology related patents in Brazil. African Journal of Biotechnology, 2021; 20(1):9-15. https://doi.org/10.5897/AJB2019.17038

2. Han K-H, Lee J-Y, Shin SW, Han K-H, Lee J-Y, Shin SW. Implant-and Tooth-Supported Fixed Prostheses Using a High-Performance Polymer (Pekkton) Framework. Inter J Prosthodont. 2016;29(5):451-4. Han KH, Lee JY, Shin SW. Implant- and Tooth-Supported Fixed Prostheses Using a High-Performance Polymer (Pekkton) Framework. Int J Prosthodont. 2016 Sep-Oct;29(5):451-4. https://doi.org/10.11607/ijp.4688.

3. Elawadly T, Radi IAW, El Khadem A, Osman RB. Can PEEK Be an Implant Material? Evaluation of Surface Topography and Wettability of Filled Versus Unfilled PEEK With Different Surface Roughness. J Oral Implantol. 2017;43(6):456-61. https://doi.org/10.1563/aaid-joi-D-17-00144

4. Skirbutis G, Dzingutė A, Masiliūnaitė V, Šulcaitė G, Žilinskas J. PEEK polymer's properties and its use in prosthodontics. A review Stomatologija, Baltic Dental and Maxillofacial Journal 2018; 20(2):54-8. https://europepmc.org/article/med/30531169

5. AL-Rabab'ah M, Hamadneh Wa, Alsalem I, Khraisat A, Abu Karaky A. Use of high performance polymers as dental implant abutments and frameworks: a case series report. J Prosthodont. 2019;28(4):365-72. https://doi.org/10.1111/jopr.12639

6. Bathala L, Majeti V, Rachuri N, Singh N, Gedela S. The Role of Polyether Ether Ketone (Peek) in Dentistry - A Review. J Med Life. 2019;12(1):5-9. https://doi.org/10.25122/jml-2019-0003

7. Chaturvedi TP. Allergy related to dental implant and its clinical significance. Clin Cosmet Investig Dent. 2013;5(1):57–61. https://doi.org/10.2147/CCIDE.S35170

8. Agarwal A, Tyagi A, Ahuja A, Kumar N, De N, Bhutani H. Corrosion aspect of dental implants—an overview and literature review. Open Journal of Stomatology. 2014;4(2):56–60. https://doi.org/10.4236/ojst.2014.42010

9. Najeeb S, Zafar MS, Khurshid Z, Siddiqui F. Applications of polyetheretherketone (PEEK) in oral implantology and prosthodontics. J Prosthod Res. 2016;60(1):12–9. https://doi.org/10.1016/j.jpor.2015.10.001

10. Blanch-Martínez N, Arias-Herrera S, Martínez-González A. Behavior of polyether-ether-ketone (PEEK) in prostheses on dental implants. A review. J Clin Exp Dent. 2021;13(5):e520-6. https://doi.org/10.4317/jced.58102

11. Fathy SM, Emera RMK, Abdallah RM. Surface Microhardness, Flexural Strength, and Clasp Retention and Deformation of Acetal vs Poly-ether-ether Ketone after Combined Thermal Cycling and pH Aging. J Contemp Dent Pract. 2021;22(2):140-5. https://www.semanticscholar.org/paper/Surface-Microhardness%2C-Flexural-Strength%2C-and-Clasp-Fathy-Emera/dba526899fbaabcc2b62cc8f1c6be340b59e45e6

12. Micovic D, Mayinger F, Bauer S, Roos M, Eichberger M, Stawarczyk B. Is the high-performance thermoplastic polyetheretherketone indicated as a clasp material for removable dental prostheses? Clin Oral Investig. 2021;25(5):2859-66. https://doi.org/10.1007/s00784-020-03603-y

13. Sahin S; Çehreli MC. The significance of passive framework fit in implant prosthodontics: current status. Implant Dent. 2001;10(2):85-92. https://doi.org/10.1097/00008505-200104000-00003

14. Hamsho R, Mahardawi B, Assi H, Alkhatib H. Polyetheretherketone (PEEK) Implant for the Reconstruction of Severe Destruction in the Maxilla: Case Report. Plast Reconstr Surg Glob Open. 2022;10(8):e4473. https://doi.org/10.1097/GOX.0000000000004473

15. Gonzalez J. The Evolution of Dental Materials for Hybrid Prosthesis. Open Dent J. 2014;8(1):85. https://doi.org/10.2174/1874210601408010085

16. de Carvalho GAP, Franco ABG, Kreve S, Ramos EV, Dias SC, do Amaral FLB. Polyether ether ketone in protocol bars: Mechanical behavior of three designs. Journal of International Oral Health. 2017;9(5):202. https://doi.org/10.4103/jioh.jioh_163_17

17. Wiskott HW, Nicholls JI, Belser UC. Stress fatigue: Basic principles and prosthodontic implications. Int J Prosthodont 1995;8:105–16. http://www.quintpub.com/journals/ijp/abstract.php?article_id=6737#.Y-ByqnbMLIU

18. Markarian RA, Galles DP, Gomes França FM. Scanning Electron Microscopy Analysis of the Adaptation of Single-Unit Screw-Retained Computer-Aided Design/Computer-Aided Manufacture Abutments After Mechanical Cycling. Int J Oral Maxillofac Implants. 2018;33(1):127–36. https://doi.org/10.11607/jomi.5588

19. Schwitalla AD, Abou-Emara M, Zimmermann T, Spintig T, Beuer F, Lackmann J, Müller WD. The applicability of PEEK-based abutment screws. J Mech Behav Biomed Mater. 2016;63(1):244-51. https://doi.org/10.1016/j.jmbbm.2016.06.024

20. Villefort RF, Tribst JPM, Dal Piva AMO, Borges AL, Binda NC, Ferreira CEA, Bottino MA, von Zeidler SLV. Stress distribution on different bar materials in implant-retained palatal obturator. PLoS One. 2020;15(10):e0241589. https://doi.org/10.1371/journal.pone.0241589

21. Frankenberger T, Graw CL, Engel N, Gerber T, Frerich B, Dau M. Sustainable Surface Modification of Polyetheretherketone (PEEK) Implants by Hydroxyapatite/Silica Coating-An In Vivo Animal Study. Materials (Basel). 2021;14(16):4589. https://doi.org/10.3390/ma14164589

22. Peng TY, Shih YH, Hsia SM, Wang TH, Li PJ, Lin DJ, Sun KT, Chiu KC, Shieh TM. In Vitro Assessment of the Cell Metabolic Activity, Cytotoxicity, Cell Attachment, and Inflammatory Reaction of Human Oral Fibroblasts on Polyetheretherketone (PEEK) Implant-Abutment. Polymers (Basel). 2021;13(17):2995. https://doi.org/10.3390/polym13172995

23. Sertgöz A, Güvener S. Finite element analysis of the effect of cantilever and implant length on stress distribution in an implant-supported fixed prosthesis. The Journal of Prosthetic Dentistry. 1996;76(2):165-9. https://doi.org/10.1016/s0022-3913(96)90301-7

24. Brillhart M, Botsis J. Fatigue fracture behaviour of PEEK: 2. Effects of thickness and temperature. Polymer. 1992;33(24):5225-32. https://doi.org/10.1177/073168449301200902

25. Korn P, Elschner C, Schulz MC, Range U, Mai R, Scheler U. MRI and dental implantology: two which do not exclude each other. Biomaterials. 2015;53:634-45. https://doi.org/10.1016/j.biomaterials.2015.02.114

26. Deng Y, Zhou P, Liu X, Wang L, Xiong X, Tang Z, Wei J, Wei S. Preparation, characterization, cellular response and in vivo osseointegration of polyetheretherketone/nano-hydroxyapatite/carbon fiber ternary biocomposite. Colloids Surf B Biointerfaces. 2015;136:64-73. https://doi.org/10.1016/j.colsurfb.2015.09.001

27. Almasi D, Iqbal N, Sadeghi M, Sudin I, Abdul Kadir MR, Kamarul T. Preparation Methods for Improving PEEK's Bioactivity for Orthopedic and Dental Application: A Review. Int J Biomater. 2016;2016:8202653. https://doi.org/10.1155/2016/8202653

28. Mangano F, Mangano C, Margiani B, Admakin O. Combining Intraoral and Face Scans for the Design and Fabrication of Computer-Assisted Design/Computer-Assisted Manufacturing (CAD/CAM) Polyether-Ether-Ketone (PEEK) Implant-Supported Bars for Maxillary Overdentures. Scanning. 2019;2019:4274715. https://doi.org/10.1155/2019/4274715

29. Mangano FG, Marchiori F, Mangano C, Admakin O. Solid index and reverse implant library for the fabrication of a bar for overdenture: a proof of concept. Int J Comput Dent. 2021;24(3):331-343. https://doi.org/10.1155/2019/4274715

30. Abdraboh AE, Elsyad MA, Mourad SI, Alameldeen HE. Milled Bar with PEEK and Metal Housings for Inclined Implants Supporting Mandibular Overdentures: 1-Year Clinical, Prosthetic, and Patient+-Based Outcomes. Int J Oral Maxillofac Implants. 2020;35(5):982-9. https://doi.org/10.11607/jomi.8399

31. Jaros OAL, De Carvalho GAP, Franco ABG, Kreve S, Lopes PAB, Dias SC. Biomechanical Behavior of an Implant System Using Polyether Ether Ketone Bar: Finite Element Analysis. J Int Soc Prev Community Dent. 2018;8(5):446-50. https://doi.org/10.4103/jispcd.JISPCD_183_18

32. Heboyan A, Lo Giudice R, Kalman L, Zafar MS, Tribst JPM. Stress Distribution Pattern in Zygomatic Implants Supporting Different Superstructure Materials. Materials (Basel). 2022;15(14):4953. https://doi.org/10.3390/ma15144953

33. Villefort RF, Diamantino PJS, Zeidler SLVV, Borges ALS, Silva-Concílio LR, Saavedra GDFA, Tribst JPM. Mechanical Response of PEKK and PEEK As Frameworks for Implant-Supported Full-Arch Fixed Dental Prosthesis: 3D Finite Element Analysis. Eur J Dent. 2022;16(1):115-21. https://doi.org/10.1055/s-0041-1731833

34. Montero J, Guadilla Y, Flores J, Pardal-Peláez B, Quispe-López N, Gómez-Polo C, Dib A. Patient-Centered Treatment Outcomes with Full-Arch PEEK Rehabilitation Supported on Four Immediate or Conventionally Loaded Implants. A Randomized Clinical Trial. J Clin Med. 2021;10(19):4589. https://doi.org/10.3390/jcm10194589

gDNA extraction from *Candida albicans* and *Candida dubliniensis* in subgingival samples in Argentina. Evaluation of different methods

Verónica A Dubois[1,2] ⓘ, Pablo A Salgado[1,2,3] ⓘ, Laura A Gliosca[1,2] ⓘ, Susana L Molgatini[1,2] ⓘ

1. Universidad de Buenos Aires. Facultad de Odontología. Hospital Odontológico Universitario. Cátedra de Microbiología y Parasitología, Buenos Aires, Argentina.
2. Universidad de Buenos Aires, Facultad de Odontología, Instituto de Investigaciones en Salud Pública, Buenos Aires, Argentina.
3. Universidad de Buenos Aires, Facultad de Odontología, Hospital Odontológico Universitario, Cátedra de Odontología Preventiva y Comunitaria, Buenos Aires, Argentina.

ABSTRACT

The oral cavity constitutes a unique ecosystem with highly variable ecological niches that harbor a great variety of microorganisms, including yeasts. Molecular methods are currently considered the gold standard for identifying species, although they involve limitations associated with the disruption of yeast cell walls to release the genomic DNA (gDNA) for amplification. **Aim:** The aim of this study was to compare the performance of different methods for extracting gDNA from Candida albicans and Candida dubliniensis, subsequently amplifying DNA by PCR. **Materials and Method:** Fifty-two isolates (16 C. albicans and 36 C. dubliniensis) were obtained from subgingival biofilm of HIV+ patients with clinical signs of periodontal disease. The study evaluated 6 gDNA extraction methods and two PCR amplification methods. Furthermore, the presence of alleles of HWP1 gene was determined in C. albicans. **Results:** Comparisons of six methods show statistically significant differences (p<0.001) except for C. albicans in two of them. For C. dubliniensis, statistical differences were observed in all comparisons. Commercial methods were more efficient for concentrating gDNA than in-house methods, and both PCRs were effective. Ten heterozygous C. albicans isolates for this allele were positive for the HWP1-1 / HWP1-2 allele, one was homozygous for Wild Type HWP1-1 allele, and 5 were homozygous for novel/rare HWP1-2 allele. **Conclusions:** This study aims to provide simple, inexpensive strategies for phenotypic identification and molecular confirmation of Candida albicans and Candida dubliniensis for non-reference laboratories with low complexity and/or low budgets.

Keywords: Candida albicans - Candida dubliniensis - gDNA - PCR - qPCR - subgingival samples.

Evaluación de diferentes métodos de extracción de gADN en *Candida albicans* y *Candida dubliniensis* en muestras subgingivales en Argentina

RESUMEN

La cavidad oral constituye un ecosistema único con nichos ecológicos muy variables, capaz de albergar una gran variedad de microorganismos, incluidas las levaduras. Los métodos moleculares son considerados actualmente los métodos de identificación definitivos ya que a diferencia de los anteriores, nos brindan una correcta sensibilidad y especificidad. Sin embargo, existen limitaciones asociadas con la ruptura de las paredes celulares de estas levaduras para liberar el ADN genómico (gADN) necesario para la amplificación. **Objetivo:** El objetivo de este estudio fue comparar el rendimiento de diferentes métodos de extracción de gADN de Candida albicans y Candida dubliniensis, amplificando posteriormente por PCR. **Materiales y Método:** Se estudiaron 52 aislamientos, 16/52 de Candida albicans y 36/52 de Candida dubliniensis obtenidos de biofilm subgingival de pacientes VIH+ con signos clínicos de enfermedad periodontal. Se evaluaron seis métodos de extracción de gADN y la posterior amplificación se realizó por dos técnicas de PCR. Además en C. albicans se determinó la presencia de alelos para el gen HWP1. **Resultados:** Las comparaciones de seis métodos son estadísticamente significativas (p<0,001) excepto para C. albicans en dos de ellos. Para C. dubliniensis se observaron diferencias estadísticas en todas las comparaciones. Los métodos comerciales mostraron una mayor eficiencia en la concentración de gADN que los métodos caseros y ambos fueron efectivos en las dos PCR. 10 aislados de C. albicans resultaron positivos para el alelo HWP1-1/HWP1-2, siendo heterocigotos para este alelo. Solo un aislamiento fue homocigoto para el alelo HWP1-1 de tipo salvaje y 5 eran homocigotos para el alelo HWP1-2 nuevo/raro. **Conclusiones:** Este estudio tiene como objetivo proporcionar estrategias simples y económicas para la identificación fenotípica y confirmación molecular de Candida albicans y Candida dubliniensis para laboratorios de no referencia con baja complejidad y/o bajo presupuesto económico.

Palabras clave: Candida albicans - Candida dubliniensis - gADN - PCR - qPCR - muestras subgingivales.

INTRODUCTION

The human oral cavity is a unique ecosystem with a great variety of ecological niches that can be colonized by microorganisms, including yeasts[1].

The advent of techniques based on DNA sequencing has enabled phylogenetic recognition of yeast species considered cryptic phylogenetically close. They were *Candida albicans*, *Candida dubliniensis* and *Candida africana*[2,3].

Correct identification of these cryptic species in a clinical setting is relevant from an epidemiological and medical standpoint, and to better understand evolution of antifungal resistance. Moreover, rapid identification is crucial to clinical treatment of local or systemic candidiasis. There are different phenotypic methods for distinguishing species, but they are laborious, time-consuming and do not provide definitive confirmation. In contrast, molecular methods are currently considered the gold standard since, unlike phenotypic methods, they provide appropriate sensitivity and specificity. [4,5,6]

There are still limitations associated with rupture of yeast walls to release gDNA for amplification. Due to the complex structure of fungal cell wall, it is difficult to produce cell lysis, which limits the sensitivity of PCR assays. In addition, the fungal load of *Candida* spp. in colonized sites is relatively low[7]. With the advent of commercial extraction kits, quality and quantity of DNA obtained has greatly improved. However, not all low-complexity laboratories can afford to purchase them for routine diagnosis.

In our experience, *C. dubliniensis* has been the species most frequently recovered from oral samples, probably due to the selective pressure caused by the administration of antifungal agents, since *C dubliniensis* has higher susceptibility profiles than *C albicans*. In order to identify these species correctly, we needed to find a simple method for rupturing the cell wall[4,8].

The aim of this study was to compare the performance of different methods for extracting gDNA from *Candida albicans* and *Candida dubliniensis*, subsequently amplifying DNA by PCR and Real Time PCR for correct molecular identification.

MATERIALS AND METHODS

This study analyzed 52 *Candida albicans* and *Candida dubliniensis* isolates obtained from subgingival biofilm from patients living with HIV with clinical signs of periodontal disease[;10], who were under high-activity antiretroviral treatment (HAART) but were not receiving antibiotic or antifungal treatment[4,8]. Informed consent was obtained according to the Declaration of Helsinki. The project and informed consent were approved by the Facultad de Odontología, Universidad de Buenos Aires (FOUBA) Ethics Committee, 023/2019-CETICA-FOUBA.

All diagnoses and treatments were conducted at the periodontics service of the High-Risk Patients Oral Care Unit (CLAPAR I), Facultad de Odontología, Universidad de Buenos Aires; Hospital general de agudos Dr. Juan A. Fernández", and Hospital de Infecciosas Francisco Javier Muñiz. Patients voluntarily signed an Informed Consent after receiving an explanation of dental practices and benefits of participating in the protocol. Subgingival *biofilm* samples were collected using the protocol described by Gliosca et al.[8].

Phenotypic methods were compared with molecular ones to identify the isolations at species level.

Phenotypic methods

Samples were seeded on CHROMagar Candida® at 37 ºC, 48 h in aerophilic conditions for presumptive identification of *Candida albicans, Candida dubliniensis* and *Candida africana*[11]. Green colonies were isolated on Sabouraud Dextrose Agar (SDA) at 37 ºC, 24 h in aerophilic conditions to perform phenotypic identification tests.

Microcultures were done on:

a) Milk agar with 1% tween 80 for germ-tube production at 37 ºC, 3h, and pseudomycelium-mycelium and chlamydospores at 28 ºC, 48 h.[12,13]

b) Cornmeal agar with 1% tween 80 for formation of pseudomycelium-mycelium and chlamydospores at 30 ºC, 48 h.[14]

c) Staib agar to assess morphology of colonies and chlamydospores at 30 ºC, 72 h[15].

Growth capacity at 45 °C and in hypertonic medium were determined on SDA 48 h[16,17], and SDA with NaCl 6% at 37 ºC, 96 h[18].

gDNA extraction methods

Six different methods were evaluated to determine their performance in obtaining *C. albicans* and *C. dubliniensis* gDNA. In all cases (in-house and commercial kits), a

single colony was taken from a 24-hour fresh culture on yeast peptone dextrose agar (YPD) to obtain the fungal gDNA. The spectrometric quantification of gDNAs was measured by triplicate in Nanodrop Biotek® and their quality was estimated considering the ratio of the readings at 260/280 nm (acceptable values between 1.7 and 2.0). Pure DNA concentrations were normalized to 1 ng/µl for use in all PCR reactions.

In-house cell disruption methods

-MET 1: A single colony was suspended in 100 µl of ddH$_2$O (double distilled water), heated at 100 °C for 15 minutes, centrifuged at 14,000 g for 3 minutes, and the supernatant was used subsequently.

-MET 2: A single colony was suspended in 100 µl of ddH$_2$O supplemented with zymolase 1000 U Zymoresearch®, incubated at 37 °C for 60 minutes, centrifuged at 14,000 g for 3 minutes, and the supernatant was separated to be used subsequently.

-MET 3: A single colony was suspended in 100 µl of ddH$_2$O, twofold heating (100 ºC) and freezing (-20 ºC for 2 minutes), followed by centrifuge at 14,000 g for 3 minutes, and the supernatant was used subsequently[19].

-MET 4: The method described by Marko Lõoke et al.[20] was applied, using lithium acetate (LiOAc) and dodecyl sodium sulfate (SDS) 1% to disrupt the cell wall.

Commercials kit methods

-MET 5: Yeast Genomic DNA Kit (Zymo Research®) was used following the manufacturer's instructions.

-MET 6: Presto TM Mini gDNA Bacteria (Geneaid®) was used following the manufacturer's instructions, but with some adaptations to enable it is used with oral samples and to recover both bacteria and yeasts. Zymolase 1000 U Zymoresearch® was added in the lysis step, incubating at 37 °C for 60 minutes; 20 µl of proteinase k was added, incubating at 60 °C for 20 minutes and eluting twice in a final volume of 75 µl.

Molecular amplifications

For all 6 extraction methods, two PCR amplification techniques were used: PCR and Real Time PCR (qPCR).

Multiplex qPCR of the ITS regions

Two species-specific primers derived from the internally transcribed spacer (ITS) region (comprising the ITS1, 5.8s rRNA and ITS2 regions) were used as described by Asadzadeh et al.[21] with some modifications according to Dubois et al. 2020[4]. Master mix was adjusted to 2X SYBR Green Supermix in a 10 µl final volume, 10 µM of each primer, and 1 µl of gDNA, in a thermal cycler CFX96 C1000 Touch (BioRad®). Cycling conditions consisted of denaturation at 95 °C for 5 minutes, followed by 39 amplification cycles at 95 °C for 15 seconds, 60 °C for 30 seconds, 65 °C for 5 minutes, and 95 °C for 5 minutes. Amplification process was evaluated using MCA (melting curve analysis) for *C. albicans* 86 ºC (+0.5) and *C. dubliniensis* 82 ºC (+ 0.5).

Multiplex PCR of HWP1 gene

To optimize the HWP1 gene detection strategies, concentrations and final volume of protocol described by Romeo 2008[22] were adjusted in a final reaction of 25 µl: Buffer 10X, dNTPs 0.2 mM each, primers 25 uM each.

Similarly, performance was evaluated for two different polymerases (PFU polymerase DSBIO 2.5 U/µl and EasyTaq® DNA Polymerase U/µl, with added SO4 Mg^{++} 20mM), gDNA 1 µl in a thermocycler Aeris-BG096 (Esco Micro®). Cycling conditions consisted of denaturation at 95 ºC for 5 minutes, followed by 30 amplification cycles at 94 ºC for 45 seconds, 58 ºC for 40 seconds, 72 ºC for 60 seconds, and 72 ºC for 10 minutes. PCR amplification products were separated by electrophoresis using 1.3% agarose gel in 1X TAE buffer with GelGreen™ (Biotium®) and visualization was performed using the Gel DocTM XR + Imaging System (Biorad®).

Presence of alleles of the HWP1 gene was evaluated according to size of fragments for *C. albicans*, one of them of 941 bp fragment being homozygous for wild-type HWP1-1 allele, an other of 839 bp fragment being homozygous for novel/rare HWP1-2 allele, and the last one with two fragments of 941 and 839 bp being heterozygous for HWP1-1/ HWP1-2 allele[22,23].

For both phenotypic and genotypic identification, reference strains of *C. albicans* ATCC 10231 and *C. dubliniensis* CD36 were used as positive controls, and *C. parapsilosis* ATCC 22019 as negative control.

Statical analysis

For all isolates, an analysis of variance (ANOVA)

was performed for the 6 extraction methods and Tukey's post hoc was applied when the results were statistically significant. In addition to means and standard deviation, the standard error and 95% confidence interval were calculated.

RESULTS

In this study, 52 yeast isolates were identified by PCR and qPCR, of which 16 were *C. albicans* and 36 were *C.dubliniensis*.

Five replicates of each gDNA extraction method were performed per isolate. Tukey's post hoc, mean concentrations, their respective standard deviation (std) and the standard error for all methods are shown in Tables 1 and 2.

Table 1. Disruption techniques

n=5 replicates		gDNA	
		C. albicans	*C. dubliniensis*
		mean CC ng/ul ± SD	mean CC ng/ul ± SD
Heating	MET 1	4.50 ± 0.98	4.75 ± 0.78
Zymolase- ddH2O	MET 2	58.00 ± 0.81	73.22 ± 0.87
Heating-freezing	MET 3	4.25 ± 0.98	3.09 ± 0.96
LiOAC / SDS	MET 4	39.75 +0.87	35.75 +0.92
Kit Zymo Research®	MET 5	26.45 +0.42	34.58 +0.33
Kit Geneaid®	MET 6	22.36 +0.28	24.25 +0.32

CC: Concentration; gDNA: Genomic DNA; ddH2O: double distilled water; LiOAC: Lithium acetate; SDS: Dodecyl sodium sulfate; MET: Method.

Table 2. Molecular techniques

		C. albicans (n=16)	*C. dubliniensis* (n=36)
		Frequency (%)	Frequency (%)
MET 1	PCR	0 (0.0%)	36 (100.0%)
	qPCR	16 (100.0%)	36 (100.0%)
MET 2	PCR	16 (100.0%)	36 (100.0%)
	qPCR	16 (100.0%)	36 (100.0%)
MET 3	PCR	8 (50.0%)	0 (0.0%)
	qPCR	16 (100.0%)	36 (100.0%)
MET 4	PCR	16 (100.0%)	36 (100.0%)
	qPCR	16 (100.0%)	36 (100.0%)
MET 5	PCR	16 (100.0%)	36 (100.0%)
	qPCR	16 (100.0%)	36 (100.0%)
MET 6	PCR	16 (100.0%)	36 (100.0%)
	qPCR	16 (100.0%)	36 (100.0%)

MET: Method; PCR: Endpoint Polymerase chain reaction; qPCR: Real-Time Polymerase chain reaction.

Results of the comparisons are statistically significant ($p<0.001$) except for *C. albicans* in MET1 with MET3. Commercial methods were more efficient for concentrating gDNA than in-house methods, although MET 2 and MET 4 provided acceptable yields. Regarding the subsequent amplification, for *C. albicans,* the use of zymolase in ddH$_2$O and LiOAc - SDS were the most effective in-house methods in PCR (100%). In qPCR, the least effective methods were heating (0%) and heating - freezing (0%) with mean melting temperature 84 ºC and std 1.5, followed by LiOAC - SDS with mean melting temperature 85 ºC and std 0.7.

For *C. dubliniensis,* statistical differences were observed in all comparisons. All in-house methods except heating followed by freezing enabled identification, though clear bands in 1.3% agarose gel were better with zymolase in ddH$_2$O, and LiOAC - SDS in PCR. For qPCR, all methods enabled identification, but the least effective regarding melting temperature were heating followed by freezing and LiOAC - SDS, with mean 81.8 and std 0.9 and 0.3, respectively. Two commercial kits were equally effective for both species in both PCRs (Figs. 1 and 2; Table 3).

Alleles of HWP1 gene in *C. albicans*

EasyTaq® polymerase enzyme performed best for genotyping alleles. Of 16 isolates, 10 were positive for HWP1-1 / HWP1-2 allele, with 2 bands of 941 and 839 bp fragments, being heterozygous for this allele.

One isolate gave a band of 941 bp, being homozygous for Wild Type HWP1-1 allele, and the other 5 gave a band of 839 bp, being
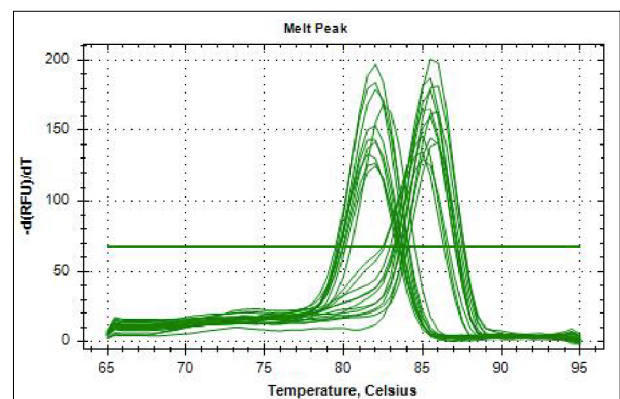

Fig. 1: Melting point of C. albicans *86°C (+0.5) and* C. dubliniens *82° C (+0.5) using as extraction method heating at 100ºC in qPCR.*
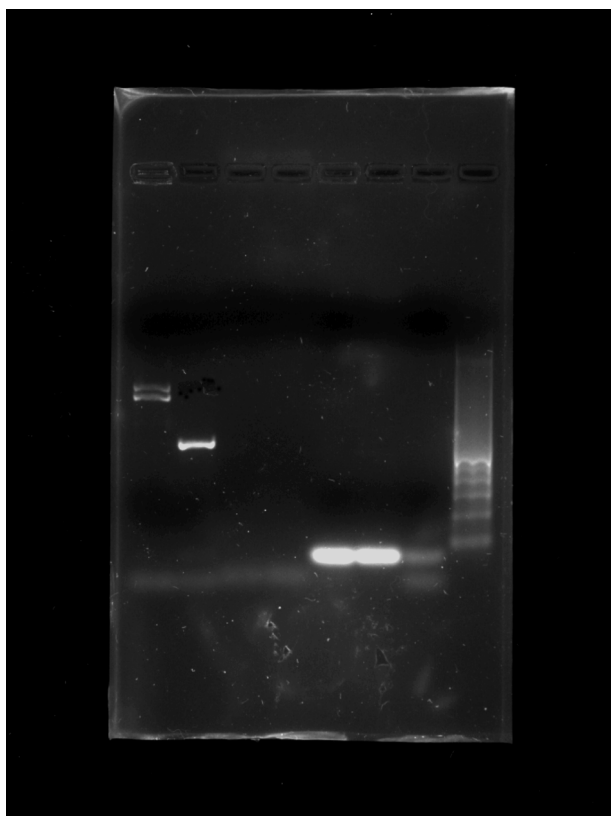
Fig. 2: 1.3% agarose gel in TAE buffer (Tris, Acetic Acid, EDTA). Block 8: Ladder 100 pb. Lane 1 positive strain for Candida albicans*, lane 2 positive strain for* Candida dubliniensis *lanes 3, 4, 5, 6 negative strains, lane 7 negative control.*

Table 3

		C. albicans Frequency (%)	*C. dubliniensis* Frequency (%)
Heating PCR	Yes	0 (0.0%)	36 (100.0%)
	No	16 (100.0%)	0 (0.0%)
Heating-freezing PCR	Yes	8 (50.0%)	0 (0.0%)
	No	8 (50.0%)	36 (100.0%)
Kit Zymo Research® PCR	Yes	16 (100.0%)	36 (100.0%)
	No	0 (0.0%)	0 (0.0%)
Kit Geneaid® PCR	Yes	16 (100.0%)	36 (100.0%)
	No	0 (0.0%)	0 (0.0%)
Zymolase- ddH$_2$O PCR	Yes	16 (100.0%)	36 (100.0%)
	No	0 (0.0%)	0 (0.0%)
LiOAC PCR	Yes	16 (100.0%)	36 (100.0%)
	No	0 (0.0%)	0 (0.0%)
Heating qPCR	Yes	16 (100.0%)	36 (100.0%)
	No	0 (0.0%)	0 (0.0%)
Heating-freezing qPCR	Yes	16 (100.0%)	36 (100.0%)
	No	0 (0.0%)	0 (0.0%)
Kit Zymo Research® qPCR	Yes	16 (1)	36 (100.0%)
	No	0 (0.0%)	0 (0.0%)
Kit Geneaid® qPCR	Yes	16 (1)	36 (100.0%)
	No	0 (0.0%)	0 (0.0%)
Zymolase- ddH O qPCR	Yes	16 (100.0%)	36 (100.0%)
	No	0 (0.0%)	0 (0.0%)
LiOAC qPCR	Yes	16 (100.0%)	36 (100.0%)
	No	0 (0.0%)	0 (0.0%)

homozygous for novel/rare HWP1-2 allele. Reference *C. albicans* 10231 presented two fragments, 941 and 839 bp, being heterozygous for HWP1-1/HWP1-2 allele.

Regarding presumptive phenotypic identification methods, only microculture in Staib agar enabled differentiation of *C. dubliniensis* isolates (Table 4).

DISCUSSION
C. albicans and *C. dubliniensis* share many phenotypic and biochemical characteristics. Presumptive identification by these methods used routinely in low-complexity laboratories continues to be a problem because they do not provide definitive identification data. Distinction between these two species is important in terms of treatment, in order to understand the clinical and epidemiological significance of the role played by *C. dubliniensis* in human infections[4,5,22,24-27].

Although *C. dubliniensis* is often isolated from oral samples in Argentina[4,8,24,26], phenotypic characterization underestimates it, and it is reported mostly as *C. albicans*. In agreement with Livério et al. 2017, none of the phenotypic tests alone, proved to be highly effective for conclusive identification of these species[27].
Molecular techniques are more sensitive and specific, but cell wall lysis is the main obstacle to efficient gDNA recovery. Conventional methods using enzymes for chemical rupture or glass beads for physical rupture, generally followed by lysis with detergents, are time-consuming and costly for application to many samples. Moreover, methods that use phenol-chloroform are hazardous to health unless used in suitable conditions[20].
Most phenotypic methods provide unsatisfactory results (false positives and negatives), so the most appropriate methods are polymerase chain reaction

Table 4. Phenotype techniques

		C. albicans n= 16		*C. dubliniensis* n= 36	
		Frequency	%	Frequency	%
CHROMagar Candida®	light green	11	68.75%	18	50.0%
	dark green	5	31.25%	13	36.1%
	white	0	0.00%	5	13.9%
Milk agar 3 h Germ-tube	yes	16	100%	32	88.9%
	no	0	0.00%	4	11.1%
Milk agar 3 h mycelium	yes	0	0.00%	6	16.7%
	no	16	100%	30	83.3%
Milk agar 24 h mycelium	yes	10	62.5%	32	88.9%
	no	6	37.5%	4	11.1%
Milk agar 24 h chlamydospores	yes	7	43.75%	29	80.6%
	no	9	56.25%	7	19.4%
Milk agar 48 h mycelium	yes	12	75.0%	33	91.7%
	no	4	25.0%	3	8.3%
Milk agar 48 h chlamydospores	yes	9	56.25%	32	88.9%
	no	7	43.75%	4	11.1%
CMA agar 24 h mycelium	yes	15	93.75%	36	100%
	no	1	6.25%	0	0.0%
CMA agar 24 h chlamydospores	yes	11	68.75%	28	77.8%
	no	5	31.25%	8	22.2%
CMA agar 48 h mycelium	yes	15	93.75%	36	100%
	no	1	6.25%	0	0%
CMA agar 48 h chlamydospores	yes	12	75.0%	29	80.6%
	no	4	25.0%	7	19.4%
Staib agar 24 h	rough colonies	1	6.25%	35	97.2%
	smooth colonies	15	93.75%	1	2.8%
Staib agar 48 h	rough colonies	1	6.25%	36	100%
	smooth colonies	15	93.75%	0	0%
SDA 45°C	yes	11	68.75%	19	52.78%
	no	5	31.25%	17	47.22%
NaCl 6.5%	yes	12	75.0%	27	75.0%
	no	4	25.0%	9	25.0%

h: Hours; SDA: Sabouraud dextrose agar; NaCl: Sodium chloride; CMA: Corn Meal agar

(PCR), mass spectrometry (MALDI-TOF) and sequencing genomics[18].

It is important to bear in mind that one of the main limitations in the use of PCR techniques to identify *Candida* spp. is that there is no consensus on the methods for cell wall rupture[29]. However, molecular methods provide conclusive identification, and are fast and accurate, though they are more expensive and require specific equipment[27].

Routine identifications, such as different phenotypic methods and amplification of the ITS regions, do not discriminate properly among the 3 species, underestimating *C. africana* and *C. dubliniensis*. However, due to polymorphism of the HWP1 gene, its amplification by PCR enables these species to be distinguished with greater certainty[30].

The qPCR technique based on melting curves analyzed with SYBR Green is a simple, fast method to distinguish *C. albicans* from *C. dubliniensis* through the ITS1 and ITS2 regions, but not for *C.*

africana[21]. Our study did not isolate *C. africana* from subgingival samples.

In 2009, a second allele for the HWP1 gene with 850 bp was described in *C. albicans*[23]. Shan et al. reported that *C. albicans* produced two DNA fragments, demonstrating that *C. albicans* isolates were heterozygous at the HWP1 locus[31]. Fontecha et al. 2019 found that most of their isolates were heterozygous, concluding that the HWP1 gene could be considered a good marker for identifying cryptic species in this complex[5], while a study in 2017 reported found 5 different genotypes[30], which provides a pattern of polymorphism presented by this gene.

CONCLUSIONS

This study aims to provide simple, inexpensive strategies for phenotypic identification and molecular confirmation of *Candida albicans* and *Candida dubliniensis* for non-reference laboratories with low complexity and/or low budgets.

The advantages of in-house extraction methods used in this study are based on their simplicity, use of minimal amounts of reagents, shorter identification time and avoiding the use of enzymes, phenol and glass beads.

The simplest, cheapest and most effective methods were heating at 100 °C for qPCR and the use of LiOAc - SDS for PCR.

REFERENCES

1. Jabra-Rizk MA, Ferreira SM, Sabet M, Falkler WA, Merz WG, Meiller TF. Recovery of Candida dubliniensis and other yeasts from human immunodeficiency virus-associated periodontal lesions. J Clin Microbiol. 2001 Dec;39(12):4520-2. https://doi.org/10.1128/JCM.39.12.4520-4522.2001

2. Brandt ME, Lockhart SR. Recent Taxonomic Developments with Candida and Other Opportunistic Yeasts. Curr Fungal Infect Rep. 2012 Sep;6(3):170-177. https://doi.org/10.1007/s12281-012-0094-x

3. Taylor JW, Jacobson DJ, Kroken S, Kasuga T, Geiser DM, Hibbett DS, Fisher MC. Phylogenetic species recognition and species concepts in fungi. Fungal Genet Biol. 2000 Oct;31(1):21-32. https://doi.org/10.1006/fgbi.2000.1228

4. Dubois VA, González MI, Martínez ME, Fedelli L, Lamas S, D Eramo LR et al. Enzyme production by Candida albicans and Candida dubliniensis in periodontal HIV-positive patients receiving and not receiving antiretroviral therapy. Acta Odontol Latinoam. 2020 Sep 1;33(2):104-111. http://www.scielo.org.ar/scielo.php?script=sci_arttext&pid=S1852-48342020000200104

5. Fontecha G, Montes K, Ortiz B, Galindo C, Braham S. Identification of Cryptic Species of Four Candida Complexes in a Culture Collection. J Fungi (Basel). 2019 Dec 17;5(4):117. https://doi.org/10.3390/jof5040117

6. Neppelenbroek KH, Seó RS, Urban VM, Silva S, Dovigo LN, Jorge JH, Campanha NH. Identification of Candida species in the clinical laboratory: a review of conventional, commercial, and molecular techniques. Oral Dis. 2014 May;20(4):329-44. https://doi.org/10.1111/odi.12123

7. Metwally L, Fairley DJ, Coyle PV, Hay RJ, Hedderwick S, McCloskey B, O'Neill HJ, Webb CH, McMullan R. Comparison of serum and whole-blood specimens for the detection of Candida DNA in critically ill, non-neutropenic patients. J Med Microbiol. 2008 Oct;57 (Pt 10):1269-1272. https://doi.org/10.1099/jmm.0.2008/002444-0

8. Gliosca LA, D Eramo LR, Bozza FL, Soken L, Abusamra L, Salgado PA, et al. Microbiological study of the subgingival biofilm in HIV+/HAART patients at a specialized dental service. Acta Odontol Latinoam. 2019 Dec 1;32(3):147-155. http://www.scielo.org.ar/scielo.php?script=sci_abstract&pid=S1852-48342019000300147

9. Papapanou PN, Sanz M, Buduneli N, Dietrich T, Feres M, Fine DH, et al. Periodontitis: Consensus report of workgroup 2 of the 2017 World Workshop on the Classification of Periodontal and Peri-Implant Diseases and Conditions. J Periodontol. 2018 Jun;89 Suppl 1:S173-S182. https://doi.org/10.1002/JPER.17-0721

10. Tonetti MS, Greenwell H, Kornman KS. Staging and grading of periodontitis: Framework and proposal of a new classification and case definition. J Clin Periodontol. 2018 Jun;45 Suppl 20:S149-S161. Erratum in: J Clin Periodontol. 2019 Jul;46(7):787 https://doi.org/10.1111/jcpe.12945

11. Odds F, Bernaerts R. CHROMagar Candida, a new differential isolation medium for presumptive identification of clinically important Candida species. J Clin Microbiol 1994; 32: 1924-29. https://doi.org/10.1128/jcm.32.8.1923-1929.1994

12. Pineda G, Scollo K, Santiso G, Lehmann E, et al. Aislamiento de Candida dubliniensis en distintos materiales clínicos. Análisis de métodos fenotípicos de diferenciación con Candida albicans. Rev. Argent. Microbiol 2008; 40: 211-17. http://www.scielo.org.ar/scielo.php?pid=S0325-75412008000400006&script=sci_arttext&tlng=en

13. Jitsurong S, Kiamsiri S, Pattararangrong N. New milk medium for germ tube and chlamydoconidia production by Candida albicans. Mycopathologia. 1993 Aug;123(2):95-8. https://doi.org/10.1007/BF01365086

14. Sullivan DJ, Westerneng TJ, Haynes KA, Bennett DE, Coleman DC. Candida dubliniensis sp. nov.: phenotypic and molecular characterization of a novel species associated with oral candidosis in HIV-infected individuals. Microbiology (Reading). 1995 Jul;141 (Pt 7):1507-21. https://doi.org/10.1099/13500872-141-7-1507

15. Staib P, Morschhäuser J. Chlamydospore formation on Staib agar as a species-specific characteristic of Candida dubliniensis. Mycoses. 1999;42(9-10):521-4. https://doi.org/10.1046/j.1439-0507.1999.00516.x.

16. Coleman DC, Sullivan DJ, Bennett DE, Moran GP, Barry HJ, Shanley DB. Candidiasis: the emergence of a novel species, Candida dubliniensis. AIDS. 1997 Apr;11(5):557-67. https://doi.org/10.1097/00002030-199705000-00002

17. Gales AC, Pfaller MA, Houston AK, Joly S, Sullivan DJ, Coleman DC, Soll DR. Identification of Candida dubliniensis based on temperature and utilization of xylose and alpha-methyl-D-glucoside as determined with the API 20C AUX and vitek YBC systems. J Clin Microbiol. 1999 Dec;37(12):3804-8. https://doi.org/10.1128/JCM.37.12.3804-3808.1999

18. Alves SH, Milan EP, de Laet Sant'Ana P, Oliveira LO, Santurio JM, Colombo AL. Hypertonic sabouraud broth as a simple and powerful test for Candida dubliniensis screening. Diagn Microbiol Infect Dis. 2002 May;43(1):85-6. https://doi.org/10.1016/s0732-8893(02)00368-1

19. Silva GA, Bernardi TL, Schaker PD, Menegotto M, et al. Rapid yeast DNA extraction by boiling and freeze-thawing without using chemical reagents and DNA purification. Braz Arch Biol Technol 2012; 55: 319–27. https://www.scielo.br/j/babt/a/VxDCyKfcKdpGJnBQhmSJwVd/?lang=en

20. Lõoke M, Kristjuhan K, Kristjuhan A. Extraction of genomic DNA from yeasts for PCR-based applications. Biotechniques. 2011 May;50(5):325-8. https://doi.org/10.2144/000113672

21. Asadzadeh M, Ahmad S, Al-Sweih N, Khan Z. Rapid and Accurate Identification of Candida albicans and Candida dubliniensis by Real-Time PCR and Melting Curve Analysis. Med Princ Pract. 2018;27(6):543-548. https://doi.org/10.1159/000493426

22. Romeo O, Criseo G. First molecular method for discriminating between Candida africana, Candida albicans, and Candida dubliniensis by using hwp1 gene. Diagn Microbiol Infect Dis. 2008 Oct;62(2):230-3. https://doi.org/10.1016/j.diagmicrobio.2008.05.014

23. Padovan AC, Chaves GM, Colombo AL, Briones MR. A novel allele of HWP1, isolated from a clinical strain of Candida albicans with defective hyphal growth and biofilm formation, has deletions of Gln/Pro and Ser/Thr repeats involved in cellular adhesion. Med Mycol. 2009 Dec;47(8):824-35. https://doi.org/10.3109/13693780802669574

24. Albaina O, Sahand IH, Brusca MI, Sullivan DJ, et al. Identification and characterization of nine atypical Candida dubliniensis clinical isolates. J Med Microbiol 2015; 64: 147-156. https://doi.org/10.1186/s12879-018-3381-5

25. Al-Tekreeti ARA, Al-Halbosiy MMF, Dheeb BI, Hashim AJ, et al. Molecular identification of clinical Candida isolates by simple and randomly amplified polymorphic DNA-PCR. Arab J Sci Eng 2018; 43: 163-170. https://doi.org/10.3389/fcimb.2022.953302

26. Isla MG, Murisengo OA, Szusz W, Vivot W, Davel G. Prevalence of Candida dubliniensis fungemia in Argentina: identification by a novel multiplex PCR and comparison of different phenotypic methods. Mycopathologia. 2011 Nov;172(5):407-14. https://doi.org/10.1007/s11046-011-9450-6

27. Livério HO, Ruiz LDS, Freitas RS, Nishikaku A, et al. Phenotypic and genotypic detection of Candida albicans and Candida dubliniensis strains isolated from oral mucosa of AIDS pediatric patients. Rev Inst Med Trop Sao Paulo 2017; 13:59:14. https://doi.org/10.1590/S1678-9946202062032

28. Mahelová M, Růžička F. Methods of Candida dubliniensis identification and its occurrence in human clinical material. Folia Microbiol (Praha). 2017 Sep;62(5):401-408. https://doi.org/10.1007/s12223-017-0510-2

29. Metwally L, Fairley DJ, Coyle PV, Hay RJ, Hedderwick S, McCloskey B, O'Neill HJ, Webb CH, Elbaz W, McMullan R. Improving molecular detection of Candida DNA in whole blood: comparison of seven fungal DNA extraction protocols using real-time PCR. J Med Microbiol. 2008 Mar;57(Pt 3):296-303. https://doi.org/10.1099/jmm.0.47617-0

30. Ngouana TK, Krasteva D, Drakulovski P, Toghueo RK, Kouanfack C, Ambe A, et al. Investigation of minor species Candida africana, Candida stellatoidea and Candida dubliniensis in the Candida albicans complex among Yaoundé (Cameroon) HIV-infected patients. Mycoses. 2015 Jan;58(1):33-9. https://doi.org/10.1111/myc.12266

31. Shan Y, Fan S, Liu X, Li J. Prevalence of Candida albicans-closely related yeasts, Candida africana and Candida dubliniensis, in vulvovaginal candidiasis. Med Mycol. 2014 Aug;52(6):636-40. https://doi.org/10.1093/mmy/myu003

Effect of chemical or mechanical finishing/polishing and immersion in staining solutions on the roughness, microhardness, and color stability of CAD-CAM monolithic ceramics

Mauro GA Brito [ID], Flávia LB Amaral [ID], Cecília P Turssi [ID], Roberta TB Hofling [ID], Fabiana MG França [ID]

Instituto e Centro de Pesquisas Odontológicas São Leopoldo Mandic, Dental Materials department, Campinas, Brazil.

ABSTRACT

During the manufacture of ceramic restorations there is an important step of finishing and polishing and the effects of different types of these procedures on the surface characteristics of ceramics are not known for sure. **Aim:** *To evaluate the effects of various surface treatments and immersion in coloring substances on the roughness, microhardness, and color stability of CAD-CAM monolithic ceramics.* **Materials and Method:** *The ceramics used were lithium disilicate reinforced with zirconium dioxide (Suprinity), lithium disilicate (E.max) or leucite (Empress). They were subjected to two surface treatments: glazing (group G) (n=20) or mechanical polishing (group P) (n=20). Then they were divided into two subgroups (n=10) to be treated with the staining substance (coffee or water). Roughness, microhardness and color were measured before and after treatment. Data were subjected to analysis of variance and multiple comparisons were performed with Tukey tests at 5% significance level.* **Results:** *Roughness was lower in all tested ceramics after polishing than after glazing. Microhardness was the same for polished and glazed E.max, higher in glazed than polished Empress, and higher in polished than glazed Suprinity. Analysis of the effects of glazing and polishing on the individual ceramics showed that the ΔE2000 and ΔWID data of the E.max ceramic subjected to polishing showed greater change. Mechanical polishing is a good option for surface treatment of monolithic ceramics.* **Conclusion:** *Glazing was inferior and less satisfactory than polishing. Glazing generates changes that can lead to color instability.*

Keywords: ceramics - dental polishing - materials testing.

Efeito do acabamento/polimento químico ou mecânico e imersão em soluções manchantes na rugosidade, microdureza e estabilidade da cor em cerâmicas monolíticas CAD-CAM

RESUMO

Durante a confecção de restaurações cerâmicas existe uma importante etapa dos procedimentos de acabamento e polimento. Os efeitos de diferentes tipos desses procedimentos nas características superficiais das cerâmicas não são conhecidos com certeza. **Objetivo:** *Avaliar os efeitos de vários tratamentos de superfície e imersão em substâncias corantes na rugosidade, microdureza e estabilidade de cor de cerâmicas monolíticas CAD-CAM.* **Materiais e Métodos:** *As cerâmicas utilizadas foram dissilicato de lítio reforçado com dióxido de zircônio (Suprinity), dissilicato de lítio (E.max) ou leucita (Empress). Foram submetidos a dois tratamentos de superfície: glazeamento (grupo G) (n=20) ou polimento mecânico (grupo P) (n=20). Em seguida, foram divididos em dois subgrupos (n=10) para serem tratados com a substância corante (café ou água). Rugosidade, microdureza e cor foram medidas antes e após o tratamento. Os dados foram submetidos à análise de variância e as comparações múltiplas foram realizadas com testes de Tukey ao nível de 5% de significância.* **Resultados:** *A rugosidade foi menor em todas as cerâmicas testadas após o polimento do que após o glazeamento. A microdureza foi a mesma para o E.max polido e vidrado, maior no Empress vidrado do que no polido, e maior no Suprinity polido do que no vidrado. A análise dos efeitos do esmaltação e polimento nas cerâmicas individuais mostrou que os dados ΔE2000 e ΔWID da cerâmica E.max submetida ao polimento apresentaram maior alteração. O polimento mecânico é uma boa opção para o tratamento superficial de cerâmicas monolíticas.* **Conclusão:** *A aplicação do glazing foi inferior e menos satisfatório que o polimento, gerando alterações que podem levar à instabilidade da cor.*

Palavras-chave: cerâmica - polimento dentário - ensaios de materiais.

INTRODUCTION

Dental ceramic technology has developed significantly over time in response to clinical needs. Feldspathic ceramic crowns were first introduced by Land, and aluminum oxide (Al2O3) was added in 1965 by McLean, with the aim of improving ceramic mechanical-physical properties. Since then, the literature records the introduction of numerous metal-free materials and systems[1].

As techniques for the fabrication of all-ceramic restorations advanced, monolithic restorations were created, i.e., parts made entirely from a single type of ceramic and at the same time. This technique eliminates the need for an overlay or top layer, thereby shortening fabrication time, eliminating problems associated with bonding between layers, and allowing more conservative tooth wear for prosthetic purposes[2].

Monolithic dental restorations using CAD-CAM technology have become popular due to their excellent mechanical properties and favorable esthetics, without the need for a veneering ceramic. Monolithic restorations can be shaped into final form using CAD-CAM equipment and materials such as zirconia, lithium disilicate ceramics, zirconia-reinforced lithium disilicate, feldspathic ceramics, leucite-based ceramics, and glass/ceramic polymer materials[3].

The complexity of tooth color does not appear to be achievable with any existing restorative material. Light reaching the surface of the tooth is partially absorbed, making it difficult for hard tooth structures to scatter, transmit or reflect it. Recent research has shown that these physical effects occur as optical phenomena on the surface and within tooth structures, and are strongly influenced by tooth type[4].

Although color change has been extensively studied in dentistry, there is still no consensus in the literature on acceptable and unacceptable values of ΔE change. The most usual classification states that ΔE values below 1 are considered clinically imperceptible and are not perceived by the human eye. Values between 1 and 3.3 are considered clinically acceptable and are perceived only by trained operators, while values above 3.3 are considered clinically unacceptable because they can be perceived by untrained observers[5].

Ceramic systems offer different opacities and a wide range of colors to suit any clinical situation and act as "biomimetic," with optical and mechanical properties similar to those of the tissue being replaced. However, these materials must be handled with care, as significant color differences have been observed between the same shades from different lot numbers and between brands with similar color designations, which may affect the esthetic outcome of the final restoration[6].

When a ceramic restoration is placed, the occlusal adjustment of a crown may roughen the surface, so the restoration must be polished and finished. Many different polishing systems are recommended for ceramic restorations, though it is unclear whether they can all achieve a smooth surface that is the same as or better than the original or untreated surface[7].

The aim of this study was to investigate the effects of chemical and mechanical finishing/polishing (glaze and manual mechanical polishing) and immersion in a coloring substance on the roughness, color stability, and microhardness of CAD-CAM lithium silicate monolithic ceramics: zirconia-reinforced, lithium disilicate-reinforced, and leucite-reinforced. The null hypothesis tested was that there was no effect of the type of ceramic, finishing/polishing type, or immersion substances on the roughness, microhardness or color stability of the materials.

MATERIALS AND METHOD
Experimental setup

Experimental units: 120 rectangular plates of ceramic CAD-CAM material (14 mm x 12 mm x 2 mm).

Factors studied:

- 3-stage ceramic CAD-CAM: (1) lithium disilicate reinforced with zirconium dioxide (SiO_2-Li_2O-ZrO_2) (VITA Suprinity® - Vita Zahnfabrik®), (2) lithium disilicate ($Li_2Si_2O_5$) (IPS E.max® CAD – Ivoclar Vivadent®) and (3) reinforced with leucite (SiO_2-Al_2O_3-K_2O) (IPS Empress® CAD - Ivoclar Vivadent®).
- Staining substances in two stages: Coffee and distilled water.
- Two surface treatments: (1) Glaze (IPS Ivocolor Glaze Paste - Ivoclar Vivadent® / Akzent Plus Glaze Paste - Vita Zahnfabrik®) and (2) mechanical polishing with sandpaper in three grit levels: 600, 800 and 1200.
- Reaction variables - evaluation of surface roughness, color and microhardness (before

and after immersion in the staining substance). Figure 1 illustrates the experimental design.

Test specimen preparation

To obtain the ceramic specimens, a high concentration diamond disk (BUEHLER® - IsoMetMT Diamond Wafering Blades 102 x 0.3 mm 15HC) was used in a metallographic cutter (BUEHLER®) to cut the ceramic blocks at a thickness of 2 mm, obtaining rectangular slices with dimensions 14 mm x 12 mm x 2 mm. The slices were placed in the ceramic oven to crystallize, according to the recommendations of the respective manufacturers.

Finishing/Polishing Process

The specimens were subjected to two types of finishing/polishing: In groups G1, G2 and G3 (n=20), a thin layer of glaze was applied according to the recommendations of the manufacturer of the respective ceramic brand. In groups P1, P2 and P3 (n=20), the specimens were mechanically polished in a polishing machine (Aropol 2V - Arotec Ind. e Comércio) with sandpaper (WetordryTM Sandpaper - 3M ESPE®) at three grit levels (600, 800 and 1200) under running water for 60 seconds. They

were then cleaned ultrasonically in distilled water for 10 minutes and air dried.

Immersion in staining solutions

The specimens were again divided into two subgroups (n=10) according to the staining substance. Each subgroup was immersed in 200 mL of either a solution of Melitta soluble coffee or distilled water (control), both refreshed daily. During immersion, the containers were sealed with PVC film to prevent evaporation. Immersion time was 3 hours daily at room temperature for a test period of 30 days.

At the end of each immersion period, specimens were washed with distilled water, dried, and stored in plastic bottles with cotton soaked in distilled water and placed in a bacteriological oven at 37ºC. Two weeks after the end of immersion, the specimens were tested for surface roughness, color, and microhardness.

Surface roughness

Specimen surface roughness (Ra) was determined after surface treatment and again after immersion in coloring substances, using a roughness meter (SJ-210, Mitutoyo, Kanagawa, Japan). Roughness
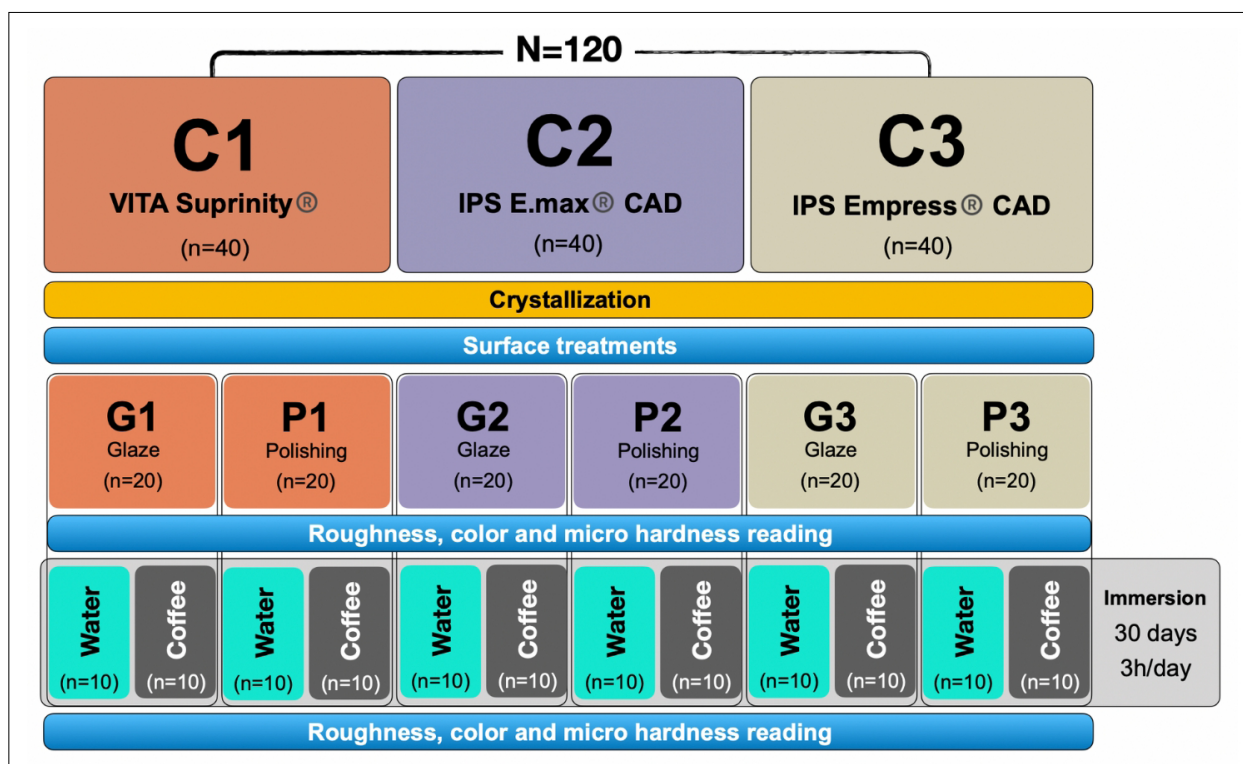

Fig. 1: Diagram showing experimental design.

values were obtained by averaging 3 measurements with a cutoff value of 0.25 mm.

Microhardness

Surface microhardness was tested before and after immersion in water and coffee using a microhardness tester (Pantec HVS, Panambra, São Paulo, SP, Brazil) and a Knoop indenter with a load of 50 grams and an application time of 5 seconds. Three impressions were made on the top of each specimen.

Color stability

Specimen color was recorded twice: after surface treatment and after immersion in the staining solutions, using a digital spectrophotometer (VITA Easyshade® - VITA Zahnfabrik), following the manufacturer's instructions. Color was evaluated based on the difference of the CIELab parameters (ΔL, Δa, Δb), $\Delta E00$ and ΔWID; according to the following formulas: $\Delta E00 = \sqrt{(\Delta L'/kLSL)2 + (\Delta C'/kCSC)2 + (\Delta H'/kHSH)2 + RT (\Delta C'/kCSC)(\Delta H'/(kHSh)}$.

In the $\Delta E00$ formula, ΔL^* represents the variation in the L^* coordinate, which indicates brightness (black-white axis); ΔC represents differences in saturation (chroma); ΔH represents differences in hue; and RT is a function that accounts for the interaction between chroma and hue differences in the blue region of the spectrum. The values of $\Delta E00$ are calculated sequentially following Sharma et al.[8]. In addition to the above formulas, the variation between the time points and the initial values of the CIEL*a*b* coordinates are calculated by the whiteness index in dentistry (ΔWID) considering the linear formula (WID) at each time point studied: $WID = 0.511L^* -2.324a^* -1.100b^*$.

Statistical analysis

The SPSS 23 program (SPSS Inc., Chicago, IL, USA) was used for the statistical calculations, and the significance level was set at 5%. The data for roughness, microhardness, and color parameters L, a, and b, obtained in the first phase of the experiment, when the ceramics had been subjected to surface treatment, were subjected to two-way ANOVA. These were also used after the glazed or polished ceramics had been immersed in distilled water or coffee. The mean differences between the values measured in the second and first stages were presented descriptively. The $\Delta E2000$- and ΔWID-data were subjected to a three-way repeated measure ANOVA. Multiple comparisons were performed using Tukey tests.

RESULTS

The results were ordered according to the analyses performed: 1) in the first phase of the experiment, when the ceramics were subjected to surface treatment; 2) in the second phase of the study, after the glazed or polished ceramics were immersed in distilled water or in coffee; 3) for $\Delta E2000$ and ΔWID.

First stage: ceramics subjected to surface treatment

The two-way analysis of variance applied to the first stage of the experiment showed statistically significant interaction between the ceramics and the surface treatments in terms of roughness, microhardness, and color parameters 'a' and 'b' (p < 0.001). For the color L parameter, there was no interaction between ceramics and surface treatments (p = 0.318), but a significant difference was observed between ceramics and between surface treatments (p < 0.001).

Roughness

For each of the ceramics tested, smoothness was significantly higher when polished than when glazed. During polishing, Suprinity and Empress ceramics, which did not differ from each other, were significantly less rough than E.max. After glazing, Empress ceramics had an average roughness significantly different from Suprinity and E.max, which were the least and most rough, respectively (Table 1).

Microhardness

For E.max ceramic, microhardness did not differ significantly between glazed and polished surfaces. For Empress ceramic, microhardness was significantly higher for glazed surface, while for Suprinity ceramic, it was significantly higher for polished surface (Table 1).

Color 'L' parameters

Significantly higher values were found when polished, regardless of the ceramic used. Regardless of whether the specimens were glazed or polished,

Table 1. Means and standard deviations of roughness, microhardness and color parameters L, a and b, according to the ceramic and its surface treatment and these groups after immersion in coffee and distilled water.

First stage of the experiment: ceramics subjected to surface treatments (glazing or polishing)

Ceramic	Roughness (µm)		Microhardness (kg/mm²)		Color 'L' parameter			Color 'a' parameter		Color 'b' parameter	
	Glazing	Polishing	Glazing	Polishing	Glazing	Polishing	Average	Glazing	Polishing	Glazing	Polishing
E.max CAD	0,603 Cb (0,170)	0,144 Ba (0,145)	511 Ba (79)	505 Ba (84)	87,9 (1,2)	90,0 (1,6)	89,0 B (1,7)	1,2 Aa (0,4)	1,0 Ba (0,1)	23,6 Aa (1,6)	24,5 Ba (0,8)
Empress CAD	0,462 Bb (0,129)	0,075 Aa (0,028)	462 Ab (60)	372 Aa (58)	88,6 (1,0)	91,5 (0,9)	90,0 B (1,7)	1,1 Ab (0,3)	0,4 Aa (0,1)	23,3 Ab (1,5)	21,6 Aa (0,9)
Suprinity	0,148 Ab (0,083)	0,054 Aa (0,046)	547 Ca (45)	616 Cb (33)	82,1 (7,6)	86,4 (1,5)	84,2 A (5,8)	8,9 Bb (4,2)	0,2 Aa (0,4)	47,7 Bb (14,3)	23,6 ABa (2,4)
Overall average	—	—	—	—	86,2 a (5,3)	89,3 b (2,5)	—	—	—	—	—

Second stage of the experiment: groups formed by ceramics with treated surface and submitted to immersion in distilled water or coffee

Ceramic and treatment	Roughness (µm)		Microhardness (kg/mm²)		Color 'L' parameter		Color 'a' parameter		Color 'b' parameter	
	Water	Coffee	Water	Coffee	Water	Coffee	Water	Coffee	Water	Coffee
E.max CAD glazing	0,563 Da (0,130)	0,715 Db (0,250)	483 Ca (66)	538 Db (52)	87,3 Aa (1,4)	88,4 ABa (1,0)	1,1 Ba (0,4)	1,1 Ba (0,4)	23,5 Aa (1,9)	23,8 ABa (1,9)
E.max CAD polishing	0,174 Ba (0,200)	0,148 Ba (0,132)	476 Ca (51)	529 Db (37)	90,1 Ba (1,9)	89,2 Ba (0,7)	1,2 Ba (0,1)	1,1 Ba (0,2)	24,9 Aa (0,9)	27,4 Ba (9,8)
Empress CAD glazing	0,409 Ca (0,125)	0,603 Cb (0,108)	440 Ba (80)	505 Cb (63)	88,5 Aa (0,8)	88,1 ABa (1,3)	1,2 Ba (1,0)	1,1 Ba (0,4)	22,2 Aa (1,4)	23,6 ABa (1,8)
Empress CAD polishing	0,078 Aa (0,071)	0,074 Aa (0,048)	377 Aa (29)	411 Ab (86)	92,0 Ba (1,0)	91,1 Ba (0,8)	0,5 Aa (0,1)	0,5 Aa (0,1)	22,0 Aa (0,6)	21,7 Aa (0,3)
Suprinity glaze	0,181 Ba (0,074)	0,176 Ba (0,101)	512 Da (49)	494 Ca (75)	96,0 Cb (9,3)	86,2 Aa (9,9)	2,4 Ca (4,0)	7,6 Cb (4,9)	24,0 Aa (12,6)	42,6 Cb (16,5)
Suprinity polida	0,052 Aa (0,039)	0,048 Aa (0,026)	575 Eb (20)	447 Ba (25)	86,0 Aa (0,8)	86,4 Aa (2,0)	0,2 Aa (0,3)	0,5 Aa (0,5)	24,5 Aa (1,2)	23,8 ABa (3,3)

Considering each response variable separately, capital letters indicate comparisons within each column (ceramics among themselves), while lowercase letters indicate comparisons within each row (glaze x polishing or distilled water x coffee). Means followed by distinct letters differ significantly from each other. Overall averages for parameter L, whose interaction effect was not significant, show comparisons between ceramics (capital letters) and between surface treatments (lower letters).

the highest L values were found for the E.max and Empress ceramics, with no significant difference between the two (Table 1).

Color 'a' parameters
No difference was found between specimens of E.max ceramics that were glazed or polished, while in the other ceramics, the values of 'a' were significantly higher when glaze was applied. No statistically significant difference was found between glazed E.max and Empress, but they both had significantly lower 'a' values than Suprinity. After polishing, the 'a' parameter was significantly higher

in E.max ceramics, with no significant difference between the other two ceramics (Table 1).

Color 'b' parameters
The results are identical to those found for the 'a' parameter. The only difference was that the Suprinity ceramic did not differ significantly from Empress when polished (Table 1).

Second stage: after immersing the glazed or polished ceramics in distilled water or coffee
Two-way analysis of variance showed that there was a statistically significant interaction for roughness

data (p = 0.017), microhardness, and parameters L, a, and b (p < 0,001). There was a statistically significant interaction between the surface-treated ceramics and the immersion factor in staining solution.

Roughness

After immersion in coffee or distilled water, there was no significant change in surface roughness of the polished specimens or the glazed Suprinity specimens. However, surface roughness of the glazed E.max and Empress specimens increased in coffee.

After immersion in water, glazed E.max had significantly higher surface roughness than Empress specimens, which in turn were rougher than polished E.max and glazed Suprinity. Polished E.max and glazed Suprinity did not differ from each other, but were rougher than polished Empress and Suprinity, which had the lowest roughness values.

After immersion in coffee, the results for the glazed or polished ceramics were identical to those described for immersion in distilled water (Table 1).

Microhardness

Except for the glazed and polished Suprinity ceramics, which showed no significant difference when immersed in coffee or water and showed significantly lower microhardness when immersed in coffee, microhardness was significantly lower for all other combinations of ceramics and surface treatment after immersion in distilled water.

After immersion in water, polished Suprinity had significantly higher microhardness than glazed Suprinity. It was followed by E.max (both polished and glazed, which did not differ significantly from each other). E.max in turn had significantly higher microhardness than the glazed Empress, while polished Empress had the lowest values under all conditions.

After immersion in coffee, polished and glazed E.max, which did not differ significantly from each other, had higher microhardness than glazed Empress and Suprinity, which also did not differ from each other. Polished Suprinity and Empress had the lowest microhardness values (Table 1).

L Parameters

The values of parameter L of the specimens immersed in water or coffee did not differ significantly for any combination of ceramics and surface treatment, except for glazed Suprinity, which showed a significantly lower L value after immersion in coffee.

After immersion in water, glazed Suprinity ceramic had a significantly higher L-value than the polished E.max and Empress ceramics (with no significant difference between the two), and these had higher values than glazed E.max, glazed Empress and polished Suprinity.

After immersion in coffee, polished and glazed Empress and E.max, which did not differ from each other, had significantly higher L values than both glazed and polished Suprinity, while glazed E.max and Empress had medium values of the color L parameter (Table 1).

Color 'a' parameters

The only ceramic whose 'a' color parameter was significantly affected by coffee was glazed Suprinity. After both water immersion and coffee immersion, this was the group that had the highest 'a' value, followed by E.max (both glazed and polished) and glazed Empress (with no significant difference between these three groups). The lowest value of a was measured in the polished Suprinity group (Table 1).

Color 'b' parameters

Coffee only increased the value of parameter 'b' significantly in glazed Suprinity.

After immersion in distilled water, there was no significant difference among the various ceramic and surface treatment combinations.

After immersion in coffee, the highest 'b' value was found for glazed Suprinity, followed by polished E.max, which was in turn higher than polished Empress. After immersion in coffee, glazed E.max, glazed Empress and polished Suprinity did not differ significantly from each other or from any of the other groups (Table 1).

ΔE2000 and ΔWID

The three-way repeated measure ANOVA found no significant interaction among the factors studied (ceramic, surface treatment, and staining solution) for either the ΔE2000 (p = 0.268) or the ΔWID (p = 0.495) data. The dual interactions between ceramics and surface treatment (ΔE2000: p = 0.127; ΔWID: p = 0.633) and between surface treatment and staining

Table 2. Means and standard deviations of the ΔE2000 and ΔWID parameters, according to the ceramic, its surface treatment and immersion in water and coffee.

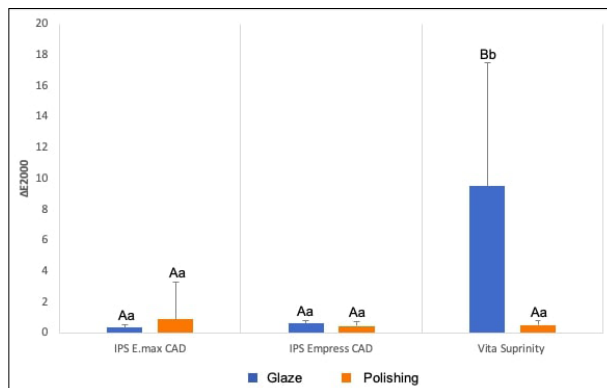| Response variable	Ceramic	Glaze		Polishing	
		Water	Coffee	Water	Coffee
ΔE2000	E.max CAD	0,40 (0,17)	0,33 (0,23)	0,31 (0,21)	1,47 (3,4)
	Empress CAD	0,64 (0,81)	0,62 (0,20)	0,33 (0,20)	0,60 (0,26)
	Suprinity	11,89 (7,18)	7,13 (8,38)	0,45 (0,27)	0,61 (0,35)
ΔWID	E.max CAD	-0,77 (0,78)	0,81 (0,89)	-0,68 (0,73)	-3,75 (10,72)
	Empress CAD	-0,04 (2,56)	0,46 (0,99)	0,22 (0,80)	-1,31 (1,04)
	Suprinity	34,87 (34,49)	23,83 (35,40)	-0,42 (1,06)	-1,49 (1,47)

Fig. 2: Column diagram of the average values of ΔE2000, according to the ceramic and its surface treatment, regardless of immersion in water and coffee.
Caption: Blue columns indicated with distinct capital letters indicate a significant difference between ceramics that received glaze. Red columns indicated with equal capital letters indicate no significant difference between polished ceramics. Columns with equal lowercase letters indicate no significant difference between glazed and polished samples, considering each ceramic separately.
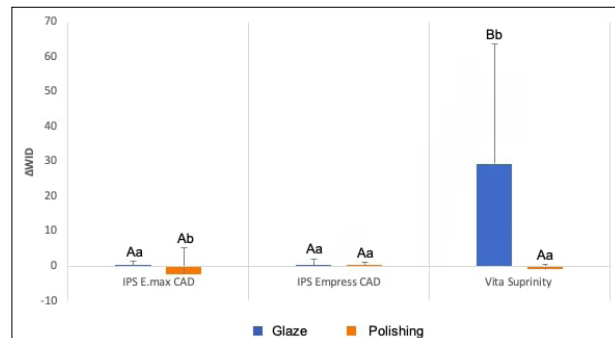

Fig. 3: Column diagram of the average values of ΔWID, according to the ceramic and its surface treatment, regardless of immersion in water and coffee.
Caption: Blue columns indicated with distinct capital letters indicate a significant difference between ceramics that received glaze. Red columns indicated with equal capital letters indicate no significant difference between polished ceramics. Columns with distinct lowercase letters indicate a significant difference between glazed and polished samples, considering each ceramic separately.

solution (ΔE2000: p = 0.083; ΔWID: p = 0.838) were not significant. The interaction between ceramic and surface treatment was statistically significant for the ΔE2000 and ΔWID data (p < 0.001) (Table 2).

Breaking down the interaction between ceramics and surface treatment for the ΔE2000 data, no difference was found between glazed and polished E.max or Empress, but for Suprinity, delta values were significantly higher for glazed. While the polished ceramics did not difer significantly from each other, glazed ceramics differed significantly, with Suprinity having significantly higher values than the other materials, between which no significant difference was found (Fig. 2).

For the ΔWID data, the comparisons between the ceramics gave the same results as for ΔE2000. Analysis of the effects of glazing and polishing

on the individual ceramics showed that the only difference from the ΔE2000 data was that polished E.max resulted in greater changes (Fig. 3).

Immersion in water or coffee had no effect on ΔE2000 values [p = 0.378; water immersion: 2.33 (5.15); coffee: 1.79 (4.29)], or on ΔWID [p = 0.363; water immersion: 5.53 (18.92); coffee: 3.09 (17.29)], regardless of the ceramic and surface treatment.

DISCUSSION

Surface roughness plays a critical role in preventing extrinsic discoloration[9]. The roughness data from this study showed that smoothness was significantly greater for polished than for glazed ceramics in all three cases (before and after immersion in solutions), although in another study, polishing was found to produce rough surfaces while glazing produced a

smoother surface[10]. The difference may be attributed to different specimen preparation techniques, polishing techniques[11], materials[12] or Ra machine used[13]. The surface roughness of polished specimens did not differ after immersion in coffee or water. Sandpaper with different grits was used for polishing in this study. A final mirror polish after milling or setting is essential to ensure smooth surfaces (< 0,2 μm) with optimal clinical performance. The E.max specimen surface roughness was below this value after each polishing application[14]. Polishing in the office is as effective as polishing in the laboratory[11].

After immersion in distilled water, microhardness was lower for all polishing and ceramic combinations. Suprinity showed lower microhardness with coffee and glaze. Empress microhardness was higher with glaze. E.max showed no difference between glaze and polish. Suprinity consists mainly of ZrO_2 (zirconia) 8-12 wt%, SiO_2 (silica) 56-64 wt%, Li_2O (lithium oxide) 15-21 wt%, and La_2O_3 (lanthanum oxide) 0.1 wt%. According to the manufacturer, the composition of E.max consists mainly of SiO_2, Li_2O, P_2O_5, ZrO_2, ZnO, K_2O and Al_2O_3, as well as additional dye ions, which are combined using glass technology through a pressure casting process (Vivadent Ivoclar). The partially crystallized blocks used for milling in E.max consist of 40% lithium metasilicate crystals (Li_2SiO_3), with sizes of 0.2 and 1.0 mm and platelet format, fixed in the glass phase together with disilicate cores of lithium (Vivadent Ivoclar). Therefore, the differences in ceramic materials can be attributed to the type and size of the crystalline phase (lithium silicate vs. lithium disilicate) or additional ZrO_2 particles.

Polishing increased the L-value regardless of the material because color stability is affected by the surface structure of the material. The higher L-value could be related to surface irregularities[12]. The discoloration caused by coffee can be attributed to the penetration of the yellow coffee dye into the microstructure of the materials. E.max and Empress achieved the highest L values, regardless of whether they were polished or glazed.

Distilled water and coffee affected the surface hardness of the materials studied, which may have increased their susceptibility to staining[15]. Fahmy et al.[16] reported a significant increase in the hardness values of a ceramic material after storage in saliva for 3 weeks. This increase in microhardness was related to ion exchange through the Si- OH layer reportedly formed on the ceramic surface[16].

After immersion in water or coffee, the ceramics, whether polished or glazed, showed no difference in the value of L. Glazed Suprinity had the lowest value of 'a' and L after immersion in coffee and the highest value of L after immersion in water. Immersion in coffee also increased the values of 'a' and 'b' for glazed Suprinity. Due to their low polarity, coffee dyes tend to soak into the ceramic[17]. Increases in 'a' and 'b' and a decrease in 'L' always occurred in the presence of glaze. The type of soaking solution can affect the extent of color change. In the present study, a coffee solution was used as the colorant. Odioso et al.[18] reported that coffee/tea consumption was one of the factors that significantly affected 'b' and 'L' values. People who drank coffee or tea daily had an average increase of 1.2 units in 'b' and a decrease of 1.5 units in L. The average time to drink a cup of coffee is 15 minutes, and for coffee drinkers, average coffee intake is 3.2 cups per day[17]. Therefore, 48 hours of storage simulated coffee consumption for 2 months[19]. It was postulated that 24 hours of immersion in vitro is approximately equivalent to one month *in vivo*[19]. Therefore, three hours per day of immersion for 30 days is equivalent to 90 days of clinical immersion.

The ΔE2000 and ΔWID data confirm that the presence of glaze on all ceramics resulted in higher delta values. Glazed Suprinity exhibited the highest values. Kilinc & Turgut[20] reported that manual polishing techniques can achieve similar results to glazing in terms of color stability, which contrasts with Yilmaz et al.[21], who found that glazed preparations had better color stability, although the observed color was not clinically noticeable in the polished preparations. Suprinity and E.max ceramics treated with different surface treatment procedures (glazing or polishing) showed significant and clinically acceptable differences in color changes after coffee thermal cycling[22]. Kilinc and Turgut[20] also reported clinically acceptable color changes in glass-ceramics, regardless of the type of surface treatment (control, manual polishing, or glazing). They reported that polishing and glazing produced similar results in terms of roughness[23].

Sarac et al.[24] investigated the effects of polishing systems on the color and surface texture of ceramics, finding significant differences between polishing techniques in terms of color differences, with ΔE values ranging from 1.03 to 3.36. Glazed specimens

showed better color stability; on the other hand, the discoloration observed in polished specimens was not clinically noticeable[12].

To conclude, mechanical polishing performed better in terms of roughness, surface microhardness, and color retention of the ceramics studied compared to glazing. Zirconia-based ceramics generally showed more homogeneous results in terms of microhardness and roughness when manual polishing and glazing were considered.

DECLARATION OF CONFLICT OF INTEREST
The authors declare no potential conflicts of interest regarding the research, authorship, and/or publication of this article.

REFERENCES

1. Silva TM, Salvia AC, Carvalho RF, Pagani C, et al. Polishing for glass ceramics: which protocol? J Prosthodont Res. 2014;58:160-170. https://doi.org/10.1016/j.jpor.2014.02.001

2. Johansson C, Kmet G, Rivera J, Larsson C, et al. Fracture strength of monolithic all-ceramic crowns made of high translucent yttrium oxide-stabilized zirconium dioxide compared to porcelain-veneered crowns and lithium dislocate crowns. Acta Odontol Scand. 2014;72:145-153. https://doi.org/10.3109/00016357.2013.822098

3. Kim HK, Kim SH. Effect of the number of coloring liquid applications on the optical properties of monolithic zirconia. Dent Mater. 2014;30:e229-237. https://doi.org/10.1016/j.dental.2014.04.008

4. PopCiutrila IS, Ghinea R, Perez Gomez MM, Colosi HA, et al. Dentine scattering, absorption, transmittance and light reflectivity in human incisors, canines and molars. J Dent. 2015;43:1116-1124. https://doi.org/10.1016/j.jdent.2015.06.011

5. Oliveira ALBM, Botta AC, Campos JADB, Garcia PPNS. Effects of Immersion Media and Repolishing on Color Stability and Superficial Morphology of Nanofilled Composite Resin. Microsc Microanal. 2014;20:1234-1239. https://doi.org/10.1017/S1431927614001299

6. Carney MN, Johnston WM. Appearance differences between lots and brands of similar shade designations of dental composite resins. J Esthet Restor Dent. 2017;29:E6-14. https://doi.org/10.1111/jerd.12263

7. Amaya-Pajares SP, Ritter AV, Resendiz CV, Henson BR, et al. Effect of finishing and polishing on the surface roughness of four ceramic materials after occlusal adjustment. J Esthet Restor Dent. 2016;28:382-396. https://doi.org/10.1111/jerd.12222

8. Sharma G, Wu W, Dalal EN. The CIEDE2000 color-difference formula: Implementation notes, supplementary test data, and mathematical observations. Color Research & Application 2005;30:21-30. https://doi.org/10.1002/col.20070

9. Kozmacs C, Hollmann B, Arnold WH, Naumova E, et al. Polishing of Monolithic Zirconia Crowns-Results of Different Dental Practitioner Groups. Dent J (Basel) 2017;5:30. https://doi.org/10.3390/dj5040030

10. Brunot-Gohin C, Duval JL, Azogui EE, Jannetta R, et al. Soft tissue adhesion of polished versus glazed lithium disilicate ceramic for dental applications. Dent Mater 2013;29(9):e205-e212. https://doi.org/10.1016/j.dental.2013.05.004

11. Matzinger M, Hahnel S, Preis V, Rosentritt M, et al. Polishing effects and wear performance of chairside CAD/CAM materials. Clin Oral Investig 2019;23:725-737. https://doi.org/10.1007/s00784-018-2473-3

12. Sarikaya I, Güler AU. Effects of different surface treatments on the color stability of various dental porcelains. J Dent Sci 2011;6:65-71. https://doi.org/10.1016/j.jds.2011.03.001

13. Guilardi LF, Werner A, Jager N, Pereira GKR, et al. The influence of roughness on the resistance to impact of different CAD/CAM dental ceramics. Braz Dent J 2021;32: 54-65. https://doi.org/10.1590/0103-6440202103951

14. Incesu E, Yanikoglu N. Evaluation of the effect of different polishing systems on the surface roughness of dental ceramics. J Prosthet Dent 2020;124:100-109. https://doi.org/10.1016/j.prosdent.2019.07.003

15. Tuncer D, Karaman E, Firat E. Does the temperature of beverages affect the surface roughness, hardness, and color stability of a composite resin? Eur J Dent 2013;7:165-171. https://doi.org/10.4103/1305-7456.110161

16. Fahmy NZ, EL Guindy J, Zamzam M. Effect of Artificial Saliva Storage on Mcrohardness and Fracture Toughness of a Hydrothermal Glass-Ceramic. J Prosthodont 2009;18:324-331.https://doi.org/10.1111/j.1532-849X.2009.00448.x

17. Ertaş E, Güler AU, Yücel AC, Köprülü H, et al. Color stability of resin composites after immersion in different drinks. Dent Mater J 2006;25:371-376. https://doi.org/10.4012/dmj.25.371

18. Odioso LL, Gibb RD, Gerlach RW. Impact of demographic, behavioral, and dental care utilization parameters on tooth color and personal satisfaction. Compend Contin Educ Dent Suppl 2000;S35-41;quiz S43.

19. Guler AU, Yilmaz F, Kulunk T, Guler E, et al. Effects of different drinks on stainability of resin composite provisional restorative materials. J Prosthet Dent 2005;94:118-124. https://doi.org/10.1016/j.prosdent.2005.05.004

20. Kilinc H, Turgut S. Optical behaviors of esthetic CAD-CAM restorations after different surface finishing and polishing procedures and UV aging: An in vitro study. J Prosthet Dent 2018;120:107-113. https://doi.org/10.1016/j.prosdent.2017.09.019

21. Yilmaz C, Korkmaz T, Demirköprülü H, Ergün G, et al. Color stability of glazed and polished dental porcelains. J Prosthodont 2008;17:20-24.

22. Alp G, Subasi MG, Johnston WM, Yilmaz B. Effect of surface treatments and coffee thermocycling on the color and translucency of CAD-CAM monolithic glass-ceramic. J

Prosthet Dent 2018;120:263-268. https://doi.org/10.1016/j.prosdent.2017.10.024

23. Vichi A, Fabian Fonzar R, Goracci C, Carrabba M, et al. Effect of Finishing and Polishing on Roughness and Gloss of Lithium Disilicate and Lithium Silicate Zirconia Reinforced Glass Ceramic for CAD/CAM Systems. Oper Dent 2018;43:90-100. https://doi.org/10.2341/16-381-L

24. Sarac D, Sarac YS, Yuzbasioglu E, Bal S. The effects of porcelain polishing systems on the color and surface texture of feldspathic porcelain. J Prosthet Dent 2006;96:122-128. https://doi.org/10.1016/j.prosdent.2006.05.009

Effect of fried sunflower oil intake on mandibular biomechanical competence of growing rats

Elisa V Macri[1] , Clarisa Bozzini[2] , Andrea G Ferreira-Monteiro[1] , Patricia N Rodriguez[1] , Fima Lifshitz[3] , Verónica J Miksztowicz[1,4] , Silvia M Friedman[1]

1. Universidad de Buenos Aires, Facultad de Odontología, Cátedra de Bioquímica General y Bucal. Buenos Aires, Argentina.
2. Universidad de Buenos Aires, Facultad de Odontología, Cátedra de Fisiología. Buenos Aires, Argentina.
3. State University of New York, Downstate Medical Center, College of Medicine, Brooklyn. Santa Barbara, CA, USA.
4. Laboratory of Experimental Cardiovascular Pathology and Arterial Hypertension, Institute for Biomedical Research, School of Medical Sciences, Pontifical Catholic University of Argentina and the National Scientific and Technical Research Council, Buenos Aires, Argentina.

ABSTRACT

*Previous studies by us demonstrated that the consumption of thermally oxidized oil diet adversely affects body growth, lipid metabolism, bone mass and femur biomechanical competence. **Aim:** The aim of this study was to evaluate the effects of a diet containing fried sunflower oil on the mandible of growing rats. **Materials and Method:** Male Wistar rats (21±1 day old) (n=21) were assigned at weaning to one of three diets for 8 weeks: a control diet (C), a diet containing sunflower oil (SFO) or a diet containing sunflower oil that had been repeatedly heated (SFOx); both SFO and SFOx were mixed with commercial rat chow at 13% (w/w). The consistency and viscosity of the 3 diets were similar. Zoometrics and food intake were recorded weekly. At wk=8, mandibular growth was assessed by measurements of anatomical points of cleaned bones, and mandible biomechanical competence was assessed to estimate the structural properties of the bone. Statistical analysis was performed by SPSS v. 20.0. **Results:** Rats fed SFOx diet attained the lowest final body weight (P=0.0074), mandibular weight (P=0.0001) and mandibular \length (P=0.0002). Load bearing capacity (Wf;N), load of yielding (Wy;N) and stiffness (Wy/dy;N/mm) of the mandible were negatively affected by both sunflower oil diets (fresh and fried) (P=0.001; P=0.002; P=0.003, respectively) though SFOx induced the most significant reduction in Wy/dy (C:44.4(5.4) > SFO:36.1(2.1) > SFOx: 26.3(3.7) N/ mm; P=0.003). The deleterious effect of SFOx on mandibular growth was more accentuated on the posterior part of the bone (C:11.4(0.3)=SFO:11.2(0.2)>SFOx: 10.7(0.2) mm; p=0.0005); the anterior/ posterior ratio (C:1.25(0.02)=SFO:1.27(0.02)<SFOx:1.32(0.03); p=0.0001) indicated that SFOx induced mandibular deformation. **Conclusion:** Consumption of SFOx diet during growth could affect mandibular morphometric properties and biomechanical competence, in terms of bone stiffness.*

Keywords: mandibular morphometrics - biomechanical competence - healthy rats - fried sunflower oil - growth.

Corresponding Author:
Silvia María Friedman
silvia.friedman@odontologia.uba.ar

Efecto del consumo de aceite de girasol termooxidado sobre la competencia biomecánica de la mandíbula, en animales en crecimiento

RESUMEN

*En estudios previos hemos demostrado los efectos adversos del consumo de una dieta rica en aceite termooxidado sobre el crecimiento corporal, el metabolismo de los lípidos, la masa ósea y la competencia biomecánica del fémur. **Objetivo:** El objetivo de este trabajo fue investigar el efecto de una dieta rica en aceite de girasol termooxidado (AGX) sobre los parámetros morfométricos y biomecánicos de la mandíbula de rata en crecimiento. **Materiales y Método:** Ratas macho Wistar de 22±1 días de edad (n=21) recibieron durante 8 semanas una de 3 dietas: control (C); dieta comercial, una dieta suplementada con aceite de girasol (AG) y una dieta suplementada con AGX. La consistencia y la viscosidad de las dietas fueron similares. Los parámetros zoométricos y el consumo de dieta se registraron semanalmente. A T=8, los animales se eutanasiaron y se obtuvieron las hemimandíbulas. El crecimiento mandibular se estimó por medidas morfométricas entre puntos anatómicos y las propiedades estructurales por biomecánica. El análisis estadístico se realizó por SPSS v. 20.0. **Resultados:** Las ratas alimentadas con AGX presentaron menor peso corporal final (p=0.0074), peso mandibular (p=0.0001) y longitud mandibular (p=0.0002). Las propiedades estructurales de la mandíbula, Wf (p=0.001), Wy (p=0.002) y Wy/dy (p=0.003), se vieron afectadas negativamente en ratas alimentadas con AG o AGX, respecto a C; pero la rigidez ósea (Wy/dy) en AGX fue significativamente menor (C:44.4(5.4) > SFO:36.1(2.1) > SFOx: 26.3(3.7) N/mm; p=0.003). El efecto deletéreo del AGX sobre el crecimiento mandibular fue más acentuado en la región posterior (C:11.4(0.3)=SFO:11.2(0.2)>SFOx: 10.7(0.2) mm; p=0.0005). La relación anterior/posterior (C=1.25 (0.02); AG= 1.27(0.02) y AGX=1.32(0.03), p=0.001) indica que AGX indujo deformación mandibular. **Conclusiones:** El efecto adverso del consumo de una dieta rica en AGX durante el crecimiento podría afectar los parámetros morfométricos y la biomecánica ósea en términos de rigidez ósea.*

Palabras clave: morfometría mandibular - competencia biomecánica - ratas sanas - aceite de girasol frito - crecimiento.

INTRODUCTION

In Argentina, sunflower oil (SFO) is commonly used for frying and is consumed in large quantities, fried potatoes being the most consumed deep-fried food[1]. Fried food consumption contributes to the development of chronic diseases such as obesity[2], atherosclerosis[3], and liver damage[4]. It also contributes to deterioration of bone histomorphometric parameters[5] and altered mechanical strength of femoral diaphysis to external loading[6,7]. The adverse effects of diets containing fried sunflower oil (SFOx) on total skeleton bone mineral content (BMC) are more evident on growing rats[8].

Bone with a faster turnover rate (modeling) could reveal potential adverse effects of inappropriate types of fat intake on the skeletal and biomechanical bone properties of a growing animal. Nutritional intake is known to affect the mechanical properties of the appendicular and axial bones.

Our previous studies indicated that growing animals fed a diet rich in olive oil or high-oleic-sunflower oil (HOSO) exhibited negative mechanical strength of femoral diaphysis in response to external loading, compared to commercial rodent diet. Moreover, HOSO with phytosterols or fish oil did not reverse the detrimental effects on femur biomechanical competence[9].

Mandible quality depends on diet intake and gender[10]. Our previous studies demonstrated impaired mechanical mandible competence in rats fed a suboptimal restricted diet[11,12] and a diet containing inadequate quality or quantity of protein[13]. However, to our knowledge, there are no studies evaluating the effect of different types of dietary fat and the biomechanical competence of the mandible during growth.

The aim of the current study was to assess the effects of two oil diets on mandible morphometric properties and biomechanical competence. The study diets contained either SFO or SFOx were compared with a control diet (C). The three diets had similar viscosity and masticatory loading capacity since the mandible is a load-bearing bone that differs from other bones in the axial skeleton. It is influenced by mechanical masticatory loading, which rapidly impacts the mass density and microarchitecture of the mandibular alveolar bone[14,15]. The importance of this study is the detrimental effect of consuming diets rich in fried oils on bone health during growth.

MATERIALS AND METHOD

Animals

The Animal Resources of the Department of Biochemistry, School of Dentistry of the University of Buenos Aires provided the male weaning Wistar rats for the study. The twenty-one rats, weighing 53.8 (42.9-64.7) g, were housed under standard conditions (light-dark 12:12 hours, $21 \pm 1^\circ C$ and 50–60% humidity) in individual steel cages, following the Principles of Laboratory Animal Care established by the National Institute of Health (NIH), USA Ethics Committee.

The protocol for this animal study was approved by the Animal Research Committee of the School of Dentistry, University of Buenos Aires (Approval number 004/17).

The mothers' nutritional status was adequate to factor directly associated with bones and body development.

Diets

The composition of the three diets consumed in the experiment is shown in Table 1. A modified commercial stock Purina chow (Gilardoni SA, Buenos Aires, Argentina) was used as the control diet (C). Chow was composed of vegetal-based ingredients such as soybean flour, corn gluten, wheat flour and wheat bran, and animal-based ingredients such as fish and meat flour. The main sources of fat in the C diet were corn oil and fish oil (Table 1).

The experimental diets were supplemented with either fresh sunflower oil (SFO) or fried sunflower oil (SFOx), thereby differing in fat concentration from the C diet. All diets were similar in particle size. The three diets were prepared by adding 3% gelatin to prepare cubes with similar viscosity and consistency[16] based on the rheological properties of several hydrogels. The ingredients of each diet were crushed and mixed, and the homogenized mixture was transferred to a press. The diets were cut manually into a similar size as the commercial chow. It was important to ensure similar consistency for all three diets because consistency affects the masticatory apparatus by producing high frequency loads of variable magnitude on the teeth and jaws. Jaws differ from the appendicular skeleton because mandibular loads cause complex patterns of bone deformation during normal function, as a result of the diverse force vectors acting on them. These forces

Table 1. Diet composition

INGREDIENTS (g/100g)	C	SFO	SFOx
Starch	48	30.7	30.7
Protein (mix of corn, wheat, soybean, fish, and meat flour)	23	14.7	14.7
Fat (acid hydrolysis) (mix of corn oil and fish oil)	7.0	4.5	4.5
SFO		13	
SFOx			13
Other source of fats: Cholesterol (ppm) Linoleic acid Linolenic acid Arachidonic acid Omega-3 fatty acids Total saturated fatty acids Total monounsaturated fatty acids	200 1.3 0.11 <0.01 1.90 1.89 1.98	128 8.79 0.08 0.03 1.98 2.53 4.88	128 6.91 0.07 0.04 1.97 3.57 5.58
Total polyunsaturated fatty acids	3.32	10.9	8.99
Fiber Minerals	6.0 6.0	3.8 3.8	3.8 3.8
Vitamins mixture Gelatin Water	1.5 3.0 5.5	0.96 3.0 23.5	0.96 3.0 23.5
Total kcal	359	351.1	351.1

C: Standard diet; SFO: C diet supplemented with fresh sunflower oil; SFOx: C diet supplemented with fried sunflower oil.

produce bone modeling and remodeling, ultimately shaping the adult jaw and providing mechanically fit morphology. During the power stroke of mastication, maximal muscle activity and bone strain occur[17], affecting mandibular bone mass, quantity and density, as well as mandibular length and width.

Lipids provided 17.5 % of the calories in the C diet, and 45% of the calories in the SFO and SFOx diets. SFO and SFOx were mixed with the rat chow at 13% (w/w) of diet. The oil compositions of the experimental diets were as follows: (1) SFO composition: n-6 Polyunsaturated Fatty acids (n-6 PUFA): 61.25%; n-3 PUFA: 0.07%; Monounsaturated Fatty acids (MUFA): 27.8%; Saturated Fatty acids (SFA): 10.1%; Trans fatty acids (TFA): 0.7%; (2) SFOx composition: n-6 PUFA: 46.78%; n-3 PUFA: 0%; MUFA: 33.15%; SFA: 18.09%; TFA: 1.66%. The diets contained calcium carbonate anhydrous at 40.04%, potassium phosphate monobasic at 22.76% and Vitamin D-3 (400 000 IU/g) (AIN-93G); 0.6 mg alpha-tocopherol equivalents/g PUFA were added to the high fat diets, as recommended by Valk and Hornstra[18].

Diets were prepared on alternate days and kept refrigerated. Food intake was measured (Mettler scale PC 4000; accuracy±1 mg) and the amount of diet consumed was expressed in grams per rat and per week (g/rat/wk) and as kcal per 100 g of body weight per day (kcal/100 g W/day).

Frying Procedure
The repeated frozen potato frying procedure was performed in standard commercially available 8L deep-fat fryer pots heated for 6 hours per day for a total 40 hours of frying. Sunflower oil oxidation was measured as previously described[8]. Polar compounds (triacylglycerol polymers, dimers, monomers, and oligomers, oxidized triacylglycerols, diacylglycerols and non-esterified fatty acids) were analyzed using a Testo device, Model 270, at 50° C.

Experimental design
The rats were randomly assigned to one of three different diets and had *ad libitum* access to food and water during the experiment.
Food was replaced on alternate days. The amount of food consumed and the total body weight were assessed weekly. Food efficiency for body weight gain (g of body weight gain/g of food intake in the same period) was calculated.
At the end of the experimental period (eight weeks), final body weights were determined and animals were euthanized by an intramuscular injection of anesthesia (0.1 ml of ketamine hydrochloride; 100 mg/ml, (Holliday Lab.) /100 g body weight mixed with 0.02 ml of xylazine; 100 mg/ml, (Konig Lab.) /100 g body weight. The right hemimandibles were dissected and cleaned of adhering soft tissue, weighed in a Mettler scale and stored at -20ºC wrapped in gauze soaked with Ringer's solution in sealed plastic bags, in accordance with Turner and Burr[6]. Each bone was thawed at room temperature and mandible weight was measured in g with a Mettler PE 600 scale (Zurich, Switzerland). Mandibular growth and mechanical properties were determined.
The same researcher measured all bone structures in order to reduce possible errors.

Zoometrics
Body weights (W) were measured in a Mettler PC 4000 scale; accuracy ± 0.001g and recorded weekly, after 2 to 4 hours fasting, throughout the experimental

period. Body weight gain was expressed in grams per rat between weeks (g/rat/wk).

Mandibular morphometric properties

Mandibular growth was assessed directly on the right hemimandible by obtaining measurements (to the nearest 0.05 mm) with digital calipers, as per Eratalay et al.[19] with modifications by Alippi et al.[20]. The dimensions, including mandibular area, length of the base, length of the mandible and mandibular height are shown in Fig. 1.

The mandibular length measurement was divided into anterior and posterior sections by a vertical line drawn perpendicular to the occlusal plane of the molars immediately posterior to the surface of the third molar.

These specific measurements were selected to provide data on the growth of the bone as a whole without taking into consideration its morphological units.

Biomechanical testing of the mandible

Mechanical properties of the rat right hemimandible were determined using a three-point bending mechanical test. Before testing, each bone was thawed at room temperature and biomechanical

Fig. 1: Mandible morphometric measurements.
Right hemimandible showing the bony points between which measurements were taken.
Mandibular height was the distance between the most posterior point of the angular process (II) and the most superior point of the coronoid process (III).
Mandibular length was determined by the distance between the most anterior superior point of the interdental space (IV) and the posterior point of the angular process (II). Mandibular length was divided into anterior and posterior sections by a vertical line drawn perpendicular to the occlusal plane of the molars immediately posterior to the surface of the third molar.
The length of the base of the jaw was estimated as the distance between I-II (the most anterior inferior bone point of the interdental space (I), the most posterior bone point of the angular process (II);
Mandible area was estimated by the triangle determined by I-II and III.

competence was determined as described in our previous publication[12].

Mechanical properties of the rat hemimandible were determined using an Instron model 4442 (Instron Corp., Canton, MA, USA), as described previously[21]. The plots of load v. deformation (W/d) were analyzed to determine the structural mechanical properties of the hemimandible; which measure the resistance to deformation (stiffness) and fracture (strength). The following measurements were recorded: Load at fracture (Wf, N), which directly expresses the resistance of the whole bone to fracture, incorporating both the elastic and the plastic behaviors; Load at yielding (Wy, N), which defines a threshold above which unrecoverable permanent deformation occurs, and Yielding deformation (dy, mm) at the yielding point, and structural stiffness or bone rigidity that represents the rigidity of the bone or the resistance to deformation (Wy/dy, N/mm)[21].

Statistical Analysis

Results were presented as mean values ± SD and/ or SE. Statistical analyses were performed using SPSS (v. 20.0 IBM Corp., Chicago, IL. USA) and GraphPad Prism (version 6.0). Comparisons between groups were analyzed by one-way analysis of variance. When a statistically significant difference was encountered, a Student–Newman–Keul's test or Dunn (non-parametric test) was performed. In all analyses, Bartlett's test for homogeneous variances was applied. Statistical significance was set at $p = 0.05$. The Kolmogorov–Smirnov test was used to determine whether data had normal distribution.

RESULTS

The incorporation of fatty acids in gelatin hydrogels caused no difference in diet viscosity; all three diets had a similar viscosity with 1.6 cPa at 20ºC. These data were similar to those reported by Lorenzo, Checmarev, Zaritzky and Califano [22].

Animal body weight patterns and food intake of all three groups are presented in Table 2 and Fig. 2A and 2B. At the beginning of the study, animal body weights did not differ significantly ($p = 0.6705$). However, total body weight was significantly altered by the type of dietary fat consumed during the experimental period. Total body weights were lower in the SFOx rats than in the other groups ($p = 0.0074$). From wk=2 to wk=6, SFOx rats ceased gaining weight ($p > 0.05$), while SFO rats gained
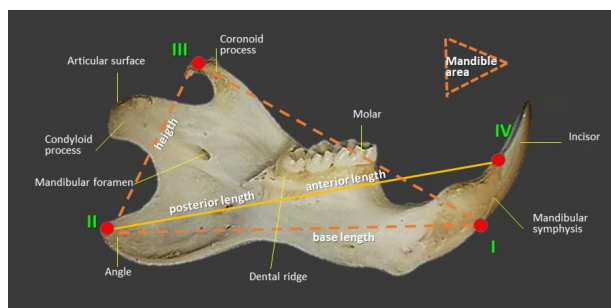
Table 2. Body weight, diet and fat intake

	CONTROL	SFO	SFOx	p†
Initial Body Weight (g)	53.8±10.9a	53.9±8.8a	57.7±7.6a	0.644ns
Final Body Weight (g)	344.3±20.4b	328.4±22.3b	307.4±13.8a	0.007**
Energy Intake (kcal/100gW/day)	24.8±1.4a	30.9 ± 2.7b	30.6 ± 2.9b	0.007**
Fat Intake (g/100gW/day)	0.49±0.1a	1.51±0.3b	1.52±0.3b	0.001***
SFA (g/100gW/day)	0.13±0.01a	0.22±0.02b	0.28±0.02c	0.001***
MUFA (g/100gW/day)	0.14±0.01a	0.44±0.07b	0.45±0.06b	0.001***
PUFA (g/100gW/day)	0.23±0.01a	0.98±0.02c	0.72±0.01b	0.001***
Linoleic acid (g/100gW/day)	0.07±0.01a	0.79±0.01c	0.55±0.02b	0.001***

C: Standard diet; SFO: C diet supplemented with fresh sunflower oil; SFOx: C diet supplemented with fried sunflower oil.
Mean values and SD for seven animals per group. Different letters mean significant differences between groups; "a" being the lowest.
†ANOVA and Student–Newman–Keul's test a posteriori
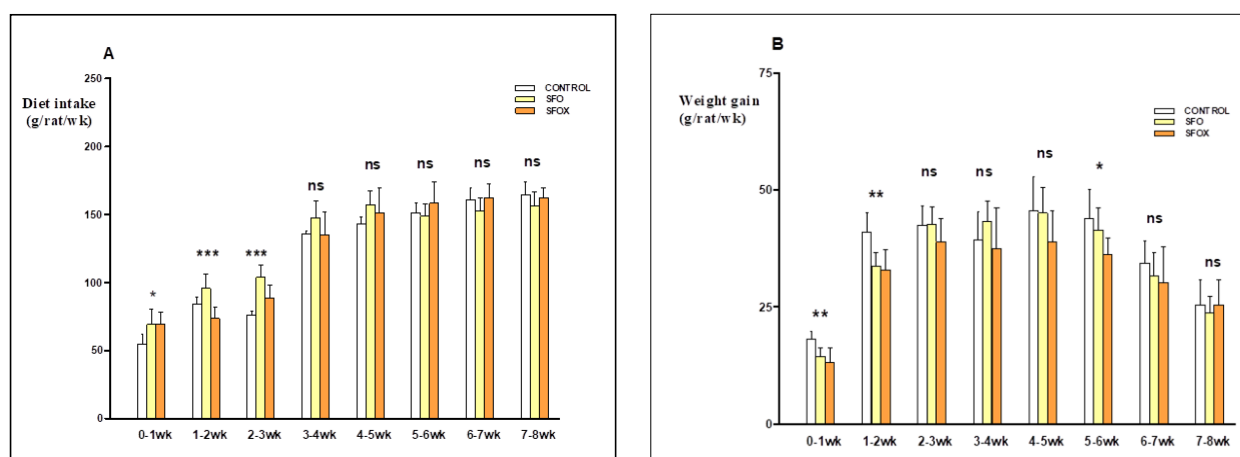** Indicates $p < 0.01$; ***$p < 0.001$, ns=no significant differences

Fig. 2: Diet intake per week throughout the study (A) and Food efficiency for body weight gain per week throughout the study (B).
Control (C): Standard diet; SFO: C diet supplemented with fresh sunflower oil; SFOx: C diet supplemented with fried sunflower oil.
†ANOVA and Student–Newman–Keul's test a posteriori
* Indicates $p < 0.05$; **$p < 0.01$; ***$p < 0.001$, ns=no significant differences

weight ($p < 0.01$). By the 6th week of the experiment, the SFOx group had the lowest body weight gain (Fig. 2B), while the body weight of SFO rats were similar to the C group ($p > 0.05$).

There was a substantial difference in food intake among the three rat groups during the first two weeks of the experiment. The SFOx rats ate less (73.4 (8.2) g/rat/wk) than the SFO (95.6 (10.7) g/rat/wk) ($p < 0.05$) and C groups (84.2 (5.3) g/rat/wk) ($p < 0.01$). However, after the third week, food intake was similar among all groups, both between weeks 2 and 5, and between weeks 6 and 8 of the

experiment (Fig. 2A). The efficiency of body weight gain per g of diet intake was assessed in the three groups when the amount of food consumed was stable (Fig. 2A, 2B). The SFOx group showed the lowest efficiency for gaining weight (C: 1.585 (0.138) = SFO: 1.516(0.136) > SFOx: 1.388(0.090) g/g; p = 0.021).

Animals that consumed SFO diets containing either fresh oil (SFO) or fried oil (SFOx) had higher energy consumption than the C rats (p = 0.0002), but there was no difference in energy intake between the two SFO groups (Table 2). SFOx consumption

Table 3. Morphometry of bone mandible

	CONTROL	SFO	SFOX	p†
Hemimandible weight (g)	0.43±0.02c	0.39±0.02b	0.36±0.02a	0.001***
Mandible height (mm)	12.6±0.24b	11.9±0.73a	11.8±0.24a	0.019*
Mandible length (mm)	25.6±0.24c	25.1±0.49b	24.6±0.24a	0.001***
Mandible base (mm)	26.03±0.65b	25.00±0.50a	24.80±0.26a	0.001***
Mandible area (mm²)	140.2±5.5b	129.5±6.9a	128.3±5.3a	0.006**
Mandible anterior part (mm)	14.24±0.45a	14.17±0.23a	14.09±0.43a	0.797ns
Mandible posterior part (mm)	11.4±0.3b	11.1±0.2b	10.7±0.2a	0.001***
Mandible anterior/posterior ratio	1.25±0.02a	1.27±0.02a	1.32±0.03b	0.004**

C: Standard diet; SFO: C diet supplemented with fresh sunflower oil; SFOx: C diet supplemented with fried sunflower oil.
Mean values and SD for seven animals per group. Different letters mean significant differences between groups; "a" being the lowest.
†ANOVA and Student–Newman–Keul's test a posteriori
*Indicates $p < 0.05$; **$p < 0.01$; ***$p < 0.001$, ns=no significant differences

caused a highly significant ($p = 0.0074$) negative consequence on body weight gain and final body weight, in comparison with the other two groups.

SFO and SFOx rats ate more total fat, monounsaturated fatty acids (MUFA) and SFA than C rats. SFO and SFOx groups did not differ significantly from each other. However, SFOx rats consumed less polyunsaturated fatty acids (PUFA), counting linoleic, arachidonic and linolenic acids, than SFO (Table 2).

The mandibular weight and length as an index of mandibular size were significantly lower in SFOx than in SFO and C rats ($p=0.0001$ and $p=0.0002$, respectively). The posterior section of the mandible of the SFOx rats was the most significantly affected area compared to the anterior section of the mandible of the rats fed on the other two diets ($p = 0.0005$); the anterior/posterior ratio indicated that SFOx ($p=0.0001$) induced mandibular deformation (Table 3 and Fig. 3).

Structural properties resulting from the slope of the load/deformation curve in the linear region of the elastic behavior are presented in Figure 4A, 4B, 4C. Load-bearing capacity (Wf) (A), load of yielding (Wy) (B) and stiffness (Wy/ dy) (C) of the mandible were adversely affected in rats that consumed either fresh SFO oil or fried SFOx, in comparison to the C group ($P = 0.001$, $P = 0.002$ and $P = 0.003$, respectively). Even though Wf and Wy did not differ significantly between SFO and SFOx groups, fried oil consumption caused a major reduction in Wy/dy.

Fig. 3: Photograph of rat mandible, lateral side, showing differential mandibular growth due to a diet containing fried sunflower oil.
Control (C): Standard diet; SFO: C diet supplemented with fresh sunflower oil; SFOx: C diet supplemented with fried sunflower oil.

DISCUSSION

To our knowledge, this is the first demonstration that a diet rich in fried sunflower oil has an impact on mandible morphometric properties and biomechanical competence, highlighting the importance of the research. This study demonstrated
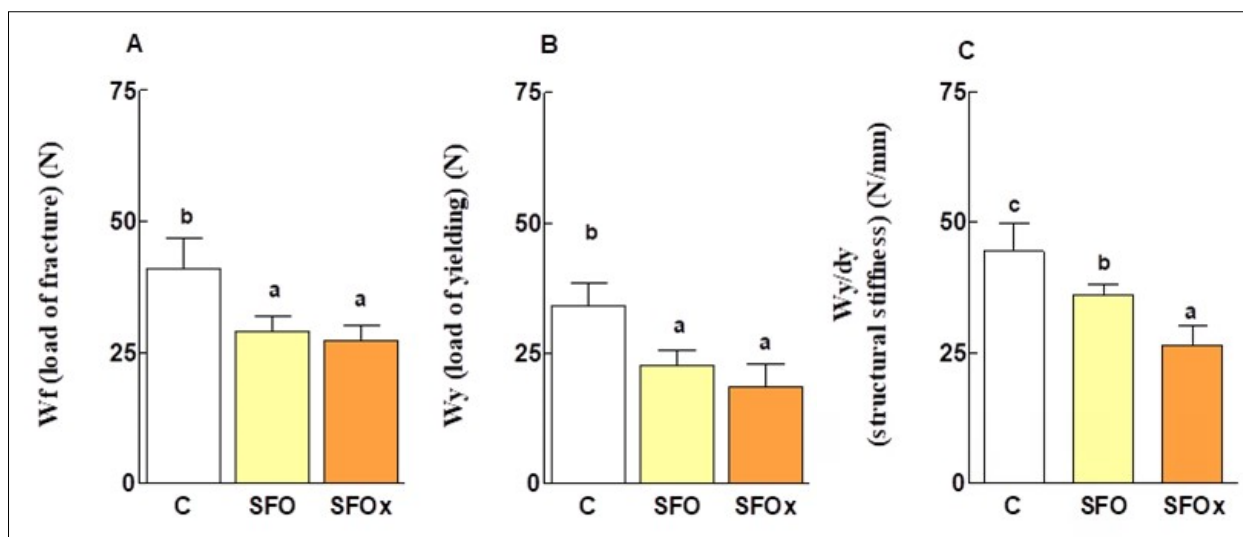
Fig. 4: Mandible structural properties
Load at fracture (Wf) (A), Load at yielding (Wy) (B) and Structural stiffness (Wy/dy) (C) of the mandible of control (C), SFO and fried sunflower oil SFOx groups. Mean values and SD for 7 animals per group. Values with different letters mean significant differences between groups (p < 0.05); "a" being the lowest.
C: Standard diet; SFO: C diet supplemented with fresh sunflower oil; SFOx: C diet supplemented with fried sunflower oil.
†ANOVA and Student-Newman-Keul's test a posteriori.

that in healthy, growing male rats, a diet containing fried sunflower oil was detrimental to body and mandible growth, and mandible biomechanics. It demonstrated that SFOx consumption caused a highly significant negative effect on body growth, compared to the other two rat groups. Additionally, the mandible of SFOx rats had significantly lower bone weight and length, as indices of mandibular size.

The study also showed that the differences in mandible stiffness and strength induced by SFOx consumption appeared to be the result of decreased gain of bone structural properties. Bone mechanical quality (structural properties) depends on the combination of the mechanical quality of the mineralized tissue (material stiffness mostly related to collagen mineralization) and the architectural quality of the structural bone design, size, shape and architectural distribution of mineralized tissue[23].

The observed mandibular changes in bone mineral content and spatial distribution of mineralized tissue did not reflect altered bone material properties of other bones; a previous study showed that the mechanical competence of the femur of SFOx rats was not affected[8]. In contrast, thermoxidazed oil consumption has been found to alter cardiovascular status, femur mass and biomechanical competence[6,7]. Rat mandible and femur have also been demonstrated

to have different performance in growing rats subjected to chronic suboptimal nutrition[12] or in those fed imbalanced diets[24].

The rat mandible may be divided into an anterior section comprising the alveolar and symphysial regions and a posterior section comprising the condyloid, the coronoid and the angular process. In the weaning rat, the length of the posterior section of the mandible is about one-half of the anterior section[15]. There is a relative enlargement of the posterior section of the mandible to more than twice as much as that of the anterior section due to the rapid growth of the condyle and the cartilage of the mandible, situated in the posterior section. The growth rates are different between the two sections of the bone mandible, which attain equal lengths in adulthood.

The condyle located in the posterior area operates as the main center of regional adaptive growth. The regulation of its development is defined by genetic and epigenetic factors that modify the expression of transcription and growth factors[25]. The mandibular condyle is a secondary cartilage that it is not surrounded by a cartilaginous matrix, and is therefore not isolated from the influences of local factors. However, the condyle responds to functional and mechanical loads; its frequent stimulation triggers a series of events that increase

the number of replicating mesenchymal cells[25].

In the current study, the masticatory load did not differ among the three diets fed to the rats. All three diets were prepared to attain similar consistency, since studies in growing rodents have demonstrated that masticatory function induces morphological modifications in the mandible[26]. Moreover, the masticatory system is a complex musculoskeletal system where activation of the masticatory muscles, movements of the jaw, loads and deformations, in both the jaw and the temporomandibular joint, are directly interconnected. The potential harmful effect of fried oil on mandibular growth becomes evident on the posterior section of the bone ("anterior/posterior ratio" altered in SFOx versus SFO and C rats [p = 0.0001]). In contrast, the anterior section, where the teeth are located and which determines the mandibular movements, was unaffected.

In rats, as in humans, most muscles are inserted in the posterior section of the mandible. In rodents, mandibular movements slide from front to back, whereas in humans, the movements open, close, and move laterally. Most of these movements depend on the incorporated muscles and are facilitated by the temporo-mandibular joint[17]. The consumption of a SFOx diet during growth appears to affect mandibular dynamics. Further studies may elucidate which sector of the posterior section was altered or whether the reduction was harmonious.

The ingredients in the diets employed for testing could also play a role in the decreased mandibular mass. The findings of the rats fed SFOx could be related to the decreased PUFA levels and/or the increase in total saturated fat rather than the source of the dietary oil. In previous studies, we demonstrated that rats fed a high-saturated fatty acid diet for eight weeks had lower bone mineral density (spine BMD) and total skeleton bone mineral content (BMC) than rats that consumed other types of vegetable oils[27]. The rats that consumed high-fat vegetable oil diets, regardless of the diverse omega-6 (n-6) polyunsaturated fatty acid (n-6 PUFA)/omega-3(n-3) PUFA ratio, gained total skeleton BMD, BMC, and BMC per total body weight (BMC/W) similar to the animals fed the control diet proposed by the American Institute of Nutrition (AIN) committee in 1993 to provide the increased nutritional requirements for rat or mouse growth (AIN 93G) formulation[28]. It is recognized that a diet rich in saturated fatty acids could increase

inflammatory cytokine expression and NF-kB ligand receptor activator, which has been found to stimulate bone resorption and disturb osteoblast genesis, leading to negative effects on bone[29,30].

The presence of dietary n-6 and n-3 PUFA are important because prostaglandins (PGs) are a group of lipid mediators formed from arachidonic acid in various tissues under several physiological and pathophysiological circumstances, and serve to sustain local homeostasis[31]. Among them, PGE works in a bimodal manner in bone metabolism; PGE2 at high concentrations powerfully induces bone resorption[32]. Further, in vitro studies have demonstrated that cyclooxygenase 2 (COX-2) and PGE2 stimulate receptor activator of nuclear factor kappa-B ligand (RANKL) expression and downregulate osteoprotegerin (OPG) expression, and that disruption of the balance of RANKL/OPG stimulates osteoclastogenesis[33]. Other studies demonstrated that the type of dietary fat conditioned age-related alveolar bone loss, and that the presence de n-6PUFA from sunflower oil was responsible for higher age-related alveolar bone loss. The mechanisms involved in this phenomenon were associated with an ablation of the cell ability to adapt to aging.

In this study, the lack of decrease in mandibular mass in the SFO group compared to SFOx rats suggests that the high n-6 PUFA content exceeded the rat requirements. Fried oils, particularly sunflower oil, induced more deleterious effects on mandible than did the excess of n-6 PUFA. The adverse consequence of consuming SFOx diet on bone mass was weakened bone strength and structural stiffness of the mandible and the mandibular area. However, mandibular mass and structural mandible strength increased proportionally with body mass. Our previous studies demonstrated the prominent role of thermoxidazed oil consumption in determining the risk for growth and cardiovascular and bone effects. The consumption of a diet rich in sunflower oil did not affect final body weight and length; in contrast, the intake of SFOx induced a lower final body growth[8].

The alterations in bone stiffness and strength induced by the consumption of SFOx diet by growing healthy male rats appeared to decrease bone structural properties with a loss in bone. In fact, the structural properties of the entire bone are established by the physicochemical nature of

its calcified matrix (material properties focused on the rigidity of the tissue) and by the architectural distribution. Changes in bone structural properties could be due to modifications in mass and its spatial distribution (geometry)[7]. Mechanical loading of the mandible during mastication affects the mass, density and microarchitecture of the mandibular alveolar bone[14,34]. Finally, our results raise an important consideration for future studies on rat mandible using micro-computed tomography (μCT) system for the evaluation of bone micro-architecture. This study was designed to feed young male rats a diet rich in fried oil that resembles the diet patterns of Argentinian children. These experimental results in growing rats may enable some responses in children fed similar diets to be foreseen. However, according to the Argentinian Second National Nutrition and Health Survey (2019), children and adolescents have eating patterns that differ from those of adults: children consume twice as many pastry products or salted snacks, and 2- to 12-year-olds eat almost three times more confectionery products than adults (26.5% vs. 10.5% respectively)[35].

CONCLUSIONS

Traditionally, the consumption of fried foods has been associated to cardiovascular diseases and obesity. We demonstrated that SFOx diets are inversely related to bone health. These findings evidenced the negative effects of fried sunflower oil consumption on total body growth and mandible alterations. These adaptations induced alterations in mandible dynamics and bone biomechanical competence, in terms of bone stiffness.

REFERENCES

1. Zapata ME, Rovirosa A, Carmuega E. Changes in the food and beverage consumption pattern in Argentina, 1996-2013. Salud Colect 2016;12(4):473-486. https://doi: 10.18294/sc.2016.936

2. Chuang H-C, Huang C-F, Chang Y-C, Lin Y-S et al. Gestational ingestion of oxidized frying oil by c57bl/6j mice differentially affects the susceptibility of the male and female offspring to diet-induced obesity in adulthood. J Nutr 2013;143(3):267-73. https://doi: 10.3945/jn.112.168948

3. Cahill LE, Pan A, Chiuve SE, Sun Q et al. Fried-food consumption and risk of type 2 diabetes and coronary artery disease: A prospective study in 2 cohorts of US women and men. Am J Clin Nutr 2014; 100(2): 667–675. https://doi: 10.3945/ajcn.114.084129

4. Owu DU, Osim EE, Ebong PE. Serum liver enzymes profile of Wistar rats following chronic consumption of fresh or oxidized palm oil diets. Acta Trop 1998;69(1):65-73. https://doi: 10.1016/s0001-706x(97)00115-0

5. Shuid AN, Chuan LH, Mohamed N, Jaarin K et al. Recycled palm oil is better than soy oil in maintaining bone properties in a menopausal syndrome model of ovariectomized rat. Asia Pac J Clin Nutr 2007;16(3):393-402. https://doi: 10.6133/apjcn.2007.16.3.02

6. Turner CH, Burr DB. Basic biomechanical measurements of bone: A tutorial. Bone 1993;14(6):595-608. https://doi: 10.1016/8756-3282(93)90081-k

7. Ferretti JL. Biomechanical Properties of Bone. In: Genant H, Guglielmi G, Jergas M, editors. Bone Densitometry and Osteoporosis. Berlin, Heidelberg: Springer Berlin Heidelberg; 1998. p. 143–161. http://link.springer.com/10.1007/978-3-642-80440-3_8

8. Macri EV, Ramos C, Bozzini C, Zago V et al. Fried sunflower oil intake affects bone quality, in growing rats. Curr Res Nutr Food Sci 2019; 7(1). http://dx.doi.org/10.12944/CRNFSJ.7.1.06

9. Alsina E, Macri EV, Lifshitz F, Bozzini C et al. Efficacy of phytosterols and fish-oil supplemented high-oleic-sunflower oil rich diets in hypercholesterolemic growing rats. Int J Food Sci Nutr 2016;67(4):441-53. https://doi.org/10.3109/09637486.2016.1161010

10. Srinivasan K, Naula DP, Mijares DQ, Janal MN et al. Preservation and promotion of bone formation in the mandible as a response to a novel calcium-phosphate based biomaterial in mineral deficiency induced low bone mass male versus female rats. J Biomed Mater Res A 2016;104(7):1622-32. https://doi.org/10.1002/jbm.a.35691

11. Compagnucci G, Compagnucci C, Olivera M, Roig M et al. Estudio comparativo morfométrico, densitométrico y biomecánico del esqueleto apendicular y axial en un modelo animal de enanismo por desnutrición. Revista Argentina de Osteología. 2005;4:10–24. Spanish.

12. Lezón CE, Pintos PM, Bozzini C, Romero AA et al. Mechanical mandible competence in rats with nutritional growth retardation. Arch Oral Biol. 2017;80:10-17. https://doi.org/10.1016/j.archoralbio.2017.03.009

13. Alippi RM, Picasso E, Huygens P, Bozzini CE et al. Growth-dependent effects of dietary protein concentration and quality on the biomechanical properties of the diaphyseal rat femur. Endocrinol Nutr. 2012;59(1):35-43. https://doi.org/10.1016/j.endonu.2011.09.005

14. van Eijden TM. Biomechanics of the Mandible. Crit Rev Oral Biol Med 2000; 11(1):123-36. https://doi.org/10.1177/10454411000110010101

15. Bozzini C, Champin GM, Bozzini CE, Alippi RM. Growth inhibition in rats fed inadequate and incomplete proteins: repercussion on mandibular biomechanics. Acta Odontol Latinoam 2013;26(1):43-53

16. Marcotte M, Hoshahili ART, Ramaswamy HS. Rheological properties of selected hydrocolloids as a function of concentration and temperature. Food Research International 2001;34:695–703. https://doi.org/10.1016/S0963-9969(01)00091-6

17. Buvinic S, Balanta-Melo J, Kupczik K, Vásquez W et al. Muscle-bone crosstalk in the masticatory system: From biomechanical to molecular interactions. Front Endocrinol (Lausanne). 2021 Mar 1;11:606947. https://doi.org/10.3389/fendo.2020.606947

18. Valk, Hornstra G. Relationship Between Vitamin E Requirement and Polyunsaturated Fatty Acid Intake in Man: a Review. Int J Vitam Nutr Res 2000;70(2):31-42. https://doi.org/10.1024/0300-9831.70.2.31

19. Eratalay YK, Simmons DJ, El-Mofty SK, Rosenberg GD, Nelson W, Haus E, Halberg F. Bone growth in the rat mandible following every-day or alternate-day methylprednisolone treatment schedules. Arch Oral Biol 1981;26(10):769-77. https://doi.org/10.1016/0003-9969(81)90172-2

20. Alippi RM, Meta MD, Boyer PM, Bozzini CE. Catch-up in mandibular growth after short-term dietary protein restriction in rats during the post-weaning period. Eur J Oral Sci 1999;107(4):260-4. https://doi.org/10.1046/j.0909-8836.1999.eos107405.x

21. Hogan HA, Groves JA, Sampson HW. Long-Term Alcohol Consumption in the Rat Affects Femur Cross-Sectional Geometry and Bone Tissue Material Properties. Alcohol Clin Exp Res 1999;23(11):1825-33. https://doi.org/10.1111/j.1530-0277.1999.tb04079.x

22. Lorenzo G, Checmarev G, Zaritzky N, Califano A. Linear viscoelastic assessment of cold gel-like emulsions stabilized with bovine gelatin. LWT - Food Science and Technology 2011;44:457–464. https://doi.org/10.1016/j.lwt.2010.08.023

23. Bozzini C, Picasso EO, Champin GM, Alippi RM et al. Biomechanical properties of the mid-shaft femur in middle-aged hypophysectomized rats as assessed by bending test. Endocrine 2012;42(2):411-8. https://doi.org/10.1007/s12020-012-9616-0

24. Bozzini CE, Champin GM, Alippi RM, Bozzini C. Biomechanical properties of the mandible, as assessed by bending test, in rats fed a low-quality protein. Arch Oral Biol 2013;58(4):427-34. https://doi.org/10.1016/j.archoralbio.2012.08.007

25. Romero Peláez CM, Torres Murillo EA, Pinto Parada YA. Crecimiento del cartílago condilar. Una revisión de la literatura. Odontol Sanmarquina 2018; 21(2):131-40. https://doi.org/10.15381/os.v21i2.14779

26. Tsolakis IA, Verikokos C, Perrea D, Bitsanis E et al. Effects of diet consistency on mandibular growth. A review. J Hellenic Vet Med Soc 2019 ;70:1603. https://doi.org/10.12681/jhvms.21782

27. Macri E V., Gonzales Chaves MM, Rodriguez PN, Mandalunis P et al. High-fat diets affect energy and bone metabolism in growing rats. Eur J Nutr 2012;51(4):399-406. https://doi.org/10.1007/s00394-011-0223-2

28. Reeves PG, Nielsen FH, Fahey GC. AIN-93 purified diets for laboratory rodents: Final report of the American Institute of Nutrition ad hoc writing committee on the reformulation of the AIN-76A rodent diet. J Nutr 1993;123(11):1939-51. https://doi.org/10.1093/jn/123.11.1939

29. Cao JJ, Gregoire BR. A high-fat diet increases body weight and circulating estradiol concentrations but does not improve bone structural properties in ovariectomized mice. Nutr Res 2016;36(4):320-327. https://doi.org/10.1016/j.nutres.2015.12.008

30. Tian L, Yu X. Fat, Sugar, and Bone Health: A Complex Relationship. Nutrients 2017;9(5):506. https://doi.org/10.3390/nu9050506

31. Narumiya S, Sugimoto Y, Ushikubi F. Prostanoid receptors: structures, properties, and functions. Physiological reviews 1999;79:1193–1226. https://doi.org/10.1152/physrev.1999.79.4.1193

32. Bilezikian JP, Clemens TL, Martin TJ, Rosen CJ. Principles of bone biology [Internet]. 1st ed. Bilezikian JP, Raisz LG (Lawrence G, Rodan GA, editors. Principles of Bone Biology. San Diego: Elsevier; 2019. Available from: https://linkinghub.elsevier.com/retrieve/pii/C20151016222.

33. Zhu C, Ji Y, Liu S, Bian Z. Follicle-stimulating hormone enhances alveolar bone resorption via upregulation of cyclooxygenase-2. Am J Transl Res. 2016 Sep 15;8(9):3861-3871.

34. Mavropoulos A, Rizzoli R, Ammann P. Different responsiveness of alveolar and tibial bone to bone loss stimuli. J Bone Miner Res. 2007 Mar;22(3):403-10. https://doi.org/10.1359/jbmr.061208

35. Abeyá Gilardon E, Drake I, Elorriaga N, Mangialavori G et al. Indicadores priorizados - Segunda Encuesta Nacional de Nutrición y Salud 2019; p. 1–78. https://www.researchgate.net/publication/339415556

The luminous transmittance of the quartz-glass fiber posts is superior to glass fiber posts

Ana CP Pasmadjian[1] , Alysson N Diógenes[2] , Camila P Perin[3] , Juliana Pierdoná[3] ,
Liliana VML Rezende[1] , Isabela R Madalena[4,5,6] , Flares Baratto-Filho[3,4] ,
Leonardo F da Cunha[1]

1. Universidade de Brasília, Faculdade de Ciências da Saúde, Brasília, Brasil.
2. Universidade Positivo, Faculdade de Engenharia Civil, Curitiba, Brasil.
3. Universidade Tuiuti do Paraná, Curitiba, Brasil.
4. Universidade da Região de Joinville, Faculdade de Odontologia, Joinville, Brasil.
5. Centro Universitário Presidente Tancredo de Almeida Neves, Faculdade de Odontologia, São João del Rei, Brasil.
6. Universidade de Uberaba, Departamento de Biomateriais, Uberaba, Brasil.

ABSTRACT

*Fiber-reinforced prefabricated intraarticular posts have gained popularity due to several favorable characteristics for clinical use compared to metallic intraradicular posts. **Aim:** To evaluate the light transmission capacity of two types of fiber posts, using two different methods. **Materials and Method:** The posts were divided into two groups: experimental group - quartz-glass fiber posts (n=10) and control group – glass fiber posts (n=10). The light transmittance of the samples was compared by means of light intensity test by photographs and ultraviolet-visible spectrophotometer. This test was analyzed by thirds: coronal, middle, and apical. The spectophotometer tested the luminous transmittance along the length of the post. The statistical analysis was conducted with a significance level of 0.05. **Results:** Light transmission was 97% on the coronal third, 68% in the middle third, and 27.66% in the apical third in the posts of the experimental group. In the posts of the control group, the light transmission was 95.33% in the coronal third, 80.66% in the middle third, and 41.33% in the apical third. Light transmission was significantly higher in the middle third of the posts of the experimental group when compared to the control group (p<0.05). The luminous transmittance of the posts of the experimental group was 97.4% with wavelengths of 400 nm, 97% at 450 and 500 nm, and 96.9% at 550 nm. In the posts of the control group, the luminous transmittance was 72.3% with wavelengths of 400 nm, 68.6% at 450 nm; 64.6% at 500 nm and 61.5% at 550 nm. The posts of the experimental group demonstrated significantly higher light transmittance than the control group (p<0.001). **Conclusion:** the luminous transmittance of quartz-glass fiber posts is higher than glass fiber posts.*

Keywords: dental pins - photoelectron spectroscopy - light.

Superioridade da transmitância luminosa dos pinos de fibra de quartzo

RESUMO

*Os pinos intra-articulares pré-fabricados reforçados com fibras têm ganhado popularidade devido a várias características favoráveis ao uso clínico em comparação com os pinos intra-radiculares metálicos). **Objetivo:** Avaliar a capacidade de transmissão de luz de dois tipos de pinos de fibra, usando dois métodos diferentes. **Materiais e Método:** Os pinos foram divididos em dois grupos: grupo experimental - pinos de fibra de vidro de quartzo e grupo controle - pinos de fibra de vidro. A transmitância de luz das amostras foi comparada por meio de teste de intensidade de luz por fotografias e espectrofotômetro ultravioleta-visível. Este teste foi analisado por terços: coronal, médio e apical. O espectrofotômetro testou a transmitância luminosa ao longo do comprimento do pino. A análise estatística foi realizada com nível de significância de 0,05. **Resultados:** A transmissão luminosa foi de 97% no terço coronal, 68% no terço médio e 27,66% no terço apical nos pinos do grupo experimental. Nos pinos do grupo controle, a transmissão de luz foi de 95,33% no terço coronal, 80,66% no terço médio e 41,33% no terço apical. A transmissão luminosa foi significativamente maior no terço médio dos pinos do grupo experimental quando comparado ao grupo controle (p<0,05). A transmitância luminosa dos pinos do grupo experimental foi de 97,4% com comprimento de onda de 400 nm, 97% em 450 e 500 nm e 96,9% em 550 nm. Nos postes do grupo controle, a transmitância luminosa foi de 72,3% com comprimento de onda de 400 nm, 68,6% em 450 nm; 64,6% a 500 nm e 61,5% a 550 nm. Os pinos do grupo experimental demonstraram transmitância de luz significativamente maior do que o grupo controle (p<0,001). **Conclusão:** a transmitância luminosa dos pinos de fibra de vidro de quartzo é maior do que pinos de fibra de vidro.*

Palavras-chave: pinos dentários - espectroscopia fotoeletrônica - luz.

INTRODUCTION

Fiber-reinforced prefabricated intraarticular posts have gained popularity due to several favorable characteristics for clinical use compared to metallic intraradicular posts.[1,2] Notable qualities of the material include dentin-like mechanical properties, the ability to adhere to the root structure, and good esthetics[2,3]. Scientific evidence demonstrates that prefabricated fiber-reinforced posts have an elastic modulus around 20 Gpa[4-6], which is very similar to dentin (18 GPa)[7]. The convergence of properties standardizes the stress distribution and reduces the risk of fracture[8-10]. Another relevant aspect of fiber-reinforced prefabricated intraradicular posts is their ability to transmit light, enhanced by the association of carbon, glass, quartz, and zirconia fibers[11]. Translucent posts can allow lighter to pass through, improving the depth and quality of polymarization of the material chosen for cementation[12-14].

Carbon fibers represent one of the first prefabricated posts available on the market. They are composed of unidirectional carbon fibers inserted in an epoxy resin matrix. They no longer represent routine use in clinical practice, mainly due to their dark color, which impairs the aesthetics of the restoration[15]. Glass fiber posts can be made of two types: S-glass and E-glass. They have different properties, but generally, are amorphous, and they are formed of a three-dimensional network of silica, with oxygen and other atoms arranged randomly[16]. Furthermore, Glass fiber posts can be associated with quartz fibers, which are pure silica in their crystallized form. Posts reinforced with glass and quartz fiber lead to better stress distribution when compared to rigid metal posts or zirconium oxide ceramic posts[14]. Fiber-reinforced posts also have advantageous optical properties over metallic post systems, reinforced by carbon fibers or metal oxide post systems[16].

Glass fibers posts have a refractive index like resin; therefore, they allow efficient light transmission[16,17]. Consequently, the addition of glass fibers to the dental composite will improve its mechanical properties without affecting the degree of conversion of the resin matrix, unlike opaque-colored fibers, as carbon, or zirconia[12,16]. The clinician must realize that there are recognizably substantial differences in the mechanical load capacity of different fiber-reinforced posts and must be aware of such differences to select an appropriate post system to use[18]. Therefore, the aim of this study was to evaluate the luminous transmittance of quartz-glass fiber posts and conventional fiberglass posts.

MATERIAL AND METHOD

Experimental design

Quartz-glass fiber posts and glass fiber posts were evaluated for light transmittance using photo light intensity test and ultraviolet visible and infrared spectrophotometer. The posts were divided into two groups: the experimental group - quartz-glass fiber posts (n=10) and the control group – glass fiber posts (n=10). The posts in the experimental group are made by optical fiber, epoxy resin and glass fiber. The exact proportion is not revealed by factory. The composition of the glass fiber posts (Exacto®, Angelus Londrina, PR, Brazil) is 80% fibers glass and 20% epoxy resin. Both have a length of 18 mm, conical with the same maximum and minimum diameters of, respectively, 1.8 and 1.0 mm.

Analysis of the light transmittance using photo light intensity test

The light intensity was made with a LED dental curing-light Radii Expert SDI and a camera Canon 70D with lens macro 100mm and exposure settings in ISO 100, aperture F18 and shutter speed 125, therefore resulting in images of 5,612x3,440 pixels in RAW format. The spectrophotometer was connected to a computer running the spectrum analyzer software (OOIBase32, Ocean Optics). The software was set in a mode to evaluate the light counts correlating with the number of photons received from the spectrometer's CCD detector. At the test of 470 nm, to each count, 30 photons were received on the equipment's detector.

The counts were registered in total light-darkness for ten posts from each group. The posts were vertically positioned over a bench with the curing light Radii Expert SDI leaning at the cervical region. Furthermore, the photos of the posts irradiated by the light-curing device were taken in complete darkness (Canon 70D with lens Macro 100mm). The photos were divided in thirds: coronal, middle and apical.

Analysis of the light transmittance using ultraviolet-visible spectophotometer

The same posts were sanitized with 70% alcohol, stored in Eppendorf flasks and always handled with procedure gloves. After distribution and sample

identification, they were submitted to an ultraviolet visible and near infrared spectrophotometer (Cary 5000 UV-Vis-NIR Spectrophotometer®, Agilent Technologies, Santa Clara, Califórnia, EUA). The mean exposure time was set at 10s, and the application distance was set at 10mm. The analyzed wavelengths were 400 nm, 450 nm, 500 nm and 550 nm. Light transmission was measured using an optical transmission microscope coupled to spectrometer. The upward referenced light source was transmitted through the edge of the cut and measured the percentage of light intensity (compared to the 100% reference) for each post. Values were given as the percentage of incident light measured at the opposite length of the post.

Statistical analysis

The analyzed all groups of specimens for means and standard deviations. The statistical analysis was performed by testing data normality using the Shapiro–Wilk test followed by Welch's t-test, with a significance level of 0.05.

RESULTS

In the transmission of light in the posts of the experimental group was 97% on the coronal third, 68% in the middle third, and 27.66% in the apical third. In the posts of the control group, the light transmission was 95.33% in the coronal third, 80.66% in the middle third, and 41.33% in the apical third (Fig. 1). Figure 2 represents the difference in light transmittance in relation to the experimental and control fiber posts, respectively. Light transmission was significantly higher in the middle third of the posts of the experimental group when compared to the control group (p=0.0155) (Table 1).
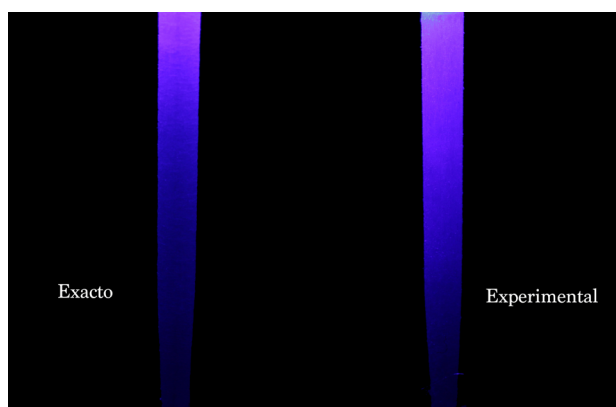

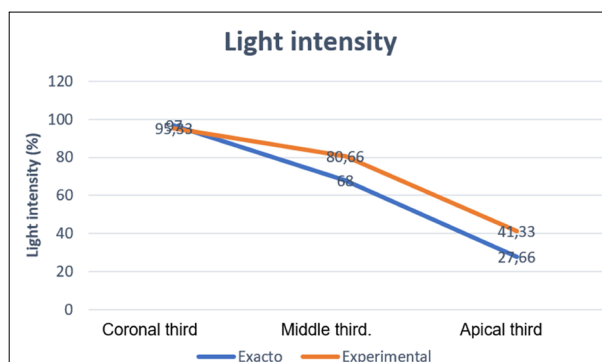*Fig. 1: Luminous transmittance between the thirds of the posts of the experimental and control groups.*

Fig. 2: Illustrated photo of the luminous transmittance between the thirds of the posts of the experimental and control groups, respectively.

Table 1. Means (standard deviations) of groups as a function of third.

Group	Coronal	Mean	Apical
Exacto	97.00 (1.00)[a]	68.00 (4.35)[c]	27.66 (1.52)[d]
Experimental	95.33 (0.57)[a]	80.66 (4.61)[b]	41.33 (9.45)[d]

*Values followed by the same letter are statistically similar (p > 0.05).

The luminous transmittance of the posts of the experimental group was 97.4% with om wavelengths of 400 nm, 97% at 450 and 500 nm, and 96.9% at 550 nm. In the posts of the control group, the luminous transmittance was 72.3% with wavelengths of 400 nm, 68.6% at 450nm; 64.6% at 500nm and 61.5% at 550 nm (Fig. 1). The values of light transmittance measured by spectrometer (mean and standard deviations) and the differences in the groups are shown in Table 2. The post of the experimental group demonstrated significantly higher light transmittance than the control group (p<0.001).

Table 2. Means (standard deviations) transmittance of the groups.

Group	Transmittance
Exacto	0.66 (0.32)[b]
Experimental	0.97 (0.02)[a]

Figure 3 is related to the linear representation of the data obtained, in which the experimental group showed greater homogeneity and stability in light transmission throughout the analyzed spectrum (close to 0.97). The control group showed the greatest change throughout the analysis, and at the wavelength of 550 nm, there was the lowest mean transmittance (0.615); while the highest transmittance occurred at 400 nm, (0.723).

Fig. 3: Values of linear representation of the data obtained from the light transmittance of the groups as a function of the wavelength.

DISCUSSION

In this study, the luminous transmittance through glass fiber posts and quartz-glass fiber posts was investigated. According to the results of this *in vitro* study, quartz-glass fiber posts showed significantly better luminous transmittance compared to glass fiber posts. The null hypothesis tested in this study that the luminous transmittance of different glass fiber posts would not differ was therefore rejected. From a clinical point of view, this may indicate better polymerization of the cementing agent used in the root canal[18].

Resin-based cement is widely used today for the cementation of various indirect dental restorations that have received intraradical support[19]. Dual-curing resin-based types of cement are clinically preferred over purely light-curing types of cement because the former can better tolerate light exposure in locations that do not allow optimal access to curing light due to indirect-direction morphology[19,20]. Compared to photopolymerizable resin-based materials, free radical-mediated polymerization of dual-polymerized materials is more complex, as two initiation reactions occur simultaneously and interact with each other[21]. Recognition of this complexity led to numerous studies on dual-polymerization resin types of cement[20] and, among other specificities, also the availability of the intraradical retainer in relation to luminous transmittance[11-14].

Scientific evidence shows that there is no difficulty for light to reach a more superficial region of the intraradicular post[14,22-25]. In this study, the evaluate of luminous transmittance was performed in thirds; the depth was defined in millimeters at six pre-established points[22]. Our results showed significantly higher luminous transmittance in the middle third of the quartz-glass fiber post when compared to the glass fiber post. This fact becomes important since favorable degrees of cure of the cementing agent have been described in depths above 8mm[23,26]. Silva et al. studied the degree of conversion after the cementation of two types of posts at three levels of depth and demonstrated statistically favorable results between the middle thirds of the two types of posts also related to translucency[23].

The luminous transmittance of glass fiber posts and zirconia, quartz, and silica have already been previously tested[27]. However, methodological differences were found in the digital camera, in the variety of posts designs such as, non-standard diameter and lengths, and a more robust sample. Thus, replication of this study is suggested, considering the results of the apical third. In the apical third, the *p-value* was very close to the significance level. The null hypothesis could be rejected if the sample was larger.

Regarding luminous transmittance analyzed by the UV/Vis spectrophotometer, better luminous transmittance was also demonstrated by the quartz-glass fiber posts, which may be related to the type and arrangement of the fibers, thus increasing the

luminous transmission values. The result of this method can be considered extremely efficient in the present study, as the posts have the same design both in length and thickness. When irradiation occurs, the light beams are distributed along the posts by total internal reflection. The critical angle is the product of the difference in refractive indices between the core and surface material. Rays that exceed the surface boundary of the material at an angle greater than the critical angles are reflected[27]. Thus, differences in optical properties are explained by variability in fiber diameter, orientation pattern and variable matrix composition. All these factors contribute to refraction

divergences and make it difficult to compare posts from different commercial brands[8,11-14,27,28].

The two luminous transmittance methods used in this study should be carefully used to estímate clinical performance. However, they can be correlated with the bond strength tests of the posts to the resin cement in the root canal, thus explaining possible favorable results for the quartz-glass fiber posts due to the greater luminous transmittance.

CONCLUSION

Quartz-glass fiber posts show significantly better light transmittance compared to glass fiber posts.

CONFLICT OF INTEREST

The authors declare no potential conflicts of interest regarding the research, authorship, and/or publication of this article.

REFERENCES

1. Wang X, Shu X, Zhang Y, Yang B et al. Evaluation of fiber posts vs metal posts for restoring severely damaged endodontically treated teeth: a systematic review and meta-analysis. Quintessence Int 2019;50:8-20 https://doi.org/10.3290/j.qi.a41499

2. Sarkis-Onofre R, Amaral Pinheiro H, Poletto-Neto V, Bergoli CD et al. Randomized controlled trial comparing glass fiber posts and cast metal posts. J Dent 2020;96:103334. https://doi.org/10.1016/j.jdent.2020.103334

3. Lassila LV, Tanner J, Le Bell AM, Narva K et al. Flexural properties of fiber reinforced root canal posts. Dent Mater 2004;20:29–36. https://doi.org/10.1016/S0109-5641(03)00065-4

4. Bateman G, Ricketts DN, Saunders WP. Fibre-based post systems: a review. Br Dent J 2003;195:43–48. https://doi.org/10.1038/sj.bdj.4810278

5. Novais VR, Quagliatto PS, Bona AD, Correr-Sobrinho L et al. Flexural modulus, flexural strength, and stiffness of fiber-reinforced posts. Indian J Dent Res 2009;20:277–281. https://doi.org/10.4103/0970-9290.57357

6. Lamichhane A, Xu C, Zhang FQ. Dental fiber-post resin base material: a review. J Adv Prosthodont 2014;6:60-5. https://doi.org/10.4047/jap.2014.6.1.60

7. Chun K, Choi H, Lee J. Comparison of mechanical property and role between enamel and dentin in the human teeth. J Dent Biomech 2014;5:1758736014520809. https://doi.org/10.1177/1758736014520809

8. Amižić I, Baraba A, Ionescu AC, Brambilla E et al. Bond strength of individually formed and prefabricated fiber-reinforced composite posts. J Adhes Dent 2019;21:557-565. https://doi.org/10.3290/j.jad.a43649

9. Ranjkesh B, Haddadi Y, Krogsgaard CA, Schurmann A et al. Fracture resistance of endodontically treated maxillary incisors restored with single or bundled glass fiber-reinforced composite resin posts. J Clin Exp Dent 2022;14:e329-e333. https://doi.org/10.4317/jced.59373

10. Santos TDSA, Abu Hasna A, Abreu RT, Tribst JPM et al. Fracture resistance and stress distribution of weakened teeth reinforced with a bundled glass fiber-reinforced resin post. Clin Oral Investig 2022;26:1725-1735. https://doi.org/10.1007/s00784-021-04148-4

11. Cekic-Nagas I, Ergun G, Egilmez F. Light transmittance of fiber posts following various surface treatments: A preliminary study. Eur J Dent 2016;10:230-33. https://doi.org/10.4103/1305-7456.178303

12. Bell-Rönnlöf AL, Jaatinen J, Lassila L, Närhi T, et al. Transmission of light through fiber-reinforced composite posts. Dent Mater J 2019;38:928-933. https://doi.org/10.4012/dmj.2018-217

13. Vieira C, Bachmann L, De Andrade Lima Chaves C, Correa Silva-Sousa YT et al. Light transmission and bond strength of glass fiber posts submitted to different surface treatments. J Prosthet Dent 2021;125:674.e1-674.e7. https://doi.org/10.1016/j.prosdent.2020.11.031

14. Haralur SB, Alasmari TA, Alasmari MH, Hakami HM. Light transmission of various aesthetic posts at different depths and its effect on push-out bond strength, microhardness of luting cement. Medicina (Kaunas) 2022;58:75. https://doi.org/10.3390/medicina58010075

15. Parčina I, Amižić S, Baraba A. Esthetic intracanal posts. Acta Stomatol Croat 2016;50:143-150. https://doi.org/10.15644/asc50/2/7

16. Safwat EM, Khater AGA, Abd-Elsatar AG, Khater GA. Glass fiber-reinforced composites in dentistry. BNRC 2021;45:190. https://doi.org/10.1186/s42269-021-00650-7

17. Khan AS, Azam MT, Khan M, Mian SA et al. An update on glass fiber dental restorative composites: a systematic review. Mater Sci Eng C Mater Biol Appl 2015;47:26-39. https://doi.org/10.1016/j.msec.2014.11.015

18 Hoshino IAE, Dos Santos PH, Briso ALF, Sundfeld RH et al. Biomechanical performance of three fiberglass post cementation techniques: imaging, in vitro, and in silico analysis. J Prosthodont Res 2023;67:103-111. https://doi.org/10.2186/jpr.JPR_D_21_00253

19 Heboyan A, Vardanyan A, Karobari MI, Marya A et al. Dental luting cements: an updated comprehensive review. Molecules 2023;28:1619. https://doi.org/10.3390/molecules28041619

20 Carek A, Dukaric K, Miler H, Marovic D et al. Post-cure development of the degree of conversion and mechanical properties of dual-curing resin cements. Polymers (Basel) 2022;14:3649. https://doi.org/10.3390/polym14173649

21 Kwon TY, Bagheri R, Kim YK, Kim KH et al. Cure mechanisms in materials for use in esthetic dentistry: cure mechanisms in dentistry. J Investig Clin Dent 2012; 3–16. https://doi.org/10.1111/j.2041-1626.2012.00114.x

22 Roberts HW, Leonard DL, Vandewalle KS, Cohen ME et al. The effect of a translucent post on resin composite depth of cure. Dental Materials 2004;20:617–22. https://doi.org/10.1016/j.joen.2006.11.015

23 Faria e Silva AL, Arias VG, Soares LE, Martin AA et al. Influence of fiber-post translucency on the degree of conversion of a dual-cured resin cement. J Endod 2007;33:303-5. https://doi.org/10.1016/j.joen.2006.11.015

24 Radovic I, Corciolani G, Magni E, Krstanovic G et al. Light transmission through fiber post: the effect on adhesion, elastic modulus and hardness of dual-cure resin cement. Dent Mater 2009;25:837-44. https://doi.org/10.1016/j.dental.2009.01.004

25 Borges MG, Faria-e-Silva AL, Santos-Filho PCF, Silva FP et al. Does the moment of fiber post cutting influence on the retention to root dentin? Braz Dent J 2015;26:141-145. https://doi.org/10.1590/0103-6440201300242

26 Teixeira ECN, Teixeira FB, Piasick JR, Thompson JY. An in vitro assessment of prefabricated fiber post systems. J Am Dent Assoc 2006;137:1006–12. https://doi.org/10.14219/jada.archive.2006.0323

27 Goracci C, Ferrari M. Current perspectives on post systems: a literature review. Aust Dent J 2011;56:77–83. https://doi.org/10.1111/j.1834-7819.2010.01298.x

28 Keul C, Seidl, J Güth, JF, Liebermann A. Impact of fabrication procedures on residual monomer elution of conventional polymethyl methacrylate (PMMA)—a measurement approach by UV/Vis spectrophotometry. Clin. Oral Investig 2020; 24:4519–30. https://doi.org/10.1007/s00784-020-03317-1

Degree of Conversion and Mechanical Properties of a Commercial Composite with an Advanced Polymerization System

Celiane MC Tapety [1], Yvina KP Carneiro[1], Yarina M Chagas[1], Lidiane C Souza[1], Nayara de O Souza[2,3], Lidia AR Valadas[4]

1. Universidade Federal do Ceará, Faculdade de Odontologia, Sobral, Brasil.
2. Universidade Federal do Ceará, Faculdade de Farmácia, Odontologia e Enfermagem, Programa de Pós-Graduação em Odontologia, Fortaleza, Brasil.
3. Faculdade Paulo Picanço, Curso de Odontologia, Fortaleza, Brasil.
4. Universidad de Buenos Aires, Facultad de Odontología, Cátedra de Odontología Preventiva y Comunitaria, Buenos Aires, Argentina.

ABSTRACT

*Advanced Polymerization System (APS) technology in a commercial composite resin enables reduction of the concentration of camphorquinone without altering composite physicochemical properties. **Aim:** The aim of this study was to evaluate the degree of conversion and mechanical properties of a commercial composite with an advanced polymerization system (APS) and compare it to other composites that do not use this system. **Materials and Method:** Five groups were analyzed. Group 1 (VT: Vittra APS - FGM); G2 (AU: Aura – SDI); G3 (ES: Quick Sigma Stelite – TOKOYAMA); G4 (FZ: Filtek Z350 XT – 3M ESPE); G5 (OP: Opallis -FGM). Degree of conversion (DC, n=3) was analyzed immediately and after 24h by analysis with FTIR spectroscopy. For Knoop hardness (KHN, n=3), 5 indentations were made at the top and bottom of specimens 2 mm thick. Flexural strength (FS, n=10) was determined by the three-point method in a universal testing machine. Polymerization stress (PS) was determined by light-curing the material (1.0 mm high) between polymethylmethacrylate rods in a universal testing machine. Light curing was performed with a Valo Cordless LED (1,000 mW/cm2 x 20 s: 20J). The results were analyzed using ANOVA and complemented by Tukey's test (α=0.05). **Results:** The highest DC values (immediate and 24h after) were observed for VT and OP resins, followed by FZ, AU and ES. FZ (top and bottom) had the highest KHN values, similar to VT top. AU, ES, OP and VT had statistically different KHN between their top and bottom surfaces. The highest RF values were observed for FZ, followed by OP/VT, ES and AU. The highest TP values were observed for FZ, OP and VT. **Conclusion:** The Vittra APS resin with a new polymerization system presents satisfactory performance for the parameters evaluated.*

Keywords: *composite resin - polymerization - camphorquinone.*

Avaliação do grau de conversão e das propriedades mecânicas de um compósito comercial com sistema avançado de polimerização

RESUMO

*A tecnologia Advanced Polymerization System (APS) presente em uma resina composta comercial permite reduzir a concentração de canforoquinona sem alterar as propriedades físico-químicas do compósito. **Objetivo:** o objetivo deste estudo foi avaliar o grau de conversão e as propriedades mecânicas de um compósito comercial com sistema avançado de polimerização (SAP) e compará-lo com outros compósitos que não utilizam esse sistema. **Materiais e Método:** cinco grupos foram analisados. Grupo 1 (VT: Vittra APS - FGM); G2 (AU: Aura – SDI); G3 (ES: Quick Sigma Stelite – TOKOYAMA); G4 (FZ: Filtek Z350 XT – 3M ESPE); G5 (OP: Opallis -FGM). O grau de conversão (GC, n=3) foi analisado imediatamente e após 24h através da análise com espectroscopia FTIR; para dureza Knoop (DK, n=3), foram feitas 5 indentações no topo e na base de corpos de prova de 2 mm de espessura; para determinar a resistência à flexão (RF, n=10), o método de três pontos foi realizado em uma máquina universal de ensaios; a tensão de polimerização (TP) foi determinada pela fotopolimerização do material (1,0 mm de altura) entre hastes de polimetilmetacrilato em uma máquina de teste universal. A fotopolimerização foi realizada com um Valo Cordless LED (1.000 mW/cm² x 20 s: 20J). Os resultados foram analisados por ANOVA e complementados pelo teste de Tukey (α=0,05). **Resultados:** os maiores valores de GC (imediato e 24h após) foram observados para as resinas VT e OP, seguidas de FZ, AU e ES. A resina FZ (superior e inferior) apresentou os maiores valores de DK, semelhante ao VT superior. As resinas AU, ES, OP e VT apresentaram DK estatisticamente diferente entre suas superfícies de topo e base. Os maiores valores de RF foram observados para FZ, seguido de OP/VT, ES e AU. Os maiores valores de TP foram observados para FZ, OP e VT. **Conclusão:** com base nos resultados, pode-se concluir que a resina Vittra APS com um novo sistema de polimerização apresenta desempenho satisfatório para os parâmetros avaliados.*

Palavras-chave: *resina composta - polimerização - canforoquinona.*

INTRODUCTION

Progress in restorative Dentistry has led to composite resins being one of the most intensively studied materials, with the aim of improving their mechanical and optical properties[1].

Over the years, in addition to changes in the composition of resins, such as the incorporation of new monomeric formulations[2], there have been changes in the photoactivation systems. Composite resins activated by visible light initiate the polymerization process by absorbing light from a photoinitiator, which, once activated, reacts with a reducing agent to produce free radicals such as camphorquinone (CQ)[3]. The methacrylate monomers then polymerize, forming a cross-linked polymer matrix, with CQ being the most frequently used photoinitiator for light-curing resin[4]. A combination of the photoinitiator/co-initiator system must be used, usually CQ and a tertiary amine, respectively[5]. Despite being the most frequently used photoinitiator, CQ has some negative aspects such as toxicity and low polymerization efficiency[5]. Furthermore, it is a solid yellow compound and, even in small amounts, can lead to an undesirable color change. Another disadvantage is that the α-diketone group derived from CQ has an absorption peak of 468 nm in the visible range of light from 400 to 500 nm, causing rapid photopolymerization under ambient light (fluorescent and dental lamps), and resulting in short therapy operating time[5].

Higher amounts of CQ promote rapid generation of large amounts of free radicals. However, this can originate polymers with lower molecular weight and reduced ability to form a suitable polymeric network. On the other hand, if the concentration of photoinitiators is too low, an inadequately polymerized resin composite may result in altered mechanical properties, and the durability of the restoration may be compromised. Therefore, the concentration and proportion of photoinitiators and co-initiators that guarantee satisfactory polymerization behavior is of essential importance[5,6]. The FGM manufacturer claims that it developed the Advanced Polymerization System (APS), which enhances the components and allows the reduction of camphorquinone concentration, in order to improve the properties of the materials it manufactures. Technically, the APS system uses a smaller amount of CQ associated with several photoinitiators that interact with each other and enhance polymerization capacity. According to the manufacturer, the system ensures a higher degree of conversion, longer handling time under ambient light, and better mechanical properties compared to conventional systems based on CQ.

In addition to new polymerization systems for composite resins, there is a current trend in the production of materials free from Bisphenol-A, a substance present in the composition of Bis-GMA monomer and related to harmful effects in the body caused by some monomers[7]. As a result, FGM launched the first Brazilian resin with an organic matrix free from Bis-GMA monomers, the Vittra APS composite resin, which contains nanospheroidal zirconia particles, and provides aesthetics due to its high polishing capacity.

In this context, the present study aimed to evaluate *in vitro* the degree of conversion and mechanical properties of Vittra APS composite resin against other composites available on the Brazilian market.

MATERIALS AND METHOD
Type of study and materials

This was an experimental *in vitro* study, in which the variables were the photoinitiator system and the composition of the composite resins studied. The materials used in the present study are described in Table 1. The color selected for all materials was A3 enamel.

Degree of Conversion (DC)

The degree of conversion (n=3) was obtained by Fourier transform near-infrared spectroscopy (FT-IR Vertex 70, Brüker Optik GmbH - United Kingdom). The reading parameters used were: 4 cm^{-1}, 32 scans in the range between 2000 and 100 cm^{-1}, and power of 100 mW.

A 1.0 mm thick sheet of condensation silicone (Optosil - Heraeus Kulzer) was made, pressed between two glass plates with spacers and insulated with liquid Vaseline. The silicones obtained were cut into rectangles measuring 3.0 x 2.0 cm and a perforation of 8.0 mm in diameter was made in the center of the silicone. Finally, each cutout was positioned in the center of glass slides.

The material was inserted into the silicone mold and pressed by another glass slide. The sets were stabilized by adhesive tapes and taken to the Vertex 70 spectrometer (Brüker Optik GmbH) to determine

Table 1. Materials used in this study (as described by the manufacturers)

Material and manufacturer	Composition	Photoinitiator system
Vittra APS, FGM Dental Products	TEGDMA, UDMA, photoinitiator composition [APS], silane, zirconia particles (200 nm), silica: 72% to 82% by weight, 52% to 60% by volume. Composite resin composed entirely of nanometric fillers (100 - 200 mm)	Camphorquinone + other photoinitiators
Aura, SDI	Limited information provided by the manufacturer	Limited information provided by the manufacturer
Estelite Sigma Quick, Tokuyama	Bis-GMA, TEGDMA. Silica-zirconia particles with an average size of 0.2µm (82% by weight and 71% by volume)	Radical Amplified Photopolymerization Technology (RAP).
Filtek Z350XT, 3M ESPE	TEGDMA, Bis-EMA, Bis-GMA, UDMA, PEGDMA. Non-agglomerated silica and zirconia particles (20 nm and 4-11 nm, respectively) and aggregated Silica/zirconia (0.6 – 10 µm). 72.5% by weight and 55.5% by volume	Camphorquinone
Opallis, FGM	Bis-GMA, Bis-EMA, TEGDMA, UDMA, co-initiator, silane. Barium aluminum silicate glass (0.5 µm) silanized (78.5% to 79.8% by weight and 57.0 to 58% by volume).	Camphorquinone

the unpolymerized spectrum. Baseline correction and curve normalization were performed using the OPUS program (Brüker Optics), increasing intensity and facilitating visualization. The peak heights of the 1610 and 1640 cm^{-1} bands were measured and recorded.

The specimens were removed from the RFS100/S equipment and light-cured with a Valo Cordless LED device (Ultradent - South Jordan, United States), with an active tip of 10 mm in diameter, for 20 seconds under an irradiance of 1,000 mW/cm^2, resulting in an energy density of 20 J/cm^2. A new reading was performed. The specimens were evaluated immediately and after 24 hours stored in a dry environment. To calculate the DC after light-curing, the values of peak heights of the bands of uncured and light-cured material were used.

Knoop hardness numbers (KHN)

Cylindrical specimens (n=3) 4.0 mm in height, 2.5 mm in width, and 2.5 mm in depth were made with the aid of a bipartite circular brass die, then positioned on a polyester strip fixed on a glass plate. The resin was inserted into the die and pressed with a transparent strip of polyester and glass slide, followed by photoactivation of the material, as described for degree of conversion.

Subsequently, the irradiated face of the specimen was polished in an EcoMetTM/AutometTM 300 polisher (Buehler - Lake Bluff, United States) under abundant irrigation with 1200 grit sandpaper for 2 minutes (20 N force; speed: 70 rpm). After 24 hours,

an ultrasonic bath was performed, followed by 5 indentations with load of 200 g for 20 seconds in a Shimadzu HMV-2 hardness tester (Tokyo, Japan), to determine the hardness values of the top and bottom surfaces (surface directly irradiated by light, and surface opposite to light irradiation, respectively).

Flexural Resistance (FR)

Specimens (n=10) were made in a bipartite steel die (10 mm long, 2 mm wide, 1 mm thick) supported by a transparent strip on a glass plate. After inserting the material, a transparent strip of polyester and a glass slide were positioned over the die to accommodate the material, followed by photoactivation, as described for degree of conversion. After disocclusion of the specimen, the excesses were removed with the aid of a scalpel blade number 11 (Solidor - Barueri, São Paulo) and the dimensions of the specimen were recorded.

The flexural strength tests were performed in a universal testing machine (model 5565, Instrom Corp - Canton, United States) with load cell of 1000 N, test speed of 0.5 mm/min and action of the incident force on the irradiated face. The distance between the supports was 8 mm, always checked between groups with a digital caliper.

Specimen breaking load values (in Newtons) and dimensions were recorded for calculation of maximum flexural strength in MPa.

Polymerization Stress (PS)

For the PS test, the method by Gonçalves et al.[7] was

used. Polymethylmethacrylate (PMMA) cylinders (Ø3mm) were sectioned into rods 13 and 28 mm long. For the 13 mm rods, one end was polished with 1200, 2000 and 4000 grit sequence sandpaper and felt with 1 µm alumina paste to allow the passage of blue light along the length of the rod at the time of photoactivation. The other faces of the other rods, both 13 and 28 mm long, were sprayed with aluminum oxide (250 µm) to improve the adhesion of the hydrophobic resin to the PMMA.

To prepare each specimen for the polymerization stress test, a layer of methyl methacrylate monomer (JET Self-polymerizing Acrylic, Clássico, Brazil) was applied to one of the sandblasted surfaces of the 28 mm rod and the sandblasted surface of the 13 mm rod to improve the wetting of the unfilled hydrophobic adhesive (Scotchbond Multiuso Plus, 3rd bottle, 3M ESPE, Brazil) applied later. After this last step, a jet of air 15 cm away from the surface of the rod was applied for 10 seconds with the aid of a triple syringe. The hydrophobic adhesive on both surfaces was individually light-cured for 20 seconds with a Valo Cordless LED device (Ultradent, South Jordan, United States).

The rods were manipulated such that contact with the treated surfaces was avoided, and then fixed in an Instron 5665 universal testing machine. The 28 mm rod was fixed in a grip connected to the load cell of the machine with the treated face facing downwards, and the 13 mm rod was positioned with the treated side facing up, in a device developed for the present test and coupled to the base of the testing machine. In order to evaluate the influence of the increment thickness on the polymerization stress, the distance (specimen height, h) between the rods was standardized at 1 mm, with 05 (n=5) being the number of specimens for each material.

After determining specimen height (distance between the rods) and recording it in the equipment memory, the load cell was moved away from the machine base and the material was inserted over the treated surface of the lower rod. The load cell was positioned according to the height parameter just memorized, so that the material could be pressed and in contact with both treated surfaces. After removing any excess material with the aid of a spatula, an extensometer (model 2360-101, Instron) was attached to the rods to keep the distance between them constant during the test.

The tip of the light-curing unit was positioned in the device slot and coupled to the base of the testing machine, directly in contact with the polished face of the base of the 13 mm rod. The tension developed during the polymerization of the materials was monitored for 15 minutes from the light-activation of the material. To determine the maximum rated polymerization stress (MPa), the maximum stress value recorded during the test (N) was divided by the cross-sectional area of each rod.

Statistical analysis

The data recoded in all tests were submitted to normality and homoscedasticity tests, then evaluated by analysis of variance (ANOVA) complemented by Tukey's test or evaluated only by the Kruskal-Wallis test ($\alpha < 0.05$).

RESULTS

Conversion Degree

Mean degree of conversion (%) for the different dental composites are shown in Figure 1. DC values immediately after curing ranged from 44.08% to 66.9%, while the 24-hour post-cure values ranged from 65.94% to 81.82%. For immediate cure, the highest to lowest mean rates of polymerization were: Vittra APS, Opallis, Filtek Z350XT, Estelite Sigma Quick and Aura. After 24 hours, DC% of Vittra APS and Opallis resins did not differ statistically, though their degree C = C conversion was higher than for Filtek Z350XT, Estelite Sigma Quick and Aura. DC after 24 h did not differ statistically between Estelite Sigma Quick and Aura. Thus, the advanced polymerization system technology in the Vittra APS resin may have influenced its performance.
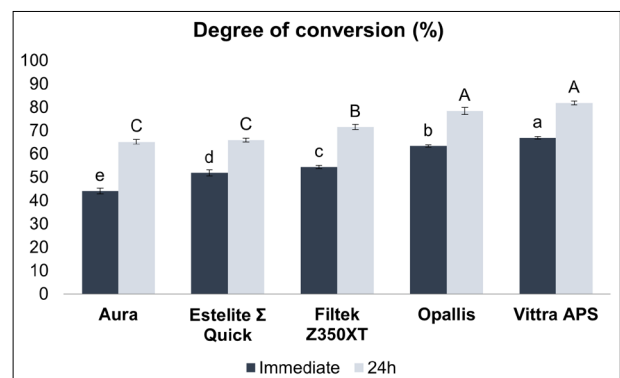

Fig. 1: Degree of conversion (%) of the resins evaluated immediately and 24 hours after light-curing.

Knoop Hardness (KHN)

The Knoop hardness results for each composite (the top of the specimen being the surface directly irradiated, and the bottom being the surface opposite to irradiation) are shown in Figure 2. Significant differences were found for bottom/top hardness among composites (p=0.010). Aura resin showed significantly lower values than the other materials. The Filtek Z350 XT resin (top and bottom) had the highest KHN values, with the bottom value being similar to the top value of Vittra APS. Despite Vittra's advanced polymerization technology, its KHN (in kilograms-force per square millimeter) at the top (44.15) was approximately double the value at the bottom (24.59).
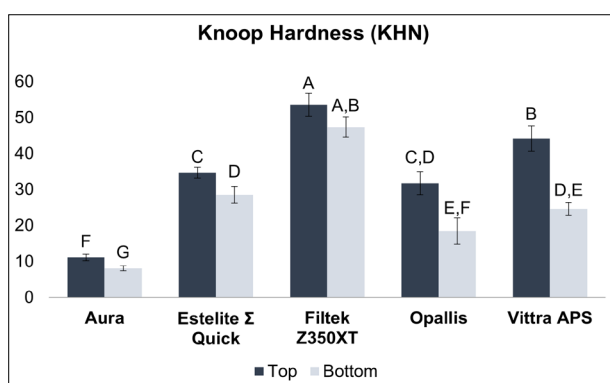

Fig. 2: Knoop hardness (KH) of the resins evaluated 24 hours after light-curing.

Flexural strength (Mpa)

The results the 3-point flexural strength (MPa) are shown in Figure 3. FS was statistically highest for Filtek Z350 XT, and lowest for Aura. Vittra APS and Opallis behaved similarly, with higher flexural strengths than Estelite, Sigma Quick and Aura.
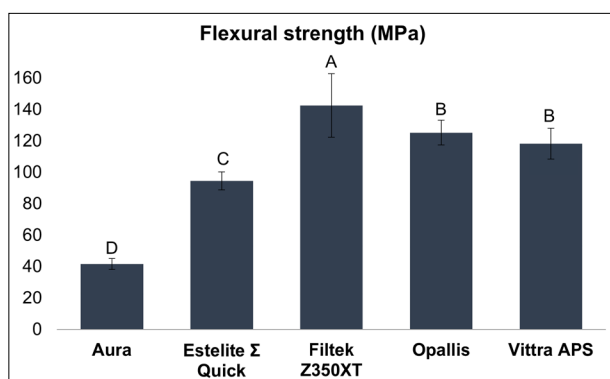

Fig. 3: Flexural strength (MPa) of the resins evaluated 24 hours after light-curing.

Polymerization Stress (Mpa)

The results of polymerization stress (MPa) are shown in Figure 4. The PS of the composite resins ranged from 2.68 MPa (Aura) to 3.84 MPa (Opallis). Polymerization shrinkage stress values differed significantly between some materials tested (p<0.001). Vittra APS showed higher polymerization stress than AURA (p=0.031). The highest values of polymerization stress were observed for Opallis, Filtek Z350 XT and Vittra APS, followed by Estelite Sigma Quick and Aura.
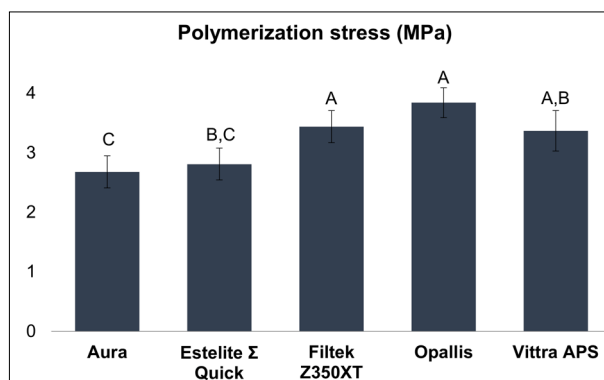

Fig. 4: Polymerization stress (MPa) of the evaluated resins.

DISCUSSION

Composite resin properties such as hardness and degree of conversion influence the clinical performance of restorations. The presence of non-converted double carbon links could increase susceptibility to degradation, reducing color stability and releasing residual monomers[8,9]. The present study observed that the DC of composite resins can vary from 34.7% to 77.1%, while the literature reports that this increase can be up to 36% in the first 24 hours[10]. Still, no material can completely convert into a polymer. In the present study, Vittra APS and Opallis resins, both from FGM, presented the highest DC, both immediately (statistically higher for Vittra APS) and 24 hours after polymerization (no statistical difference between the two). For Vittra APS, this can be explained by the presence of the APS system, which despite the low concentration of CQ, contains secondary photoinitiators not informed by the manufacturer and capable of guaranteeing high monomer conversion.

AURA (SDI) presented a statistically lower percentage than all the other resins tested in the immediate and 24 hours after readings. However, according to Alshali et al.[10], a minimum DC value

has not yet been established for adequate clinical performance. It should be noted that little information was made available by the manufacturer about this material. Many factors can affect polymerization efficiency, whether intrinsic (type and concentration of photoinitiator, matrix viscosity and optical properties) or extrinsic (light type and spectrum, irradiation parameters, curing mode, temperature and light tip positioning)[11]. This study used the same light source for all tests and resins, setting the same distance from the tip to the specimen and in the same work environment, in order to eliminate as far as possible any other variables that could affect the DC.

Despite being controversial, some studies have shown a correlation between DC and hardness[12,13], which can be explained by the fact that the strength of the material is determined not only by the inorganic fraction, but also by the creation of a dense, cross-linked polymeric network[12]. A base-to-top hardness ratio (B/T) ranging from 0.8 to 0.9 is an important criterion to verify the efficiency of polymerization in deeper areas in relation to the light source. Theoretically, the base surface hardness of a polymerized composite should be at least 80% (0.8) of the top surface hardness[6].

In the present work, AURA (SDI) had the lowest KHN hardness values (B/T). Opallis and Estelite Sigma Quick showed statistically similar mean KHN hardness values at the top. Hardness at the base of Opallis did not reach the desirable 80% B/T. Vittra hardness was higher at the top, compared to the aforementioned resins, and statistically similar to the Z350 XT resin base. Z350 XT top hardness was statistically significantly the highest among the tested resins.

A study on the effect of adding zirconia particles to a commercial composite (Vittra APS) reported that regardless of its concentration, zirconia increases hardness values compared to the control group in which the manufacturer provided the composition[14]. The presence of nano spheroidal zirconia particles combined with the expected dense polymeric network at the top of the specimens due to the presence of APS technology may account for the high hardness value compared to the base of the same material. In this case, the presence of the APS system does not seem to guarantee greater depth of polymerization.

Widely used in laboratory tests of dental composites,

flexural strength is one of the main parameters for assessing a material's resistance to fracture[14]. Flexural strength represents the stress experienced by a material at the time of its rupture and is expressed in megapascals. Z350 XT had the highest flexural strength, with statistical significance. Opallis and Vittra APS had intermediate and similar values, followed by Estelite and Aura. Aura had the lowest flexural strength among the tested resins.

According to ISO standard 4049, used to evaluate the flexural strength of restorative materials, the minimum acceptable value for composite resins is 100 Mpa[15]. Borges et al.[16] evaluated the flexural strength of 8 direct composite resins, which were microparticulate, microhybrids, hybrids and just a nanocluster, containing silica particles. This nanocluster presented the highest values for flexural strength, which were close to 150 Mpa. In the present study, the nanoparticulate resins also presented the highest values for flexural strength, with Z350 XT above 140 MPa, and Vittra APS with a value close to 120 MPa, which are values higher than those required by ISO 4049.

Borges et al.[16] report that increasing the amount of filler significantly improves all mechanical properties of composite resins. In our study, Vittra APS had a higher percentage of filler than the other composites tested, only lower than Opallis, though statistically similar. The size of the filler particles also affects the material's strength, that is, composites with nanometer-scale filler particles present greater resistance to fracture.

During polymerization, monomer molecules join to form a network of polymers. As the network is formed, the molecules approach each other so that new bonds can form[17]. This approach among molecules causes volume contraction, which can cause cracks, margins, pigmentation, microleakage, secondary caries, and postoperative sensitivity, in addition to causing tensions in the tooth-restoration interface. These tensions, in turn, can cause microfractures and failures[18]. The shrinkage stress is proportional and may be related to the volumetric shrinkage and the elastic modulus of the composites[18,3]. Other factors such as filler content, resin matrix composition and degree of monomeric conversion can also influence polymerization tension[19]. Despite the presence of the APS system in the Vittra resin, it did not present low polymerization stress, but had results like Filtek Z350 XT, Opallis

and Estelite. The lowest polymerization stress values were observed for Aura, possibly related to its low degree of monomeric conversion. Despite the limitations of the study, the resin with the APS system showed encouraging outcomes, both for aesthetic and mechanical properties.

CONCLUSION

In this study, Vittra APS resin, with a new polymerization system, presents satisfactory performance for the parameters evaluated when compared to the other materials tested. Despite having a high degree of conversion and polymerization stress like the other resins, it was inferior to Filtek Z350 XT in the Knoop hardness and flexural strength tests.

DECLARATION OF CONFLICTING INTERESTS

The authors declare no potential conflicts of interest regarding the research, authorship, and/or publication of this article.

REFERENCES

1. Alzraikat H, Burrow MF, Maghaireh GA, Taha NA. Nanofilled Resin Composite Properties and Clinical Performance: A Review. Oper Dent. 2018;43(4):E173-E190. https://doi.org/10.2341/17-208-T.
2. Hahnel S, Dowling AH, El-Safty S, Fleming GJ. The influence of monomeric resin and filler characteristics on the performance of experimental resin-based composites (RBCs) derived from a commercial formulation. Dent Mater. 2012;28(4):416-423. https://doi.org/10.1016/j.dental.2011.11.016.
3. Guimarães GF, Marcelino E, Cesarino I, Vicente FB, Grandini CR, Simões RP. Minimization of polymerization shrinkage effects on composite resins by the control of irradiance during the photoactivation process. J Appl Oral Sci. 2018;26: e20170528. https://doi.org/10.1590/1678-7757-2017-0528.
4. Bittencourt BF, Dominguez JA, Pinheiro LA, Farago PV, Santos EBD, Campos LA et al. Effect of the Bis-Dimethylamino Benzydrol Coinitiator on the Mechanical and Biological Properties of a Composite. Braz Dent J. 2017;28(6):744-748. https://doi.org/10.1590/0103-6440201701585
5. Schneider AC, Mendonça MJ, Rodrigues RB, Busato PMR, Camilott. Influence of three modes of curing on the hardness of three composites. Polímeros. 2016; 26(1): 37-42. https://doi.org/10.1590/0104-1428.1855
6. Grohmann CVS, Soares EF, Souza-Junior EJC, Brandt WC, Puppin- Rontani RM, Geraldeli S et al. Influence of different concentration and ratio of a photoinitiator system on the properties of experimental resin composites. Braz. Dent. J. 2017;28(6):726-730. https://doi.org/10.1590/0103-6440201701372
7. Gonçalves F, Pfeifer CS, Ferracane JL, Braga RR. Contraction stress determinants in dimethacrylate composites. J Dent Res. 2008;87(4):367-371. https://doi.org/10.1177/154405910808700404.
8. Lopes-Rocha L, Ribeiro-Gonçalves L, Henriques B, Özcan M, Tiritan ME, Souza JCM. An integrative review on the toxicity of Bisphenol A (BPA) released from resin composites used in dentistry. J Biomed Mater Res B Appl Biomater. 2021 Nov;109(11):1942-1952. https://doi.org/10.1002/jbm.b.34843
9. Imazato S, Tarumi H, Kobayashi K, Hiraguri H, Oda K, Tsuchitani Y. Relationship between the degree of conversion and internal discoloration of light-activated composite. Dent Mater J. 1995 Jun;14(1):23-30. https://doi.org/10.4012/dmj.14.23
10. Alshali RZ, Silikas N, Satterhwaite JD. Degree of conversion of bulk-fill compared to convencional resin-composites at two time inervals. Dent Mater. 2013;29(9):e213-217. https://doi.org/10.1016/j.dental.2013.05.011
11. Leprince JG, Palin WM, Hadis MA, Devaux J, Leloup G. Progress in dimethacrylate-based dental composite technology and curing efficiency. Dent Mater. 2013;29(2):139-156. https://doi.org/10.1016/j.dental.2012.11.005
12. Price RB, Whalen JM, Price TB, Felix CM, Fahey J. The effect of specimen temperature on the polymerization of a resin-composite. Dent Mater. 2011;27(10):983-989. https://doi.org/10.1016/j.dental.2011.06.004
13. Dimer AR, Arossi GA, Sanbtos LH, Kappaun DR. Effect of different post-cure polymerization treatment on composite resin hardness. RGO-Revista Gaúcha de Odontologia. 2015; 63(4): 426-431. https://doi.org/10.1590/1981-863720150003000082908
14. Marovic D, Panduric V, Tarle Z, Ristic M, Sariri K, Demoli N, Klaric E, Jankovic B, Prskalo K. Degree of conversion and microhardness of dental composite resin materials. J Mol Struct. 2013;1044:299-302. https://doi.org/10.1016/j.molstruc.2012.10.062
15. Souza ROA, Mesquita AMM, Pavanelli CA, Nishioca RS, Botinho MA. Avaliação da resistência à flexão de três resinas compostas de uso laboratorial IJD. 2005 4(2):50-54. https://periodicos.ufpe.br/revistas/dentistry/article/view/13848 .
16. Borges LAS, Borges AB, Barcelos DC, Saavedra GSFA. Paes Júnior TJA, Rode SM. Avaliação da resistência flexural e módulo de elasticidade de diferentes resinas compostas indiretas. Revista de Pós-Graduação. 2012; 19(2): 50-56. http://www.scielo.org.ar/pdf/aol/v25n1/v25n1a18.pdf .
17. Oliveira KM, Lancellotti AC, Ccahuana-Vásquez RA,

Consani S. Shrinkage stress and degree of conversion of a dental composite submitted to different photoactivation protocols. Acta Odontol Latinoam. 2012;25(1):115-122. http://www.scielo.org.ar/pdf/aol/v25n1/v25n1a18.pdf .

18. Kaisarly D, Gezawi ME. Polymerization shrinkage assessment of dental resin composites: a literature review. Odontology. 2016;104(3):257-270. https://doi.org/10.1007/s10266-016-0264-3 .

19. Calheiros FC, Daronch M, Rueggeberg FA, Braga RR. Effect of temperature on composite polymerization stress and degree of conversion. Dent Mater. 2014;30(6):613-618. https://doi.org/10.1016/j.dental.2014.02.024 .

In vitro cytotoxicity of resin cement and its influence on the expression of antioxidant genes

Priscila FA Moralez [ID], Kamila R Kantovitz [ID], Elizabeth F Martinez [ID], Lucas N Teixeira [ID], Ana PD Demasi [ID]

Faculdade São Leopoldo Mandic, Campinas, Brazil.

ABSTRACT

*Aim: This study evaluated cytotoxicity and antioxidant gene expression of resin cements on human gingival fibroblasts (hGF). **Materials and Method:** RelyX Ultimate™(RXU), Variolink™II(VLII), and RelyXU200™(RXU200) resin cements were incubated with culture medium for 24 h to obtain eluates. Then, the eluates were applied over hGF to assess cell viability at 24 h, 48 h, and 72 h and antioxidant gene expression at 24 h. hGF cultures non-exposed to the eluates were used as Control. Data were submitted to ANOVA and Bonferroni tests (α≤0.05). **Results:** RXU and RXU200 reduced the number of viable cells in 24 h. Longer exposure to cement extracts caused cell death. Gene expression showed peroxiredoxin 1 (PRDX1) induction by all resin cement types, and superoxide dismutase 1 (SOD1) induction by RXU200 and VLII. Moreover, RXU200 induced not only PRDX1 and SOD1, but also glutathione peroxidase 1 (GPX1), catalase (CAT), and glutathione synthetase (GSS). **Conclusions:** All resin cements showed toxicity, and induced antioxidant genes in hGF. Antioxidant gene induction is at least partly associated with cytotoxicity of tested cements to oxidative stress experience.*

Keywords: *resin cement - dental cement - oxidative stress.*

Avaliação *in vitro* da toxicidade de cimentos resinosos e sua influência na expressão de genes antioxidantes em fibroblastos humanos

RESUMO

*Objetivo: O objetivo deste estudo foi avaliar a toxicidade dos cimentos resinosos Rely X Ultimate 2, Rely X U200 e Variolink II, bem como sua influência na expressão de genes antioxidantes em fibroblastos gengivais humanos. **Materiais e Método:** Corpos de prova de cada cimento foram colocados em meio de cultura por 24 h e os extratos correspondentes foram aplicados aos fibroblastos. A viabilidade celular foi avaliada após 24, 48 e 72 h de exposição pelo ensaio de exclusão do azul de tripano e MTT. A expressão gênica foi avaliada por PCR quantitativo após 24 h de exposição aos extratos. Estes parâmetros foram comparados aos das células não expostas aos cimentos. Os dados foram submetidos ao teste ANOVA, seguido pelo pós-teste de Bonferroni (a≤0.05). **Resultados:** Os resultados demonstraram que todos os cimentos promoveram redução do número de células viáveis e da atividade mitocondrial nos períodos de 48 e de 72 h (p< 0,01), sendo que o Variolink II apresentou o menor efeito e os cimentos Rely X Ultimate e Rely X U200 promoveram similarmente os maiores efeitos. A análise de expressão gênica evidenciou influência significativa em todos os cimentos avaliados sobre os níveis de transcritos de PRDX1, SOD1, GPX1 e GSS (p> 0,05), com um aumento considerável no Rely X U200. **Conclusão:** A indução de genes antioxidantes está, pelo menos em parte, associada à citotoxicidade dos cimentos testados para a experiência de estresse oxidativo.*

Palavras-chave: *cimento resinoso - cimento odontológico - estresse oxidativo.*

Corresponding Author:
Kamila R Kantovitz.
kamila.kantovitz@slmandic.edu.br;
kamilark@yahoo.com.br

INTRODUCTION

Dental resin cements are used to fill the space between indirect restorative material and tooth preparation or implant abutment to prevent dislodgement of the restoration during the masticatory function[1]. Because of their high retentive strength, resistance to wear, and the low solubility of bonded ceramic restorations in relation to anterior and extensive posterior restorations, clinical studies describe a survival rate of up to 81%[2].

Three kinds of resin cement are available on the market, classified according to their curing mechanism: light-cured, self-cured and dual-cured[3]. Self- and dual-cured alternatives can be used for all cementation applications. However, light-cured resin cements should be limited to porcelain veneers and glass-ceramic restorations, which allow the curing light to penetrate the porcelain. Despite the reformulations of resin cements introduced on the market, the improvements have been related to physicochemical properties and a reduction in the clinical steps[4]. Notwithstanding these improvements, the thickness, microstructure, and shade of the ceramic continue to adversely affect the degree of conversion of methacrylate-based dental resin cements, and pose a risk associated with the toxic effects of residual monomers released into the oral tissues adjacent to dental restorations, such as the mucosa and dental pulp[4].

The main monomers are 2,2-bis[4-(2-hydroxy-3-methacryloxypropoxy) phenyl] propane (BisGMA) and urethane dimethacrylate (UDMA), in combination with co-monomers of lower viscosity, such as triethylene glycol dimethacrylate (TEGDMA) and 2-hydroxyethyl methacrylate (HEMA)[3,4]. Toxins may be released both early in the process, owing to defective photopolymerization, and over time, owing to erosion and degradation, influenced by thermal, mechanical, enzymatic and chemical factors[5]. It is estimated that about 1.5 to 5% of the methacrylic groups remain unreacted[6,7]. In fact, TEGDMA (triethylene glycol dimethacrylate) and UDMA (urethane dimethacrylate) have been detected in dental composite water and artificial saliva eluates by High Performance Liquid Chromatography (HPLC) in concentrations higher than those reported to be cytotoxic in primary human oral fibroblast cultures[8,9].

Resin monomer cytotoxicity has been related to the depletion of glutathione (GSH), the major non-enzymatic antioxidant of cells[10-12]. This depletion is accompanied by augmented levels of reactive oxygen species (ROS), causing damage to biomolecules and consequent cell death[13,14]. TEGDMA has been found to induce lipid peroxidation and mitochondrial damage in gingival hGFs, leading to cell death[13]. HEMA, and especially TEGDMA, have been found to induce the formation of micronuclei, leading to chromosomal aberrations *in vitro*, and TEGDMA has increased the frequency of gene mutations in mammalian cell cultures by more than ten-fold[15]. DNA damage has also been assessed through single-cell microgel electrophoresis (Comet) assay, which indicates the initiation of DNA strand breaks by TEGDMA and HEMA in human lymphocytes and salivary gland tissue[14,16].

Considering the reduced cellular detoxifying potency of monomer-exposed cells due to glutathione depletion, it is crucial to the survival of these cells to have an adaptive response that can activate the expression of enzymatic components of the antioxidant system. Thus, this study aimed to evaluate the cytotoxicity and antioxidant gene expression of three resin cements with different polymerization processes. The genes analyzed were those encoding superoxide dismutase 1 (*SOD1*), peroxiredoxin 1 (*PRDX1*), glutathione peroxidase (*GPX1*), catalase (*CAT*) and glutathione synthetase (*GSS*). *SOD1* accelerates the conversion of the superoxide anion radical to hydrogen peroxide, while *PRDX1*, *GPX1* and *CAT* convert hydrogen peroxide to water. *GSS* is the second enzyme in the *GSH* biosynthesis pathway. The tested hypothesis was that the polymerization process would affect toxicity and antioxidant gene expression in human fibroblasts.

MATERIALS AND METHOD
Resin cements and specimen preparation
All the tested materials and their compositions are listed in Table 1. The materials were hand-mixed in a flow chamber, following the manufacturer's instructions to use a 1:1 ratio, a metal spatula, and a block of waterproof paper. Briefly, the materials were placed in sterile bipartite metal molds (1-mm high and 14 mm-diameter), inserted in a single increment, and pressed between polyester strips and glass slides to prevent the formation of an oxygen-

Table 1. Material, type, composition, manufacturer, and batch number of cements used in the study

Material	Type	Composition*	Manufacturer/ Batch #
RelyX Ultimate™ *RXU*	Dual-curing Adhesive resin cement	50-60% glass powder 20-30% methacrylated phosphoric acid esters 10-20% TEGDMA 1-10% silane-treated silica < 1% sodium persulfate	3M/ESPE St. Paul, MN, USA 130720
Variolink™II (Base) *VLII*	Dual-curing (*Applied in the light-curing technique only*) Adhesive resin cement	10-25% Bis-GMA 2.5-10% UDMA 2.5-10% TEGDMA	Ivoclar Vivadent Schaan, Liechtenstein U25861
RelyX U200™ *RXU200*	Dual-curing Self-adhesive resin cement	45-55% glass powder 20-30% methacrylated phosphoric acid esters 10-20% TEGDMA 1-10% silane-treated silica < 3% sodium persulfate	3M/ESPE St. Paul, MN, USA 160920

* Bis-GMA = 2,2-bis[4-(2-hydroxy-3-methacryloxypropoxy) phenyl] propane; UDMA = urethane dimethacrylate; TEGDMA= Triethyleneglycol Dimethacrylate.

inhibited surface layer. Next, they were polymerized according to the characteristics of each cement. Although VLII is a dual-curing cement, it may be applied only with a light-curing technique, and was used for this sole purpose. Photoactivation was performed with a light-emitting diode, at a curing intensity of 1000 mW/cm^2, set to standard power, with a 9.6-mm lens diameter and wavelength of 395-480 nm, and kept plugged into an electrical outlet (VALO™, Ultradent Products, South Jordan, UT, USA). Each disc side was exposed for 20 s. All the samples were subjected to disinfection by ultraviolet light for 20 minutes on each side.

Cell Culture

To obtain samples, three healthy subjects were submitted to a gingival biopsy after approval by the Institutional Ethics Committee (protocol #1.303.768). Briefly, primary cultures were isolated using the explant technique, after being enzymatically digested by a 0.25% trypsin-EDTA solution for 1 h at 37°C. The cells were cultured in Dulbecco's Modified Eagle's Medium (DMEM), supplemented with 10% fetal bovine serum and 1% antibiotic-antimycotic solution (penicillin-streptomycin), and incubated under standard cell culture conditions (37°C, 100% humidity, 95% air and 5% CO_2).

Extract Preparation and Cell Exposure

Extracts were obtained by incubating the resin cements of the specimens in DMEM medium, in a proportion of 0.2 g/mL at 37°C for 24 h[17]. The cells were plated on 6-well (1x10^6 cells/well) or 24-well (2x10^4 cells/well) plates. After 24 h, the culture medium was removed and replaced by the different extracts taken from the 3 cements – RelyX Ultimate™ (RXU), Variolink™II (VLII), and RelyX U200™ (RXU200) – or in the DMEM medium (control). The cells were cultured under standard cell cultivation for up to 3 days, as described above.

Cell Viability (Trypan blue exclusion test)

After 24 h, 48 h and 72 h of exposure to different cements extracts, vital trypan blue exclusion was used to evaluate cell viability. Cells were removed enzymatically from the plates, and the cell pellet obtained from the centrifugation was suspended in 1 mL of medium. Ten µL of the cell suspension was added to 10 µL of Trypan Blue solution 0.4% (Sigma-Aldrich, St. Louis, MO, USA) and the solution was gently mixed for 30 sec. After that, the solution was

left to stand for 5 min. Then, 1 µL of this solution was placed in a hemocytometer (Neubauer-Fisher Scientific, Pittsburgh, PA, USA), and observed for cell count and analysis using a phase microscope (Nikon Eclipse TS100, Tokyo, Japan).

Expression of antioxidant genes (quantitative real-time PCR)

After 24 h of exposure to different cements extracts, total RNA was extracted from cell cultures using Trizol reagent (Thermo Scientific, Waltham, MA, USA) according to the manufacturer's instructions. Briefly, cells were collected and homogenized with 1 mL of Trizol, and the aqueous and organic phases were separated by adding chloroform (0.2 mL), followed by centrifugation (12,000 g, 15 minutes, 4°C). RNA was precipitated from the aqueous phase with 0.5 mL of isopropanol (12,000 g, 15 minutes, 4°C), washed with 75% ethanol, and suspended in water. Reverse transcription was performed using 1 µg of each RNA sample, treated with 1 U DNase I, and the RevertAid H Minus First Strand cDNA Synthesis Kit (Thermo Scientific). Briefly, reactions were initiated by using 1 µg of RNA, 0.5 µg of oligo (dT) 18, 1 mM of dNTP mix, 200 U of RevertAid H Minus M-MuLV Transcriptase, and 20 U of RiboLock RNase Inhibitor at 42°C for 60 minutes. The reactions were then terminated by heating the samples at 70°C for 5 minutes. The reactions were initiated by using 40 ng of cDNA and 0.3 µM of pairs of primers, added to the Maxima SYBR Green qPCR Master Mix (Thermo Scientific) (Table 2). The primer sets were as follows: Peroxiredoxin I (PRDX1; Forward 5'-GGATTCTCACTTCTGT-CATCTAGCA-3'; Reverse 5'-TGTTCATGGGTC-CCAGTCCT-3'), Glutathione Peroxidase I (GPX1; Forward 5'-CCGACCCCAAGCTCATCA-3'; Reverse 5'-GAAGCGGCGGCTGTACCT-3'), Catalase (CAT; Forward 5'-GATAGCCTTCGACCCAAG-CA-3'; Reverse 5'-ATGGCGGTGAGTGTCAG-GAT-3'), Superoxide dismutase 1 (SOD1; Forward 5'-AGGTCCTCACTTTAATCCTCTATCCA-3'; Reverse 5'-ACCATCTTTGTCAGCAGTCACATT -3'), Glutathione synthetase (GSS; Forward 5'-ATTTGACCAGCGTGCCATAGAG-3'; Reverse 5'-TCCAGAGACCCCTTTTCAGAGATATC-3'), and for internal gene reference Glyceraldehyde-3-phosphate dehydrogenase (GAPDH; Forward 5'-ACCCACTCCTCCACCTTTGA-3'; Reverse 5'-TGTTGCTGTAGCCAAATTCGTT-3'). The conditions required to elicit a reaction consisted of maintaining the samples 10 minutes at 95°C, followed by 40 cycles at 95°C. Each cycle consisted of keeping the samples 15 s at 95°C, and 1 min at 60°C. The relative expression among the samples was calculated by comparing the threshold cycle values, based on the $2^{-\Delta\Delta Ct}$ formula. The GAPDH gene was used to normalize the expression levels.

Statistical Analysis

Data distribution and homoscedasticity were analyzed by the Shapiro-Wilks and the Levene tests, respectively ($p \geq 0.05$), and the data were analyzed by ANOVA followed by the Bonferroni test, with a significance level of 5%.

Table 2. Analyzed genes and sequences of the primers used

Gene name and symbol	Gene Bank (NM)	Sequences of primers
Peroxiredoxin I *PRDX1*	181696.1[*] 181697.1[*] 002574.2[*]	F 5'-GGATTCTCACTTCTGTCATCTAGCA-3' R 5'-TGTTCATGGGTCCCAGTCCT-3'
Glutathione Peroxidase I *GPX1*	000581.2[*] 201397.1[*]	F 5'-CCGACCCCAAGCTCATCA-3' R 5'-GAAGCGGCGGCTGTACCT-3'
Catalase *CAT*	001752.3	F 5'-GATAGCCTTCGACCCAAGCA-3' R 5'-ATGGCGGTGAGTGTCAGGAT-3'
Superoxide dismutase 1 *SOD1*	000454.4	F 5'-AGGTCCTCACTTTAATCCTCTATCCA-3' R 5'-ACCATCTTTGTCAGCAGTCACATT -3'
Glutathione synthetase *GSS*	000178	F 5'-ATTTGACCAGCGTGCCATAGAG-3' R 5'-TCCAGAGACCCCTTTTCAGAGATATC-3'
Glyceraldehyde-3- phosphate dehydrogenase *GAPDH*	002046.3	F 5'-ACCCACTCCTCCACCTTTGA-3' R 5'-TGTTGCTGTAGCCAAATTCGTT-3'

* variants of transcripts

RESULTS
Cell viability
The toxicity of the resin cements was assessed by exposing the fibroblasts to the respective extracts, and then determining the number of viable cells (Fig. 1). A significant reduction was observed in the number of viable cells after 24 h of exposure to RXU and RXU200 extracts, but not to VLII, compared to the control medium ($p < 0.05$). All the cements caused a reduction in the viable cell number, but the more drastic effects were observed with exposure to the RXU and RXU200 extracts (5-fold), compared to the control medium ($p < 0.05$; Fig. 1).
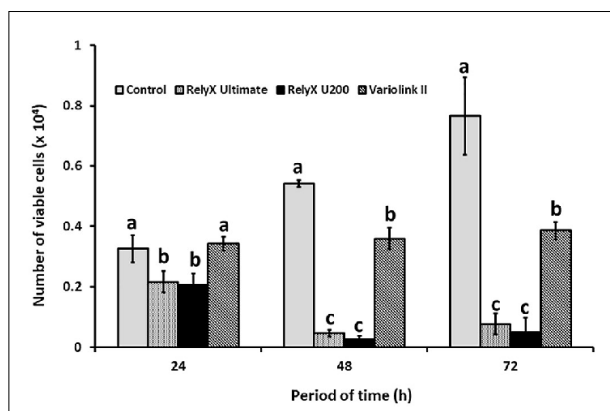

Fig. 1: Influence of the resin cement extracts on the viability of human gingival fibroblasts. Gingival fibroblasts were exposed to the extracts of RelyX Ultimate, RelyX U200 and Variolink II, or to the culture medium (Control) for 24, 48 and 72 h, and the number of viable cells was obtained by the vital trypan blue exclusion test. The data represent mean and standard deviation. Different lowercase letters show that there was significant difference for viable cell number for ANOVA and Bonferroni tests (p<0.05).

Expression of antioxidant genes
To gain better understanding of how well resin cements induce oxidative stress and antioxidant adaptive cellular response, the expression of *PRDX1*, *GPX1*, *CAT*, *SOD1* and GSS antioxidant genes was analyzed in fibroblasts exposed to the resin cement extracts, and the levels were compared to those of the cells grown in the culture medium (control). This analysis showed a significant increase in *PRDX1* transcript levels, caused by the extracts of all the tested cements ($p < 0.05$), as well as *SOD1* induction by the RXU200 and VLII cement extracts ($p < 0.05$) (Fig. 2). The other genes (*GPX1*, *CAT* and *GSS*) were induced significantly only by the RXU200 extract ($p < 0.05$). The highest levels of expression of these genes were observed

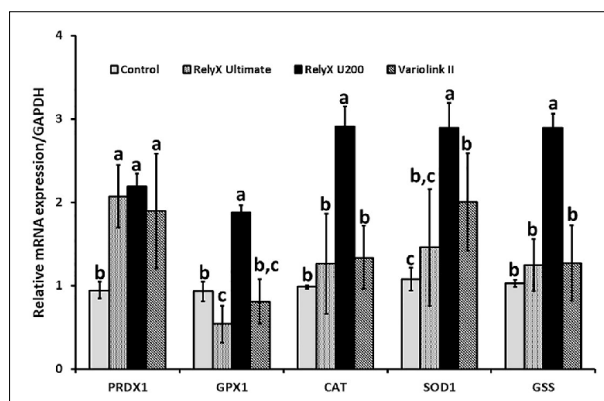with the exposure to the RXU200 cement extract (Fig. 2).

Fig. 2: Influence of the resin cement extracts on the expression of antioxidant genes in human gingival fibroblasts. Gingival fibroblasts were exposed to the extracts of RelyX Ultimate, RelyX U200 and Variolink II or to the culture medium (Control) for 24 h, and the expression of PRDX1, CAT, GPX1, SOD1 and GSS was assessed by qPCR. The data represent mean and standard deviation.
Different lowercase letters for each gene show differences by ANOVA and Bonferroni tests (p<0.05).

DISCUSSION
In the present study, the toxicity of different cements was assessed by exposing fibroblasts to the extracts obtained from resin materials. The results demonstrated that VLII cement was less toxic than RXU and RXU200, as observed by a greater number of viable cells during the 72 h of exposure to the corresponding extracts. One of the determining factors for the concentration of residual monomers is the polymerization process. It is important to emphasize that only the basal surface of this cement was used for this analysis, since polymerization of the cement is dependent exclusively on light, according to the photoactivation process, thus eliminating the need to mix the base and catalyst pastes. RXU and the RXU200 cements required dual polymerization, and presented the most exacerbated toxic effects, which were statistically similar. This could be attributed to the longer time required for polymerization, leading to more methacrylic groups remaining unreacted. In agreement, Kurt et al. showed that all resin cements were toxic to fibroblasts, but that RXU200 had the greatest toxic effect[9].

It is assumed that the combination of different methacrylates potentiates their toxicity, compared with uncombined forms. Ratanasathien et al. studied the isolated effects of methacrylates, and determined

that the most toxic cements, in decreasing order, are those containing Bis-GMA, followed by UDMA and TEGDMA, which are less toxic[18]. In our study, all the cements were formulated with Bis-GMA. However, considering the associations of methacrylates, TEGDMA had the lowest cytotoxicity, and VLII had comparatively lower toxicity, hence corroborating the findings of Ratanasathien et al. On the other hand, toxicity studies on isolated methacrylate components reported that TEGDMA and Bis-GMA are the most toxic monomers, compared to EDMA and UDMA[19,20]. Different experimental conditions may be associated with the divergent results in the study mentioned. It is known that even small amounts of monomers can induce toxic effects in cells, and that toxicity increases significantly at higher concentrations[21].

Lefeuvre et al. suggested that the death of cells exposed to TEGDMA, BIS-GMA and other resin monomers occurs due to an intracellular increase in ROS subsequent to a decrease in the GSH antioxidant agent[13]. These monomers were found to cause drastic and rapid GSH depletion in gingival fibroblast pulp cells[10,22], based on a suggested mechanism involving the formation of GSH-monomer adducts[23,24]. In line with this mechanism, N-acetylcysteine (NAC), ascorbate and Trolox antioxidants were shown to prevent TEGDMA-induced toxicity, and partially restore GSH levels in gingival fibroblasts[10]. In addition, Kurt et al. showed that the TEGDMA released from resin cements (including RXU200) increased in artificial saliva over time (1, 24 and 72 h)[9]. They also showed that stimulated ROS production increased the genotoxicity of resin cements more than 3-fold relative to that of the control, and decreased cell viability in L-929 mouse fibroblasts exposed to the cements, compared to non-exposed fibroblasts. In line with ROS involvement in resin cement toxicity, our results showed an increase in *PRDX1* expression in human gingival fibroblasts exposed to all the cement extracts, compared to those left unexposed. This increase indicates an attempt by the cells to survive a disturbance in their redox balance by increasing their antioxidant defense.

ROS generation is expected to be lower when an exclusively light-cured system is applied, such as that used with VLII cement. This is because the formation of these species is totally dependent on the presence of photons at a depth that does not exceed a few millimeters[4]. On the other hand, when chemical curing is used, free radicals are formed throughout the bulk of the curing material, regardless of depth. Hence, use of the dual cements requires a broader defense response. In fact, our results showed that not only *PRDX1* antioxidant genes, but also RXU200 cement caused an increase in the transcript levels of all the other genes studied (*GPX1*, *CAT*, *SOD1* and *GSS*). However, this broader effect was not observed in cells exposed to RXU. Since the curing system cannot explain the different expression pattern induced by the two RX dual cements, and their composition is very similar, we can only speculate that it could be related to the concentration of the ingredients. Although exact percentages are declared as trade secrets in manufacturers' safety data sheets, it is known that sodium persulfate may reach a higher percentage by weight in RXU200 (<3 for RXU200 and <1 for RXU). The same is true for the percentage of tert-butyl peroxy-3,5,5-trimethylhexanoate (<0.50 for XU200 and <0.25 for RXU). Persulfate salts and organic peroxides are radical initiators of cross-linking methacrylate monomers, and have strong oxidizing properties. It has been reported that the ammonium salt of persulfate-induced ROS generation in mast cells and basophils[25], and also MCF-7 breast cancer cells, leads to oxidative stress[26]. Thus, we can hypothesize that the higher percentage of these chemical initiators in RXU200 may have led to higher levels of ROS formation in the cells, activating additional signaling pathways responsible for the induction of a greater variety of antioxidant genes. Even so, the suggested activation of the oxidative stress response does not seem entirely efficient. This may be the reason why a drastic reduction in the number of viable cells was observed when the cells were exposed to any of the dual cements, especially after 48 h. Regarding the results of the exposed VLII base cells, ROS formation was mostly attributed to residual monomers left unpolymerized, rather than to the release of residual chemical initiators. Thus, *PRDX1* and *SOD1* induction by the cells exposed to this cement may have contributed to their survival during the exposure interval (72 h). These results support the proposition that cement cytotoxicity was at least partly related to the formation of ROS.

The findings of the present study showed that biological principles must be considered during operative and restorative procedures; hence, it

is critical to determine the professional clinical choice of whether to involve the patient. Therefore, it is generally accepted that *in vitro* tests, mostly based on cell culture systems, must precede *in vivo* approaches when testing the health risk of dental materials. This is a major concern and ongoing issue.

CONCLUSIONS

All resin cements showed toxicity to human fibroblasts, and VLII was the least toxic. Induction of antioxidant genes supports the idea that cement cytotoxicity was at least partly related to the formation of reactive oxygen species in the cells.

REFERENCES

1. Hill EE, Lott J. A clinically focused discussion of luting materials. Aust Dent J. 2011 Jun;56 Suppl 1:67-76. https://doi.org/10.1111/j.1834-7819.2010.01297.x
2. Blatz MB, Vonderheide M, Conejo J. The Effect of Resin Bonding on Long-Term Success of High-Strength Ceramics. J Dent Res. 2018 Feb;97(2):132-139. https://doi.org/10.1177/0022034517729134
3. Sulaiman TA, Abdulmajeed AA, Altitinchi A, Ahmed SN, Donovan TE. Mechanical properties of resin-based cements with different dispensing and mixing methods. J Prosthet Dent. 2018 Jun;119(6):1007-1013. https://doi.org/10.1016/j.prosdent.2017.06.010
4. Rueggeberg FA, Giannini M, Arrais CAG, Price RBT. Light curing in dentistry and clinical implications: a literature review. Braz Oral Res. 2017 Aug 28;31(suppl 1):e61. https://doi.org/10.1590/1807-3107bor-2017.vol31.0061
5. Goldberg M. In vitro and in vivo studies on the toxicity of dental resin components: a review. Clin Oral Investig. 2008 Mar;12(1):1-8. https://doi.org/10.1007/s00784-007-0162-8
6. Ferracane JL. Elution of leachable components from composites. J Oral Rehabil. 1994 Jul;21(4):441-52. https://doi.org/10.1111/j.1365-2842.1994.tb01158.x
7. Bationo R, Rouamba A, Diarra A, Beugré-Kouassi MLA, Beugré JB, Jordana F. Cytotoxicity evaluation of dental and orthodontic light-cured composite resins. Clin Exp Dent Res. 2021 Feb;7(1):40-48. https://doi.org/10.1002/cre2.337
8. Moharamzadeh K, Van Noort R, Brook IM, Scutt AM. HPLC analysis of components released from dental composites with different resin compositions using different extraction media. J Mater Sci Mater Med. 2007 Jan;18(1):133-7. https://doi.org/10.1007/s10856-006-0671-z
9. Kurt A, Altintas SH, Kiziltas MV, Tekkeli SE, Guler EM, Kocyigit A, Usumez A. Evaluation of residual monomer release and toxicity of self-adhesive resin cements. Dent Mater J. 2018 Jan 30;37(1):40-48. https://doi.org/10.4012/dmj.2016-380
10. Stanislawski L, Lefeuvre M, Bourd K, Soheili-Majd E, Goldberg M, Périanin A. TEGDMA-induced toxicity in human fibroblasts is associated with early and drastic glutathione depletion with subsequent production of oxygen reactive species. J Biomed Mater Res A. 2003 Sep 1;66(3):476-82. https://doi.org/10.1002/jbm.a.10600
11. Walther UI, Siagian II, Walther SC, Reichl FX, Hickel R. Antioxidative vitamins decrease cytotoxicity of HEMA and TEGDMA in cultured cell lines. Arch Oral Biol. 2004 Feb;49(2):125-31. https://doi.org/10.1016/j.archoralbio.2003.08.008
12. Schweikl H, Spagnuolo G, Schmalz G. Genetic and cellular toxicology of dental resin monomers. J Dent Res. 2006 Oct;85(10):870-7. https://doi.org/10.1177/154405910608501001
13. Lefeuvre M, Amjaad W, Goldberg M, Stanislawski L. TEGDMA induces mitochondrial damage and oxidative stress in human gingival fibroblasts. Biomaterials. 2005 Sep;26(25):5130-7. https://doi.org/10.1016/j.biomaterials.2005.01.014
14. Krifka S, Spagnuolo G, Schmalz G, Schweikl H. A review of adaptive mechanisms in cell responses towards oxidative stress caused by dental resin monomers. Biomaterials. 2013 Jun;34(19):4555-63. https://doi.org/10.1016/j.biomaterials.2013.03.019
15. Schweikl H, Schmalz G, Spruss T. The induction of micronuclei in vitro by unpolymerized resin monomers. J Dent Res. 2001 Jul;80(7):1615-20. https://doi.org/10.1177/00220345010800070401
16. Kleinsasser NH, Schmid K, Sassen AW, Harréus UA, Staudenmaier R, Folwaczny M, Glas J, Reichl FX. Cytotoxic and genotoxic effects of resin monomers in human salivary gland tissue and lymphocytes as assessed by the single cell microgel electrophoresis (Comet) assay. Biomaterials. 2006 Mar;27(9):1762-70. https://doi.org/10.1016/j.biomaterials.2005.09.023
17. International Organization for Standardization. Biological evaluation of medical devices – Part 12: Sample preparation and reference materials (ISO 10993–12). 4th revision, Geneva: International Organization for Standardization, 2012; 1–20.
18. Ratanasathien S, Wataha JC, Hanks CT, Dennison JB. Cytotoxic interactive effects of dentin bonding components on mouse fibroblasts. J Dent Res. 1995 Sep;74(9):1602-6. https://doi.org/10.1177/00220345950740091601
19. Geurtsen W, Lehmann F, Spahl W, Leyhausen G. Cytotoxicity

of 35 dental resin composite monomers/additives in permanent 3T3 and three human primary fibroblast cultures. J Biomed Mater Res. 1998 Sep 5;41(3):474-80. https://doi.org/10.1002/(sici)1097-4636(19980905)41:3<474::aid-jbm18>3.0.co;2-i"

20. Issa Y, Watts DC, Brunton PA, Waters CM, Duxbury AJ. Resin composite monomers alter MTT and LDH activity of human gingival fibroblasts in vitro. Dent Mater. 2004 Jan;20(1):12-20. https://doi.org/10.1016/S0109-5641(03)00053-8

21. Bakopoulou A, Papadopoulos T, Garefis P. Molecular toxicology of substances released from resin-based dental restorative materials. Int J Mol Sci. 2009 Sep 4;10(9):3861-3899. https://doi.org/10.3390/ijms10093861

22. Jiao Y, Ma S, Wang Y, Li J, Shan L, Liu Q, Liu Y, Song Q, Yu F, Yu H, Liu H, Huang L, Chen J. N-Acetyl Cysteine Depletes Reactive Oxygen Species and Prevents Dental Monomer-Induced Intrinsic Mitochondrial Apoptosis In Vitro in Human Dental Pulp Cells. PLoS One. 2016 Jan 25;11(1):e0147858. https://doi.org/10.1371/journal.pone.0147858

23. Nocca G, Ragno R, Carbone V, Martorana GE, Rossetti DV, Gambarini G, Giardina B, Lupi A. Identification of glutathione-methacrylates adducts in gingival fibroblasts and erythrocytes by HPLC-MS and capillary electrophoresis. Dent Mater. 2011 May;27(5):e87-98. https://doi.org/10.1016/j.dental.2011.01.002

24. Samuelsen JT, Kopperud HM, Holme JA, Dragland IS, Christensen T, Dahl JE. Role of thiol-complex formation in 2-hydroxyethyl- methacrylate-induced toxicity in vitro. J Biomed Mater Res A. 2011 Feb;96(2):395-401. https://doi.org/10.1002/jbm.a.32993

25. Pignatti P, Frossi B, Pala G, Negri S, Oman H, Perfetti L, Pucillo C, Imbriani M, Moscato G. Oxidative activity of ammonium persulfate salt on mast cells and basophils: implication in hairdressers' asthma. Int Arch Allergy Immunol. 2013;160(4):409-19. https://doi.org/10.1159/000343020

26. Song C, Wang L, Ye G, Song X, He Y, Qiu X. Residual Ammonium Persulfate in Nanoparticles Has Cytotoxic Effects on Cells through Epithelial-Mesenchymal Transition. Sci Rep. 2017 Sep 18;7(1):11769. https://doi.org/10.1038/s41598-017-12328-0

SAIO
SOCIEDAD ARGENTINA
DE INVESTIGACION ODONTOLOGICA

División Argentina de la International
Association for Dental Research

DESDE 1961

The 101st General Session & Exhibition of the IADR, IX Meeting of the Latin American Region (LAR), was held from June 21-24 in Bogota, Colombia. We are proud to announce that we had a record attendance of researchers from the Argentine Division (SAIO).

The attendees had the opportunity to present their own papers and projects (26 in total), which resulted in constructive discussions and valuable exchanges of knowledge, leading the way to future advances in our respective areas and interdiscipline.

Participation of the Argentine Delegation in 2023 IADR/LAR General Sesion

On behalf of the entire SAIO Board of Directors we would like to express our most sincere congratulations to the elected LAR Board of Directors (2023-2026). Their role anticipates the continued growth of dental research in the Latin American Region of the IADR.

Term 2023-2026
President: Gabriel Sánchez
Vice President: Paulo Cesar
Secretary: Daniel Di Croce
Treasurer: Mariana Picca
Executive Director: Aldo Squassi

LAR Board of Directors 2023-2026

CTOR.

CTOR Award for Student Excellence in Orthodontics

Maria Lorena Cabirta

"Three-Dimensional Study of Orthodontic Tooth Movement in Hypercholesterolemic Rats"

The CTOR Award for Excellence in Orthodontics Research acknowledges excellence in Orthodontics Research conducted and presented by dental students and graduate students. The finalists were selected and were invited to present their work during the 101st General Session & Exhibition of the IADR, IX Meeting of the Latin American Región 2023, Bogotá, Colombia. Congratulations to Dr. Maria Lorena Cabirta on winning the CTOR award 2023 for the Argentinian Division (SAIO).

CTOR Award for Excellence in Orthodontics Research, Orthodontic Research Group (ORG) at 101st General Session & Exhibition of the IADR, IX Meeting of the Latin American Region (June 21-24, Bogotá, Colombia).

SAIO 2023
LVI Reunión Científica Anual
09 al 11 NOV
CORDOBA - ARGENTINA

We are pleased to inform you that the LVI Annual Meeting of the Argentine Society of Dental Research will be held on November 9-11, 2023 in the city of Córdoba. The Schools of Dentistry of the Catholic University and the National University of Córdoba will host the event. The event is organized by the Organizing Committee of the 2023 Annual Meeting, whose President is Dr. Gabriela Martín. It will include the participation and lectures by leading experts in current dental research, awards ceremony and presentation of research papers in the form of oral and poster presentations.

LVI SAIO 2023 Annual Meeting, Córdoba-Argentina